The Abdus Salam International Centre for Theoretical Physics

1959-3

Workshop on Supersolid 2008

18 - 22 August 2008

Non-classical response of solid helium confined in porous media

E. Kim
KAIST, Republic of Korea

Superflow in solid helium

Eunseong Kim

KAIST, Republic of Korea

Outline

- Brief history on supersolid experiments
- ^{3}He effects
- New experiments at KAIST

The first observation of superflow in solid helium & ^{3}He effects at Penn State

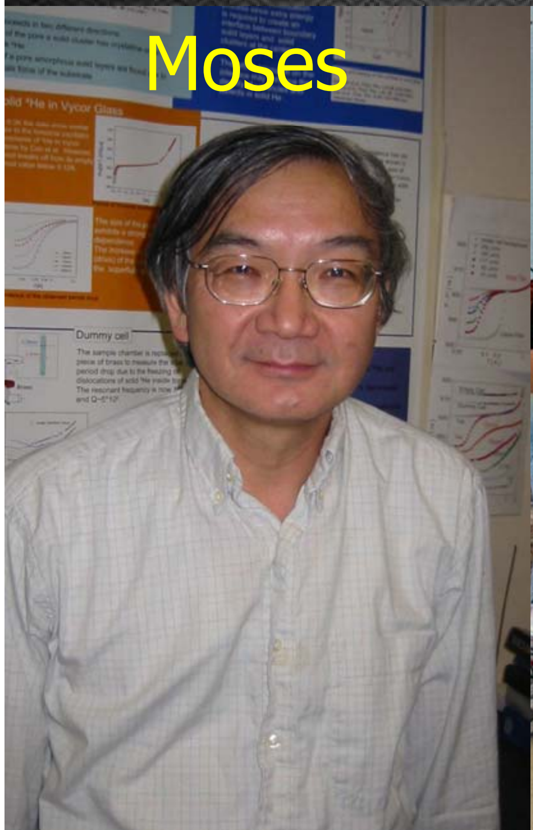

Dr. Xia @ UF

Supersolid experiments at KAIST

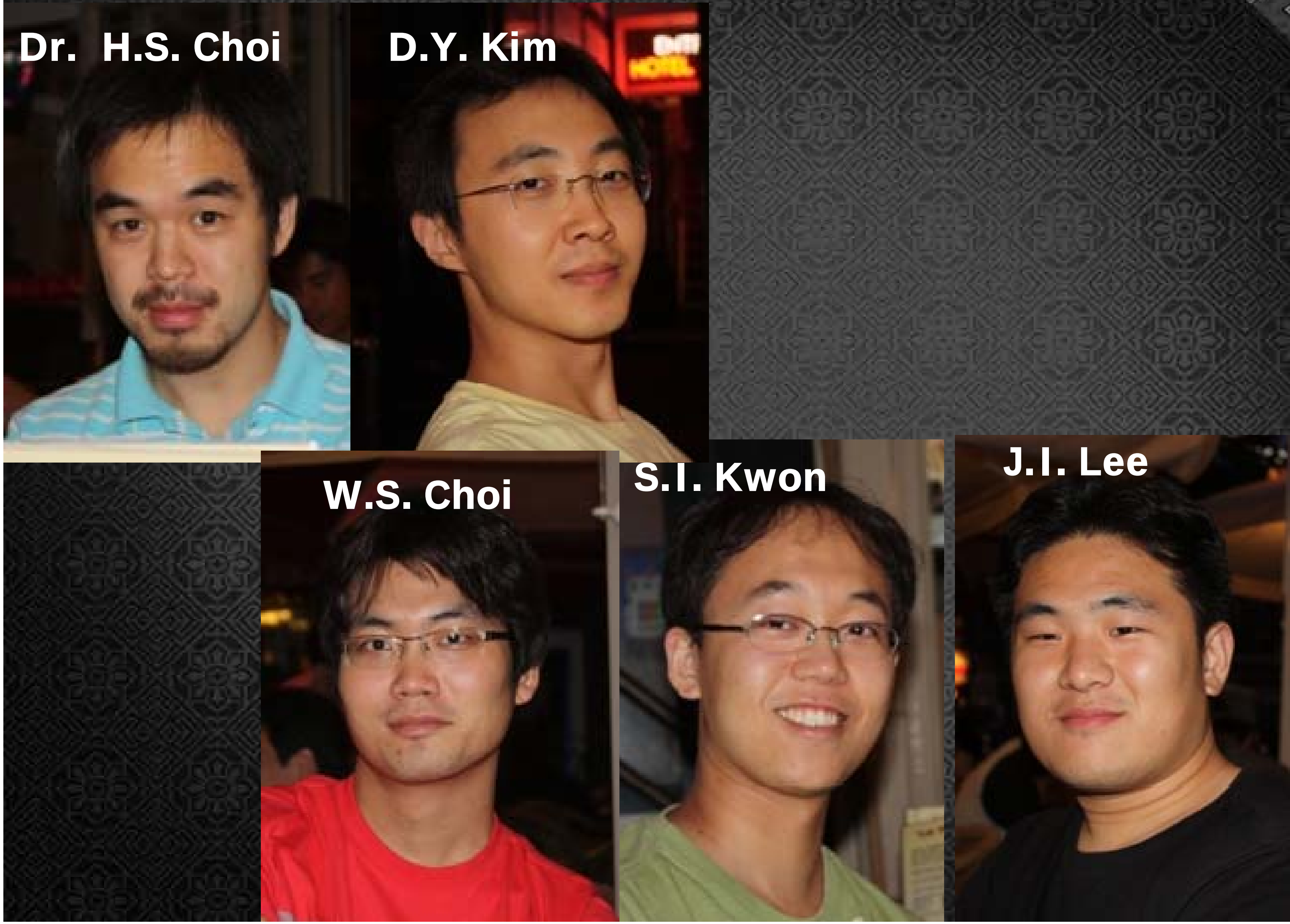

Part 1

BRIEF HISTORY OF SUPERSOLID EXPERIMENTS

Observation of Non-Classical Rotational Inertia

E. Kim and M. Chan

Superfluidity & Bose Einstein Condensation

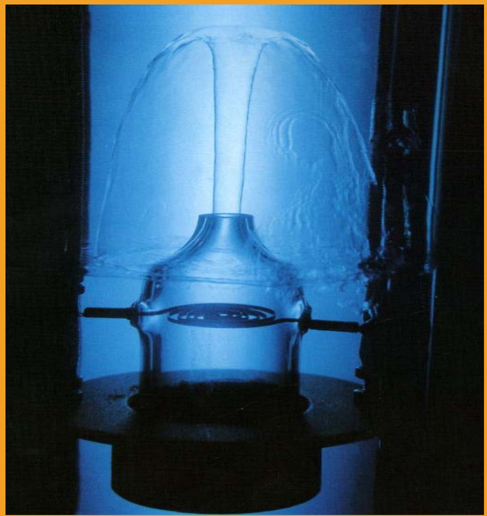

Superfluid ^4He
Kapitza
(1978)

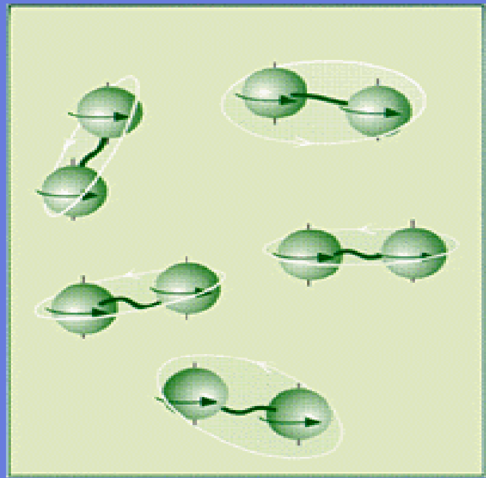

Superfluid ^3He
Lee, Osheroff, Richardson
(1996)

Theory
Leggett (2003)

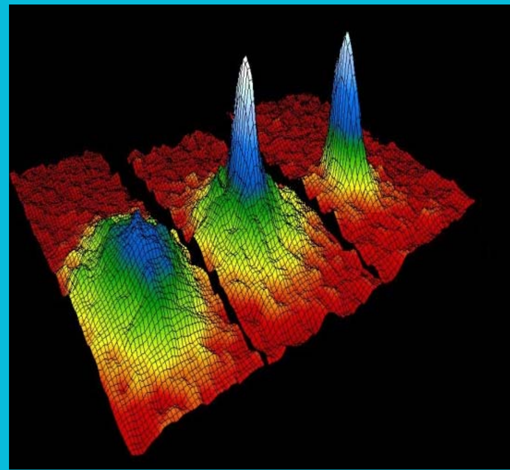

BEC in a bose gas
= Super-gas
Cornell, Ketterle, Wieman
(2001)

Super-Solid= Solid with Superfluidity?

Supersolid ?

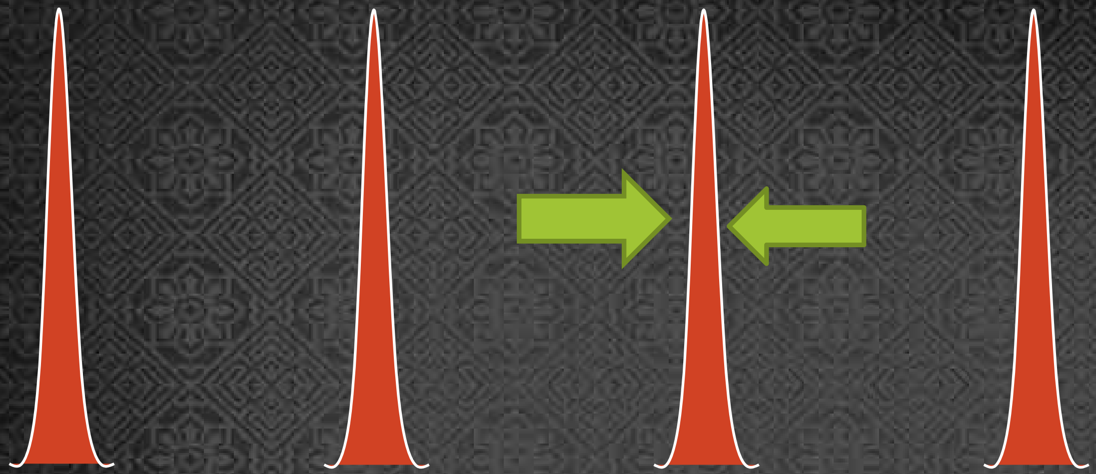

T>T_O

$$\lambda_{dB} \propto \sqrt{\frac{1}{T}} << a$$

Overlap of wavefunctions ~ Exchange amplitude
~ nearly zero in classical solid

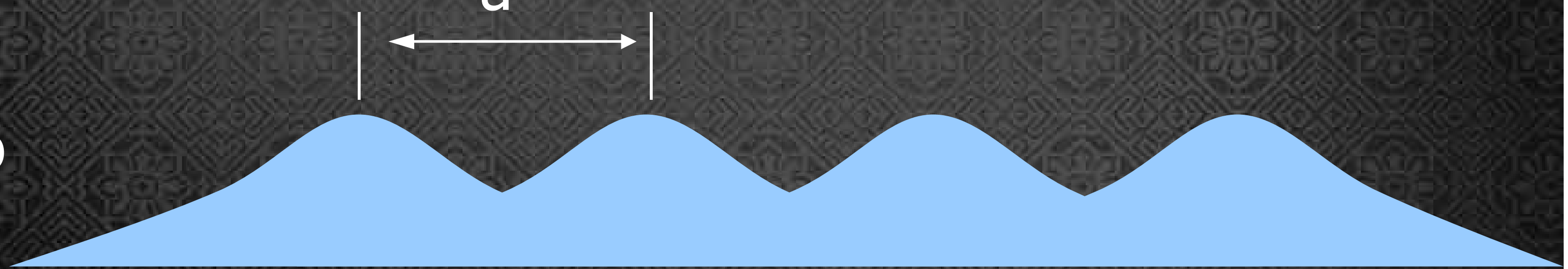

T<T_O

Finite exchange amplitude
→ Coherent exchange at very low temperature

Superfluidity in solid is not impossible!

- If solid ^4He can be described by a Jastraw-type wavefunction that is commonly used to describe liquid helium then crystalline order (with finite fraction of vacancies) and BEC can coexist.

  G.V. Chester, *Lectures in Theoretical Physics* Vol XI-B(1969); *Phys. Rev. A* **2**, 256 (1970)

  J. Sarfatt, *Phys. Lett.* **30A**, 300 (1969) L. Reatto, *Phys. Rev.* **183**, 334 (1969)

- Andreev and Liftshitz assume the specific scenario of zero-point vacancies and other defects (e.g. interstitial atoms) undergoing BEC and exhibit superfluidity.

  Andreev & Liftshitz, *Zh.Eksp.Teor.Fiz.* **56**, 205 (1969).

No experimental evidence of superflow in solid helium prior to 2004.

- Plastic flow measurement
  Andreev et al. Sov. Phys. JETP Lett **9**,306(1969)
  Suzuki J. Phys. Soc. Jpn. **35**, 1472(1973)
  Tsymbalenko Sov. Phys. JETP Lett. **23**, 653(1976)
  Dyumin et al. J. Low Temp. Phys. **15**,295(1989)

- Torsional oscillator
  Bishop et al. Phys. Rev. B **24**, 2844(1981)

- Mass flow
  Greywall Phys. Rev. B **16**, 1291(1977)

- $P_V(T)$ measurement
  Adams et al. Bull. Am. Phys. Soc. **35**,1080(1990)
  Haar et al. J. low Temp. Phys. **86**,349(1992)

- Ultra sound Measurements
  Goodkind Phys. Rev. Lett. **89**,095301(2002) and references therein

Ultrasound velocity and dissipation measurements in solid ^4He with 27.5ppm of ^3He

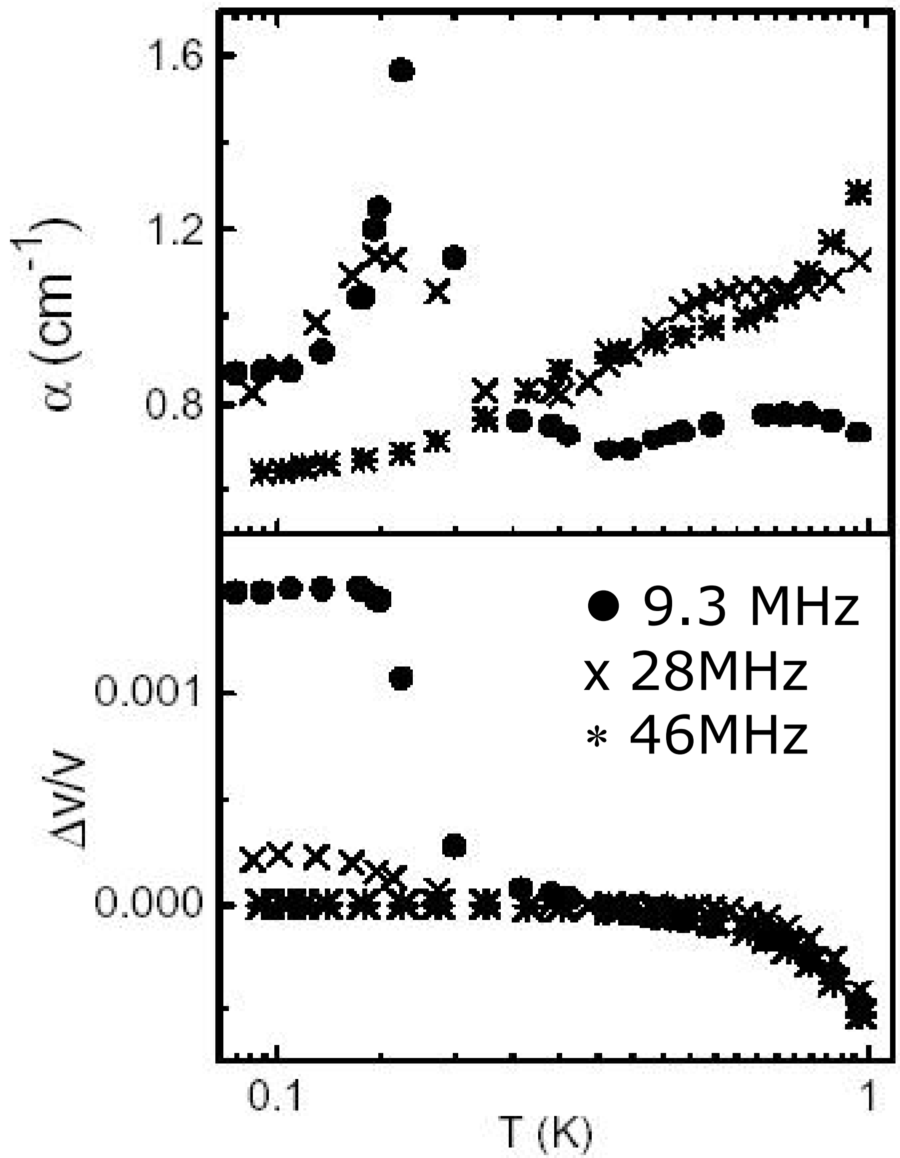

The results are interpreted by the authors as showing BEC of thermally activated vacancies above 200mK.

P.C. Ho, I.P. Bindloss and J. M. Goodkind, *J. Low Temp. Phys.* **109**, 409 (1997)

However, such a clear 'anomaly' was not seen in other ultrasound experiments of Goodkind.

Ideal detection of supersolid

Non-classical rotational inertia (NCRI)

A. J. Leggett, PRL 25, 1543 (1970)

Quantum exchange of particles arranged in an annulus under rotation leads to a measured moment of inertia that is smaller than the classical value

$$I(T)=I_{classical}[1-f_s(T)]$$

$f_s(T)$ is the supersolid fraction. Its upper limit is estimated by different theorists to range from 10^{-6} to 0.4; Leggett: 10^{-4}

Ideal torsional oscillator

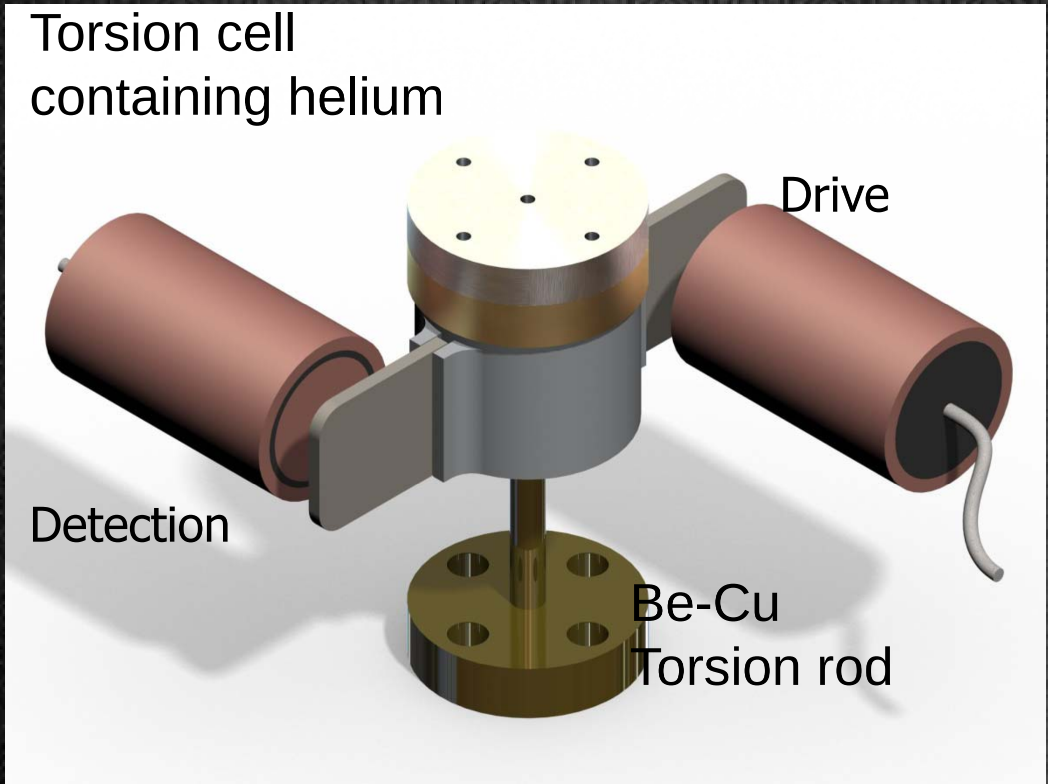

Ideal torsional oscillator

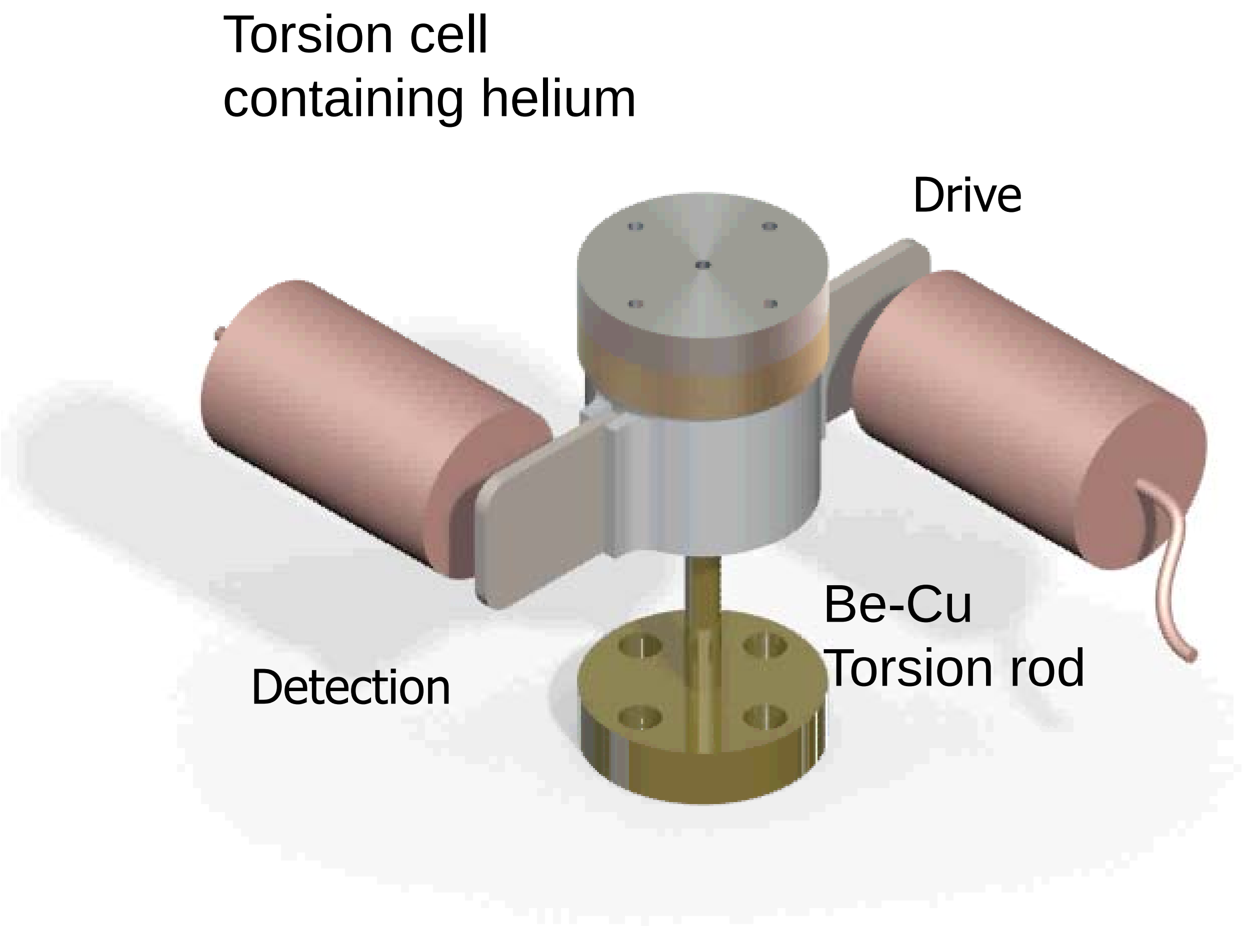

Ideal Torsional oscillator

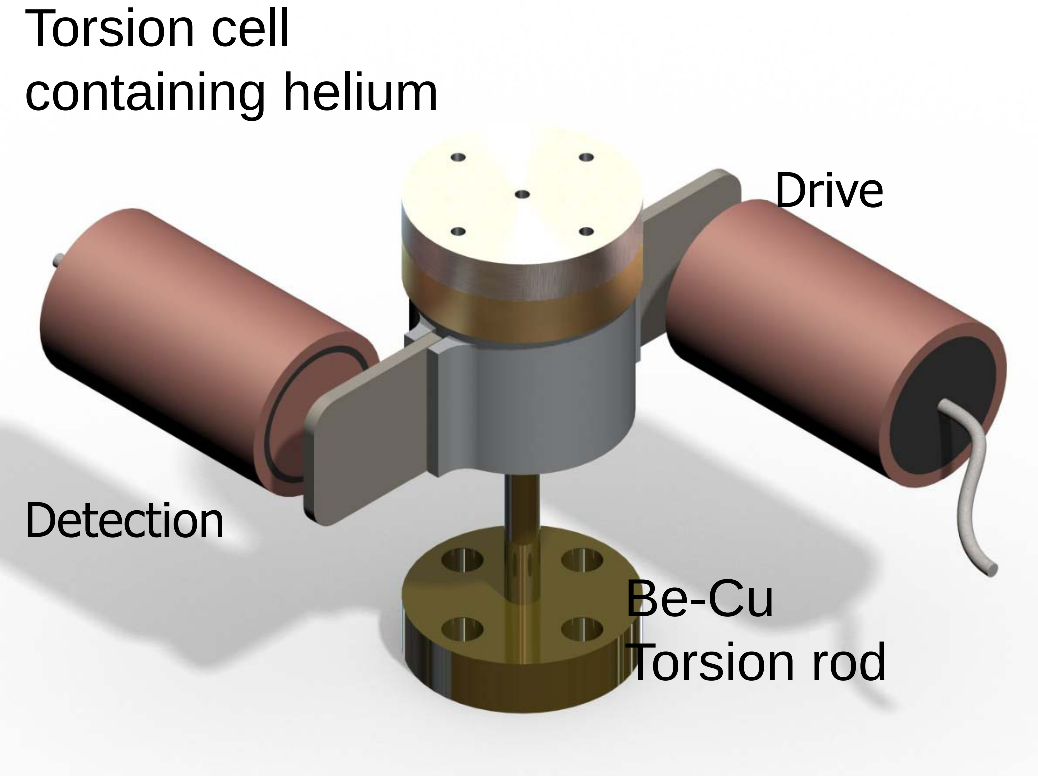

$$\tau_o = 2\pi\sqrt{\frac{I}{K}}$$

I : rotational inertia of torsion cell
K: torsion constant of the torsion Rod

Change of rotational inertia, *I*, can be detected by increase (or decrease) of the resonant oscillation period, τ_o.

→ **Detection of NCRI**

Torsional Oscillator for solid helium confined in Vycor glass

Torsion cell
with Vycor glass

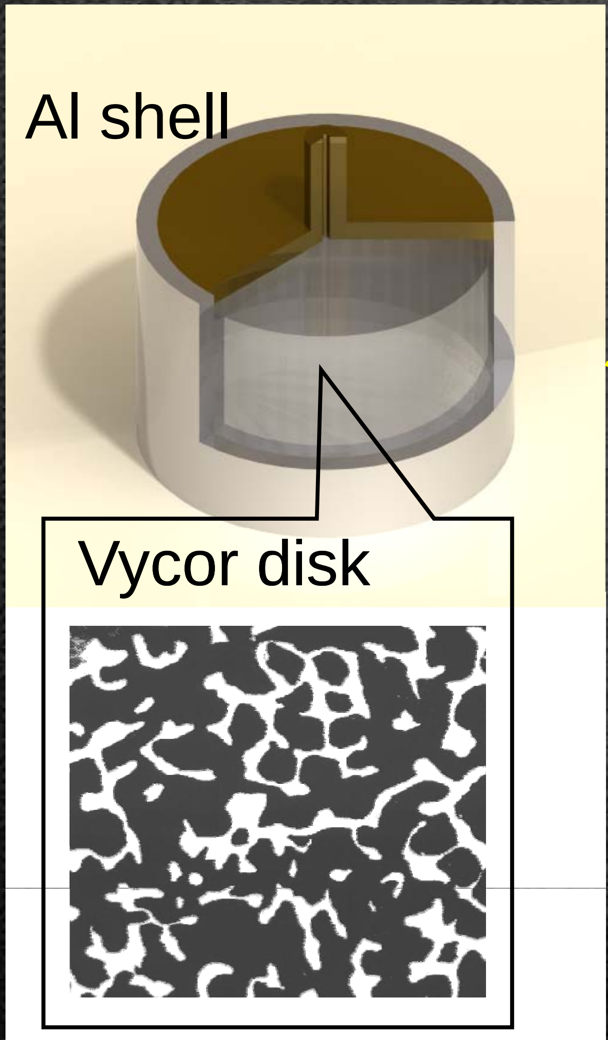

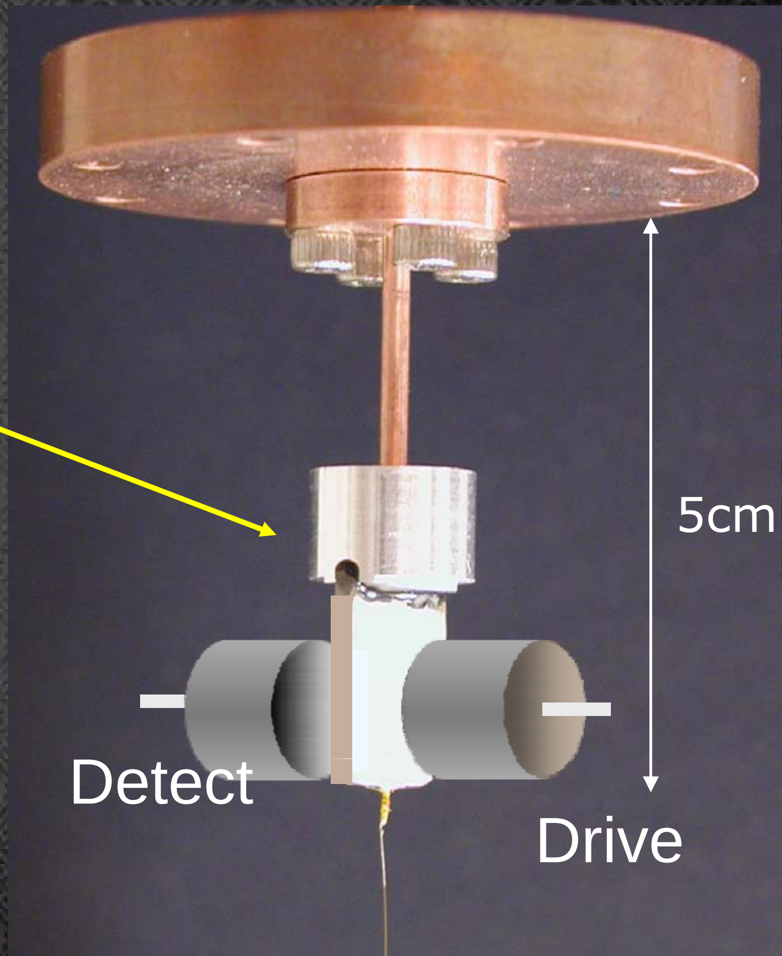

Solidification of helium in Vycor

Vycor glass

Characteristic
Pore diameter=7nm

Porosity = 30%

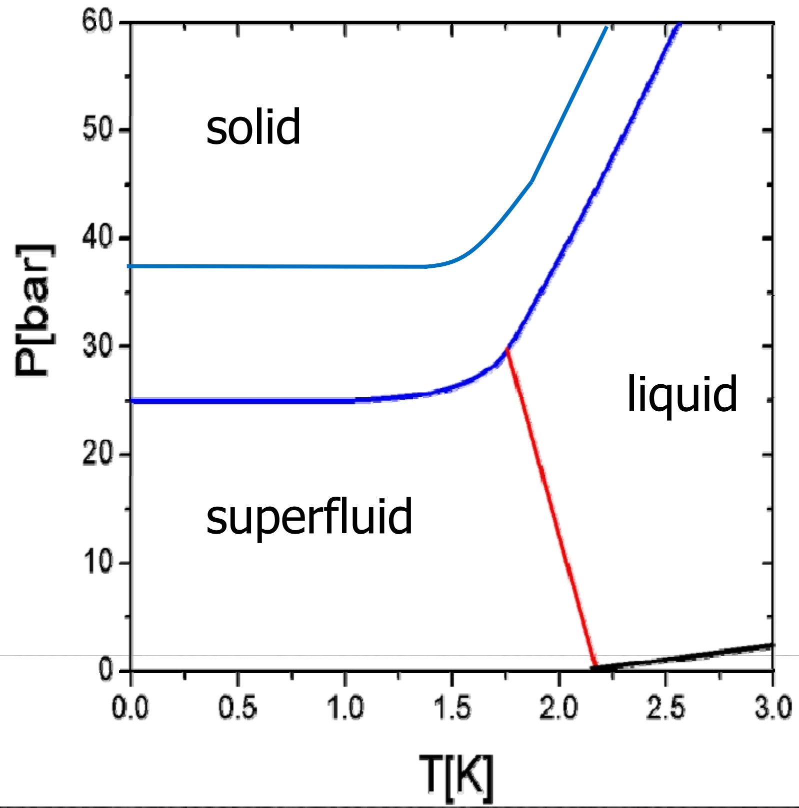

Blocked Capillary methods: Solidification of helium

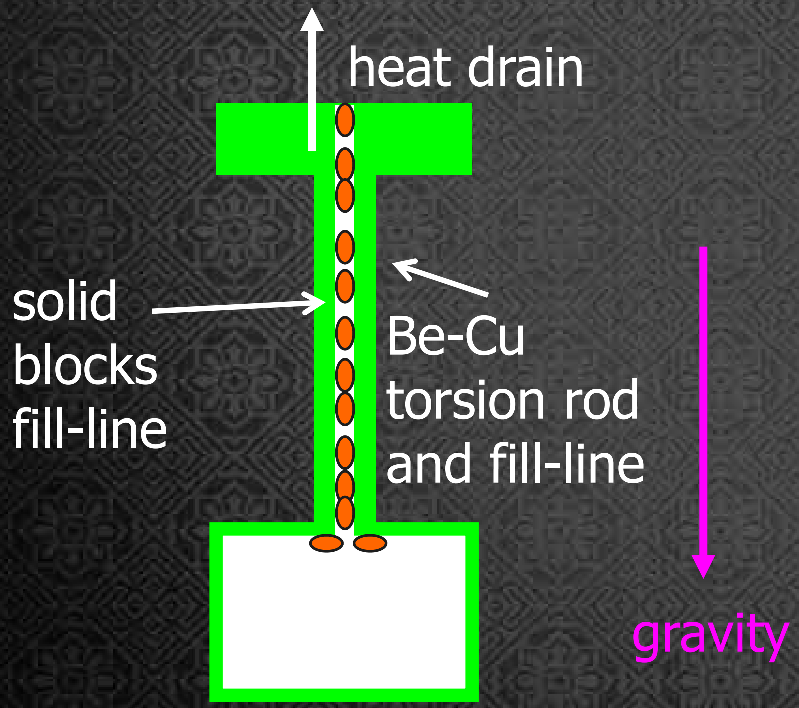

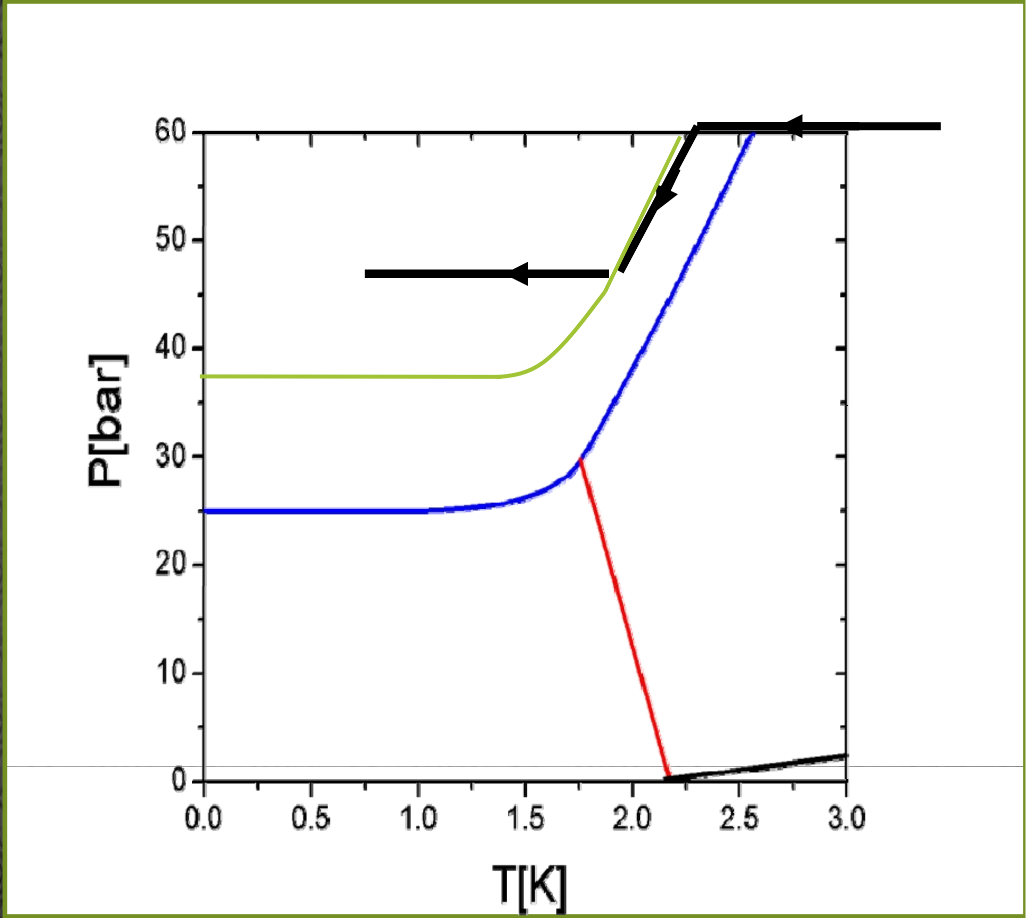

Solid ^{4}He at 62 bars in Vycor glass

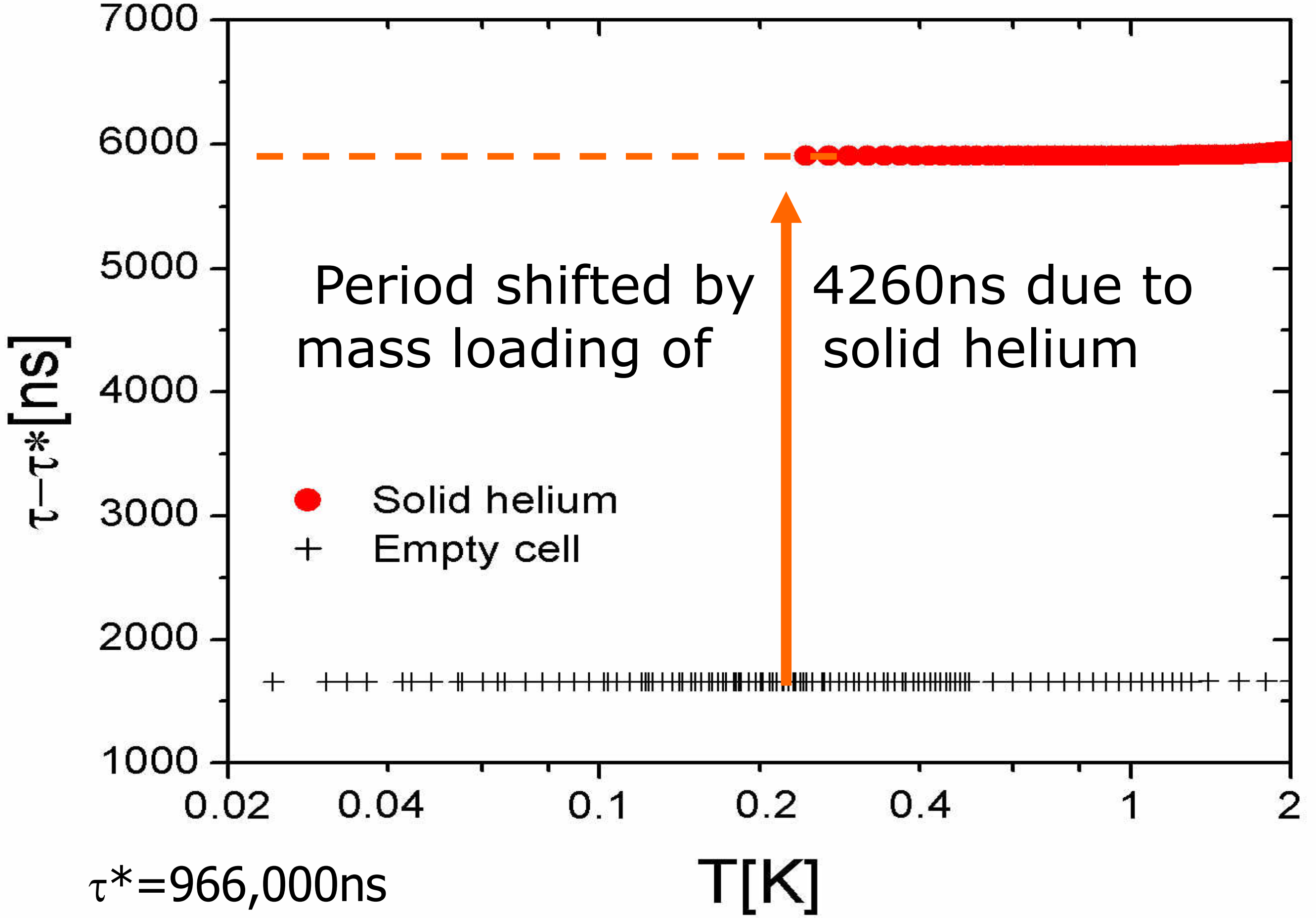

τ^*=966,000ns

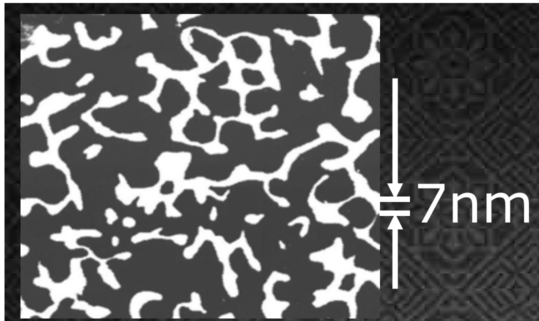

Solid helium in Vycor glass

f_0=1024Hz

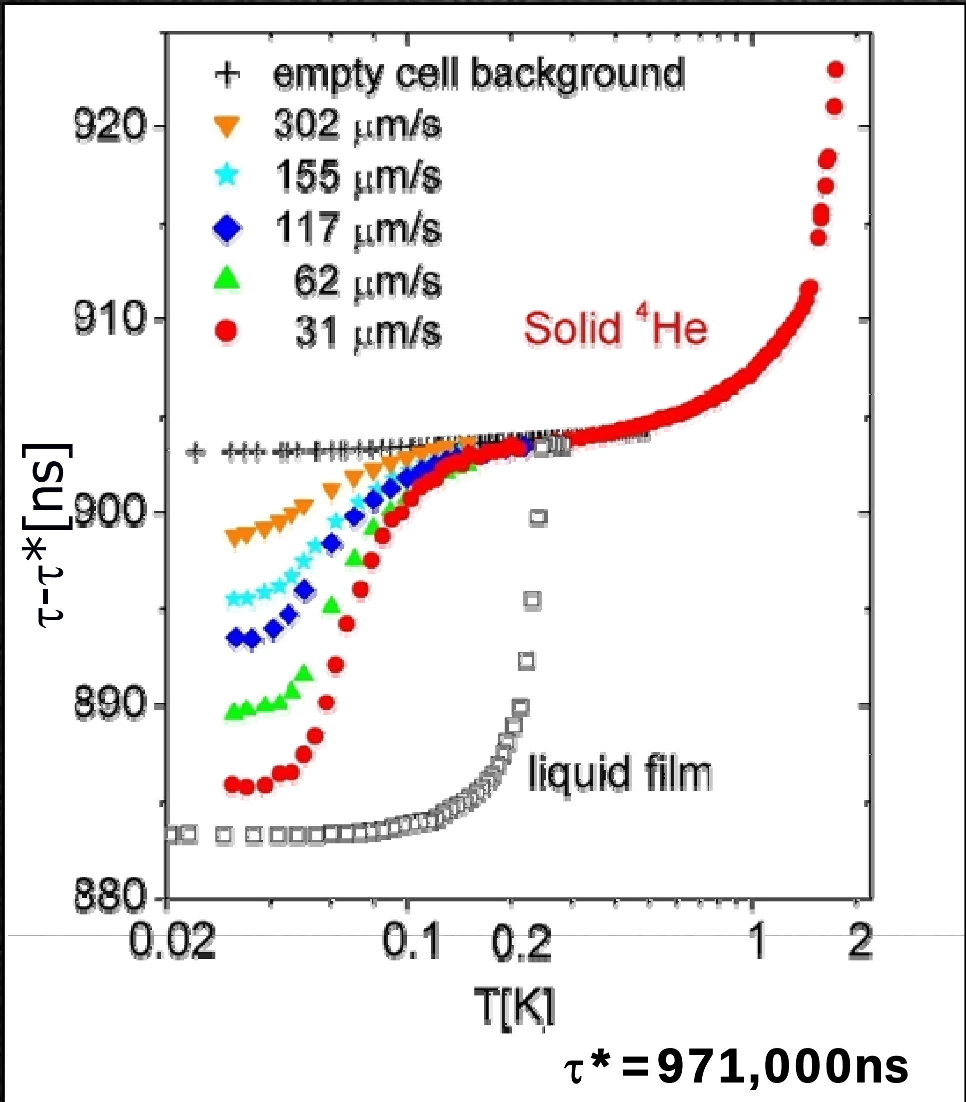

- Pressure= 62bar
- Total mass loading = 4260ns
- Measured decoupling, $-\Delta\tau_o$=17ns
- NCRIF = 0.4%

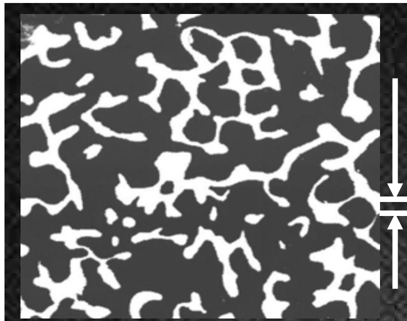

Solid helium in Vycor glass

f_0=1024Hz

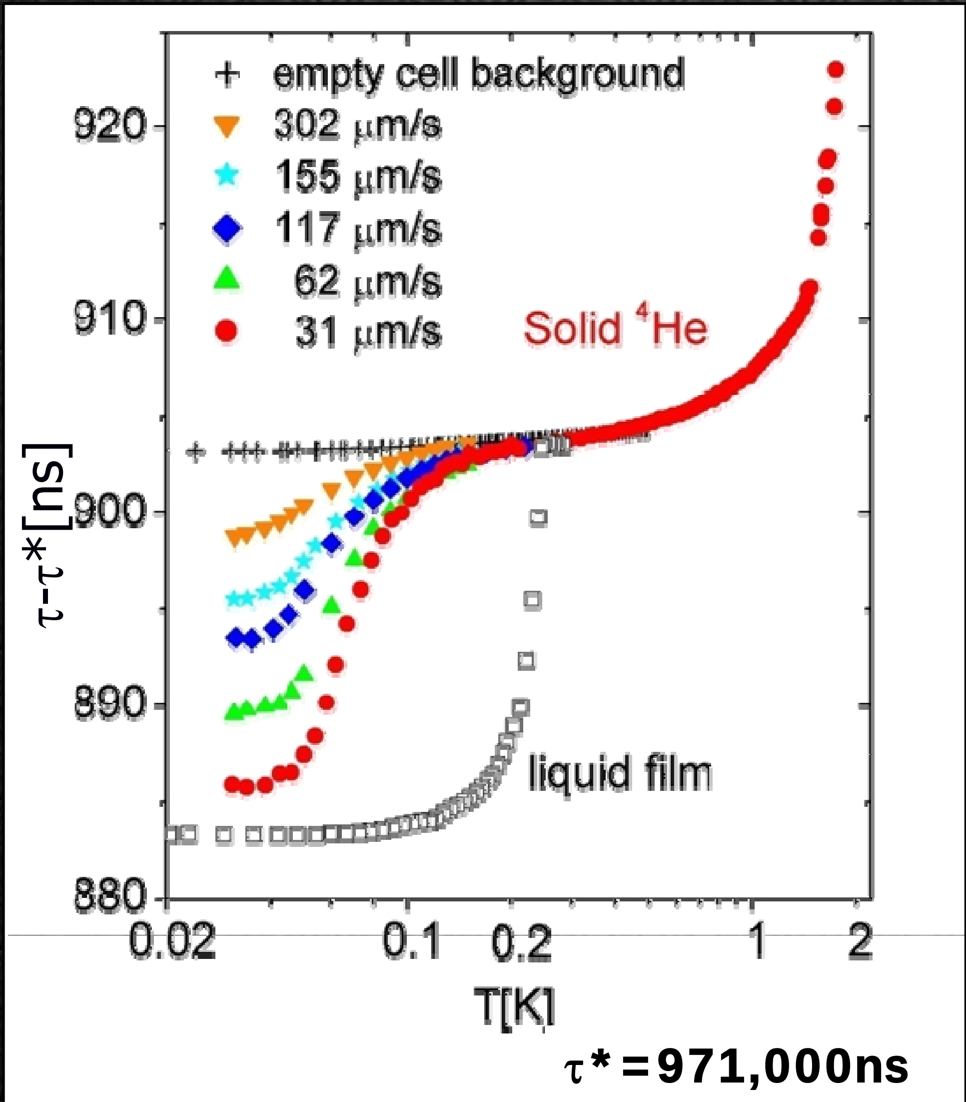

- Its viscosity should be smaller than 1.5×10^{-11} Pa·s, which is 10^5 times smaller than that of normal liquid helium.
- Viscosity penetration depth <<7nm

Strong velocity dependence

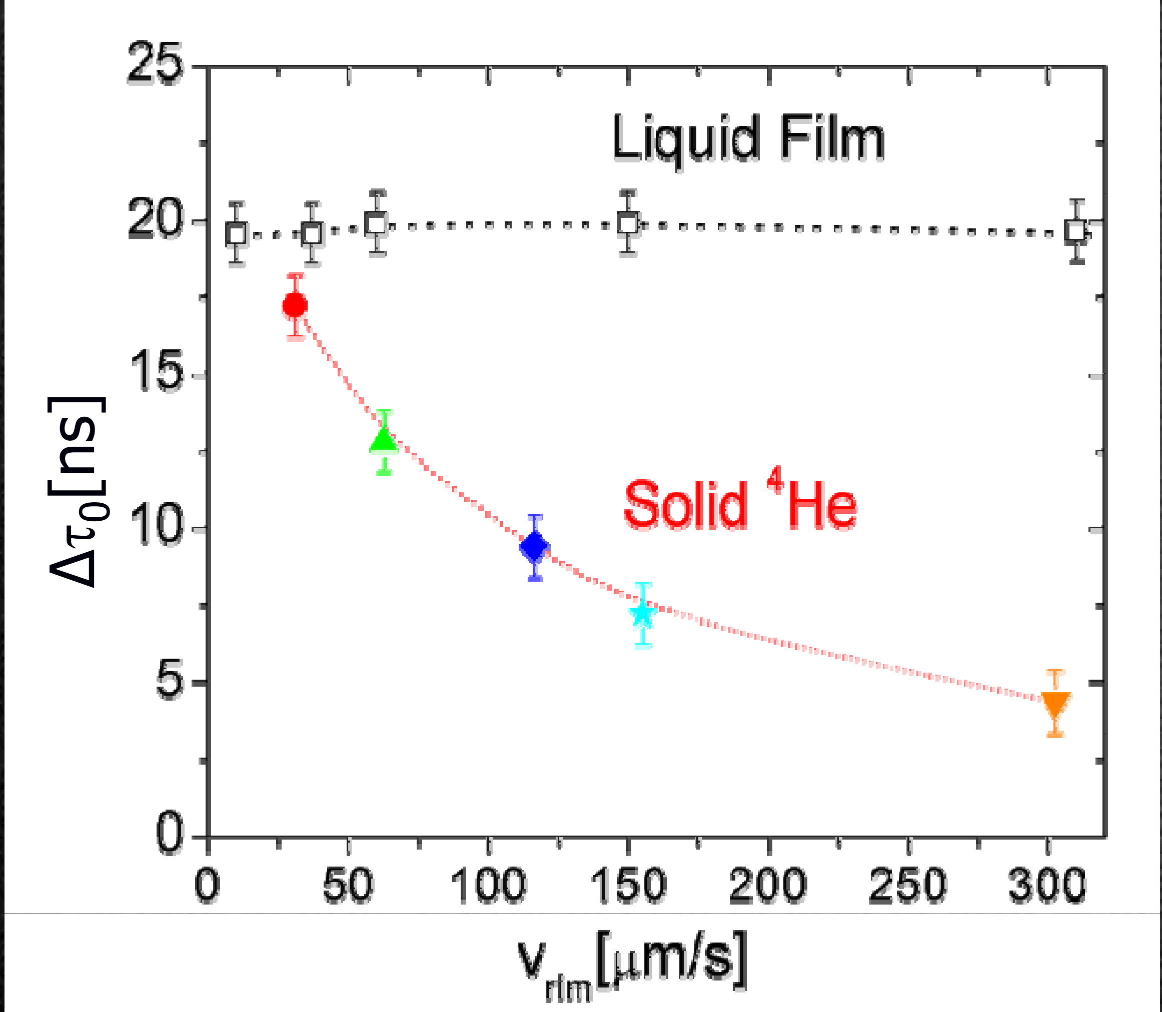

- For liquid film adsorbed on Vycor glass

  v_c > 20cm/s

M.H.W. Chan et.al., PRL 32, 1347 (1974).

- For superflow in solid ^{4}He

  v_c < 30 μm/s

Weak Pressure Dependence from 40 to 65 bar

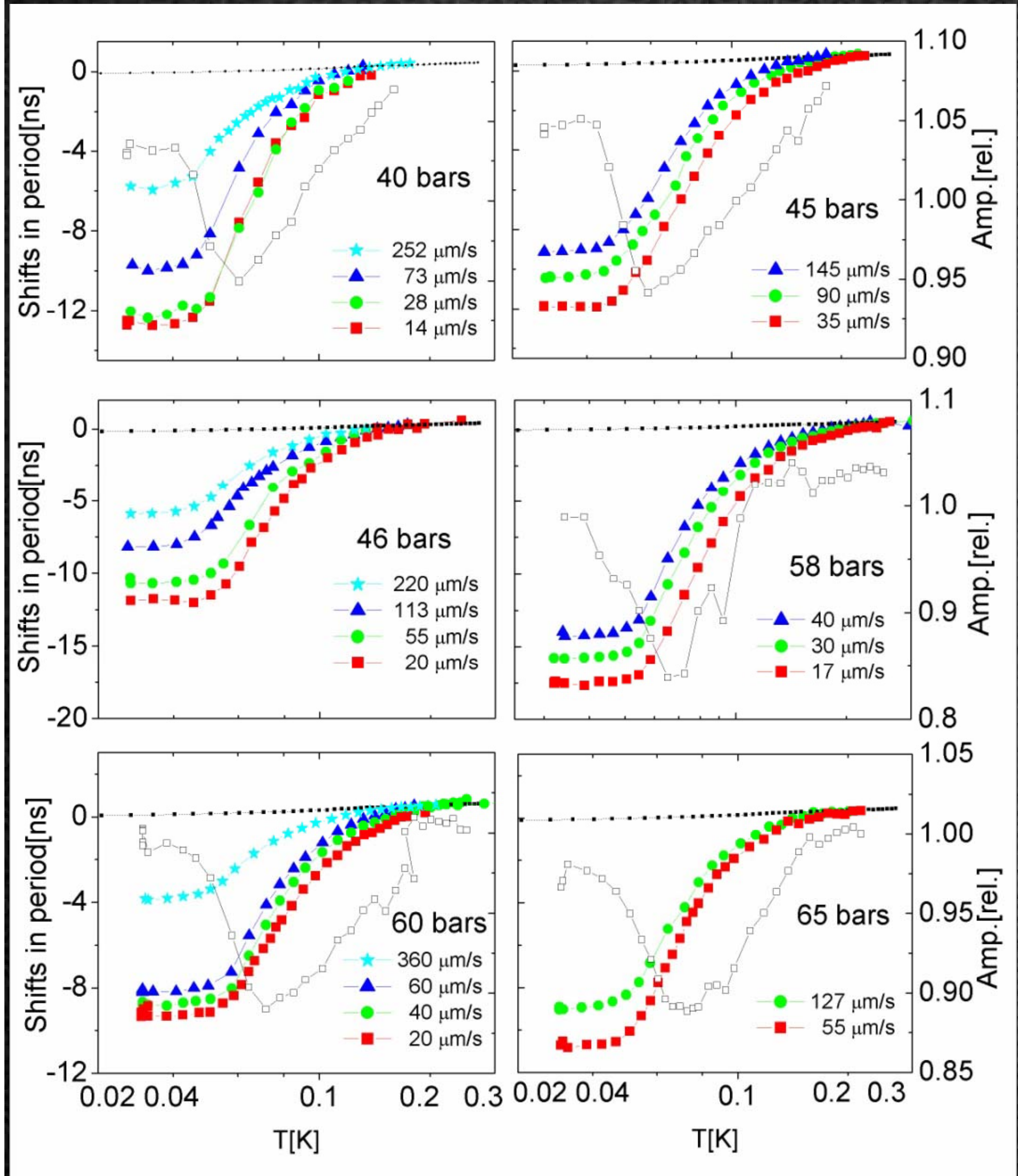

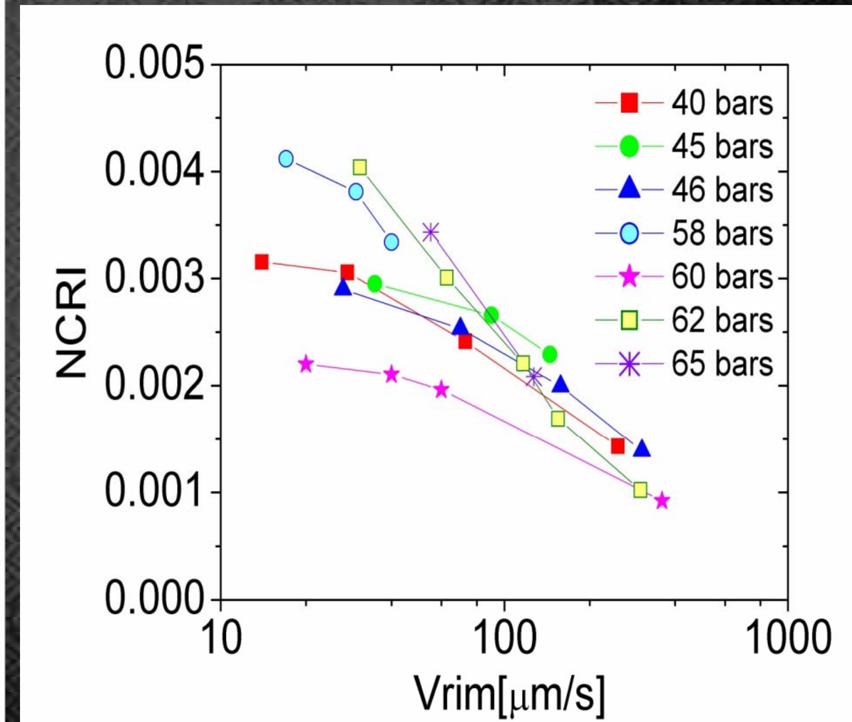

Control experiment: solid (bcc) ^{3}He

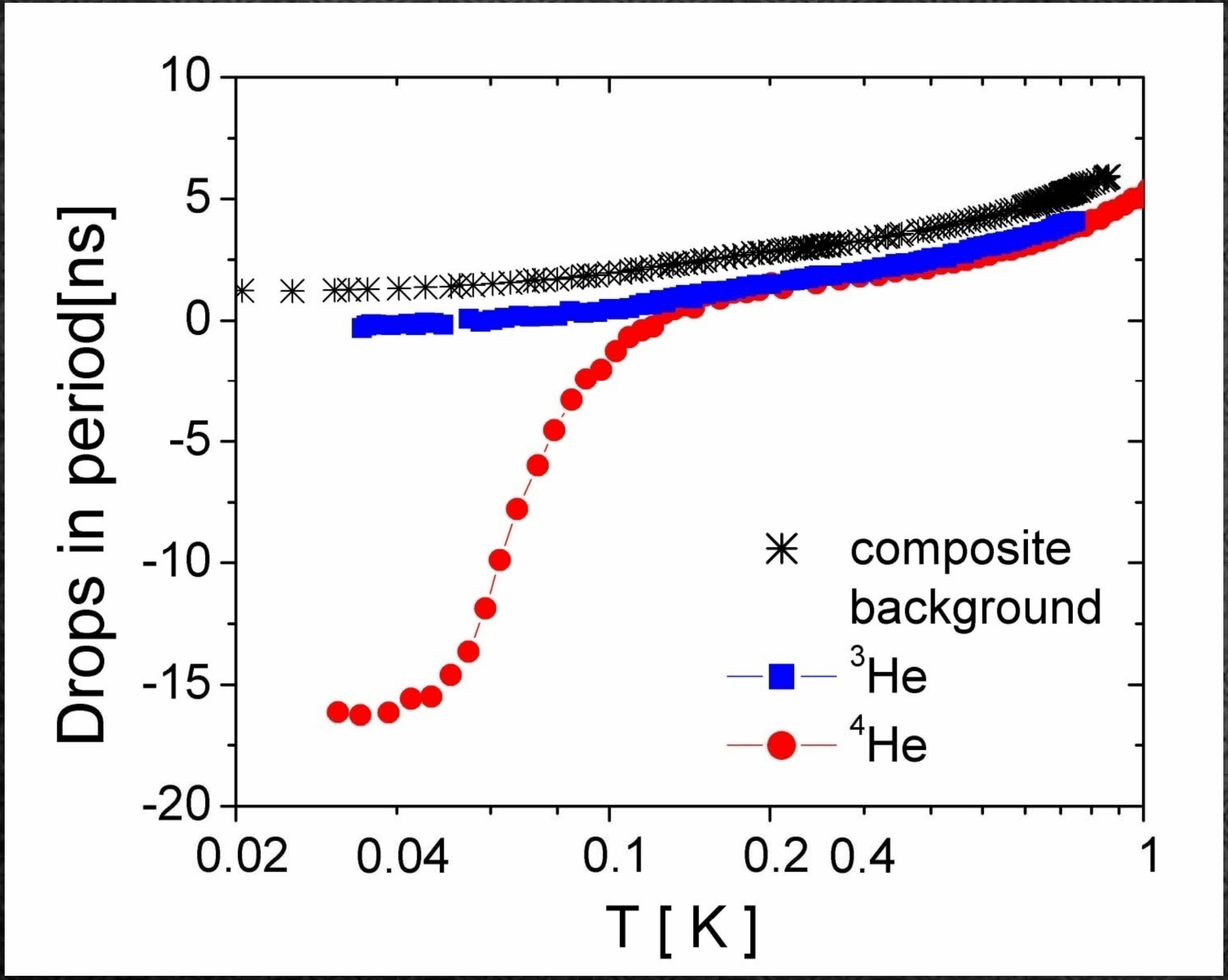

Effect of ^{3}He impurities

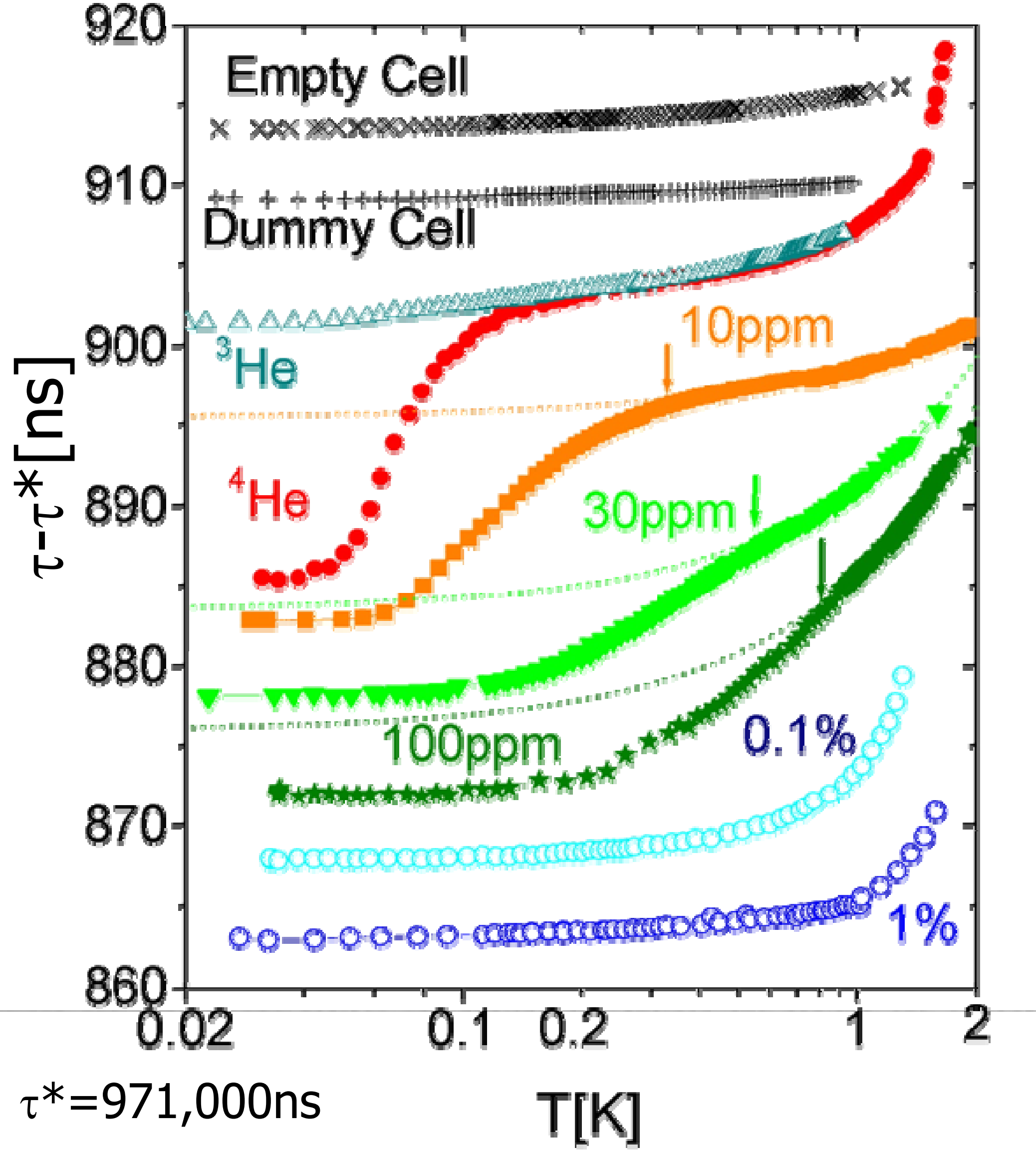

τ*=971,000ns

Data shifted vertically
for easy comparison

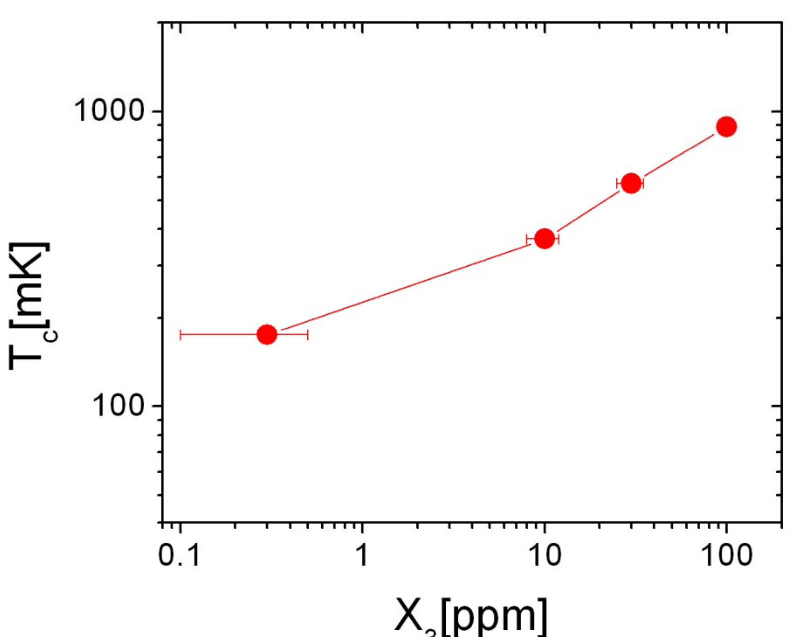

Bulk solid helium in annulus

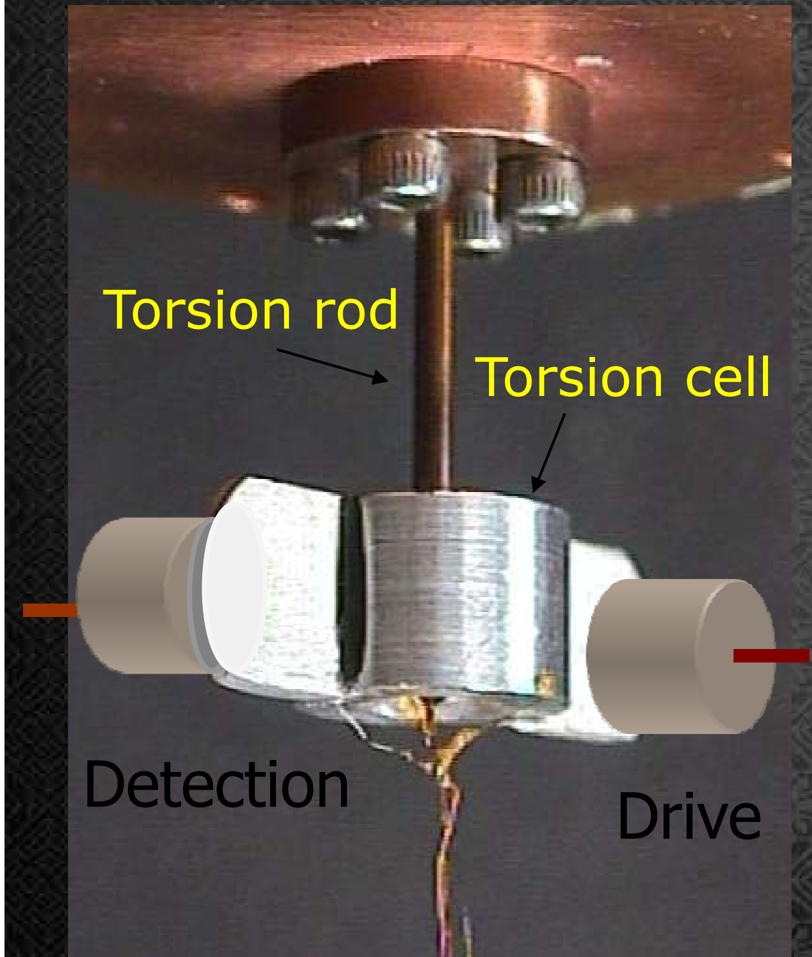

Torsion cell
with helium in annulus

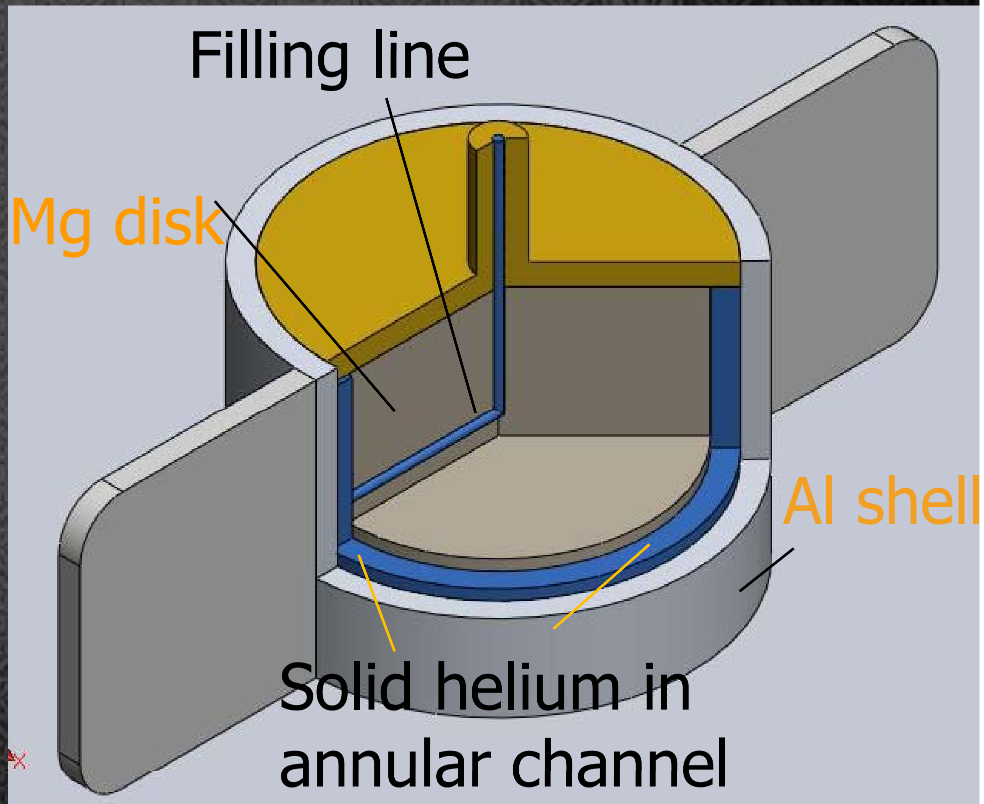

Superflow in bulk solid helium

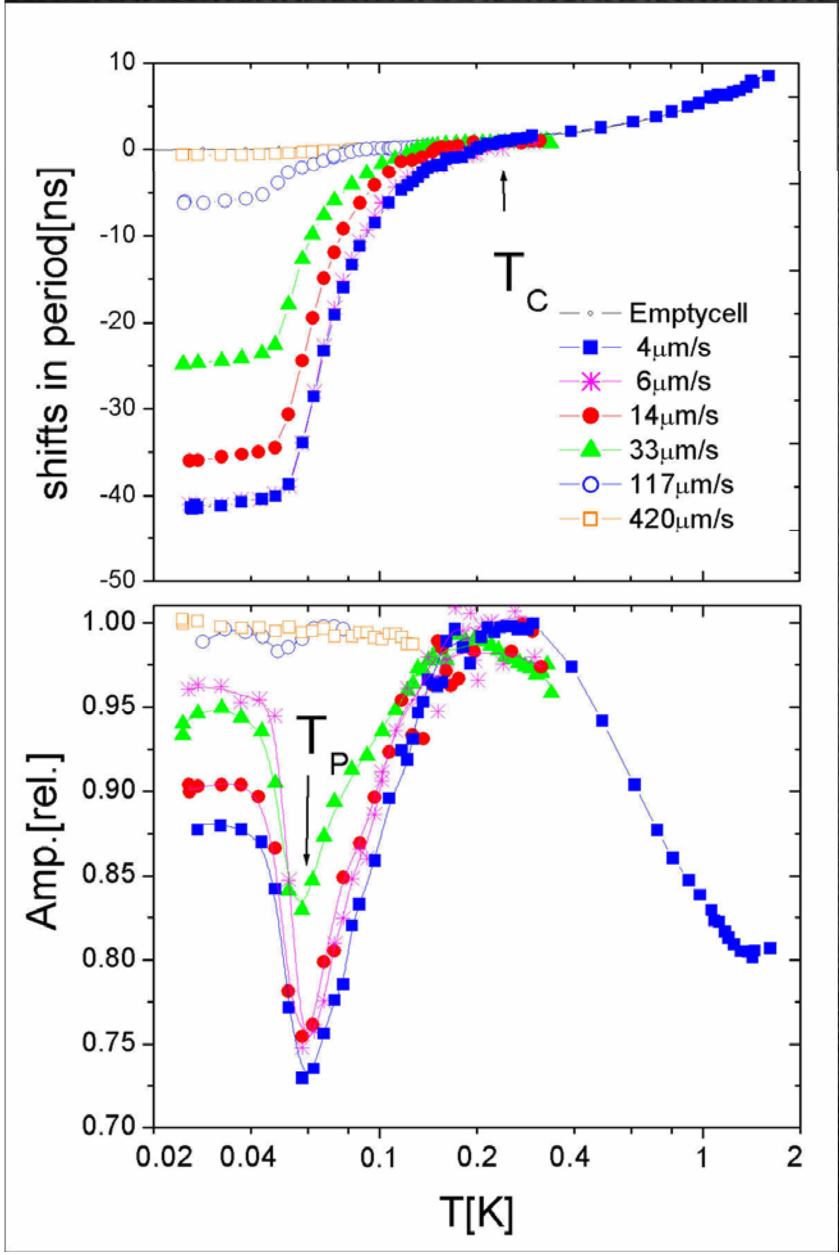

E. Kim and M. H. W. Chan, *Science* 305, 1941 (2004)

- ✓ Resonant frequency= 912 Hz
- ✓ Sample pressure 51bar
- ✓ Total mass loading = 3012ns
- ✓ Mass decoupling, $-\Delta\tau_o$=41ns
- ✓ NCRIF = 1.4%

Non-Classical Rotational Inertia Fraction

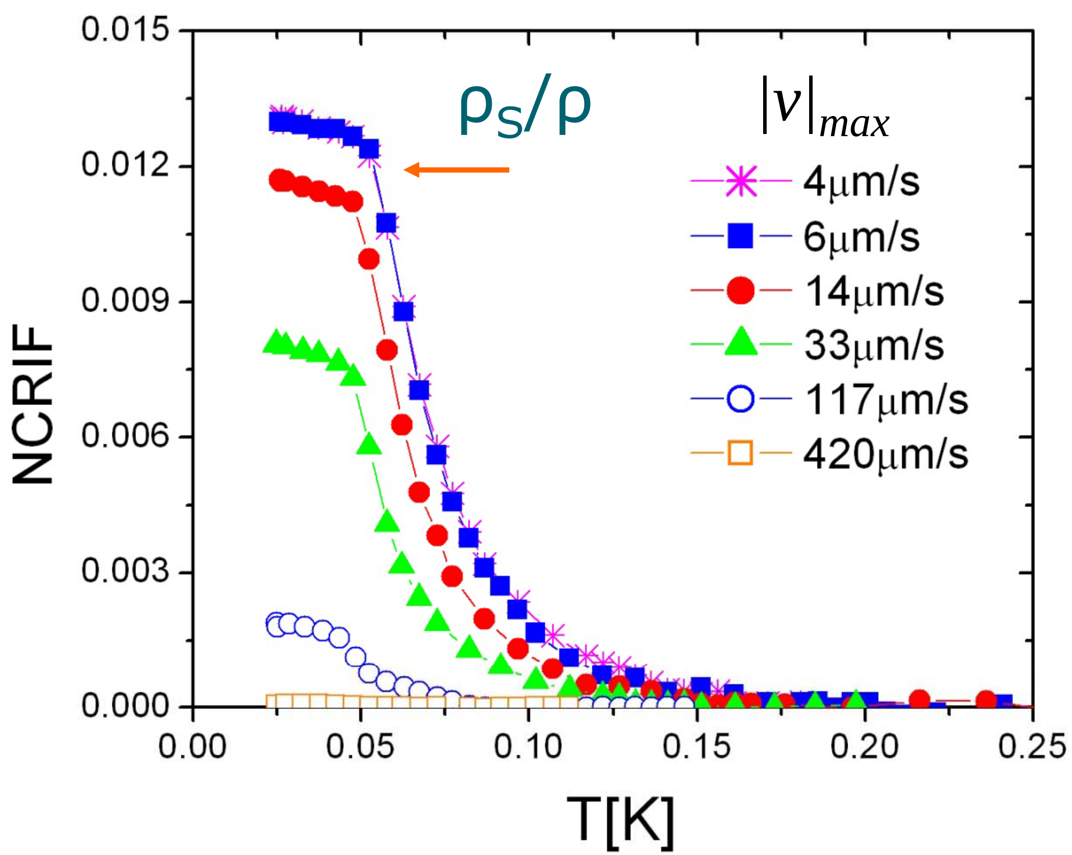

$$NCRIF = \frac{\Delta\tau}{\text{total mass loading}}$$

Total mass loading
=3012ns at 51 bars

Solid ^4He at various pressures show similar temperature dependence, but the measured supersolid fraction shows scatter with no obvious pressure dependence

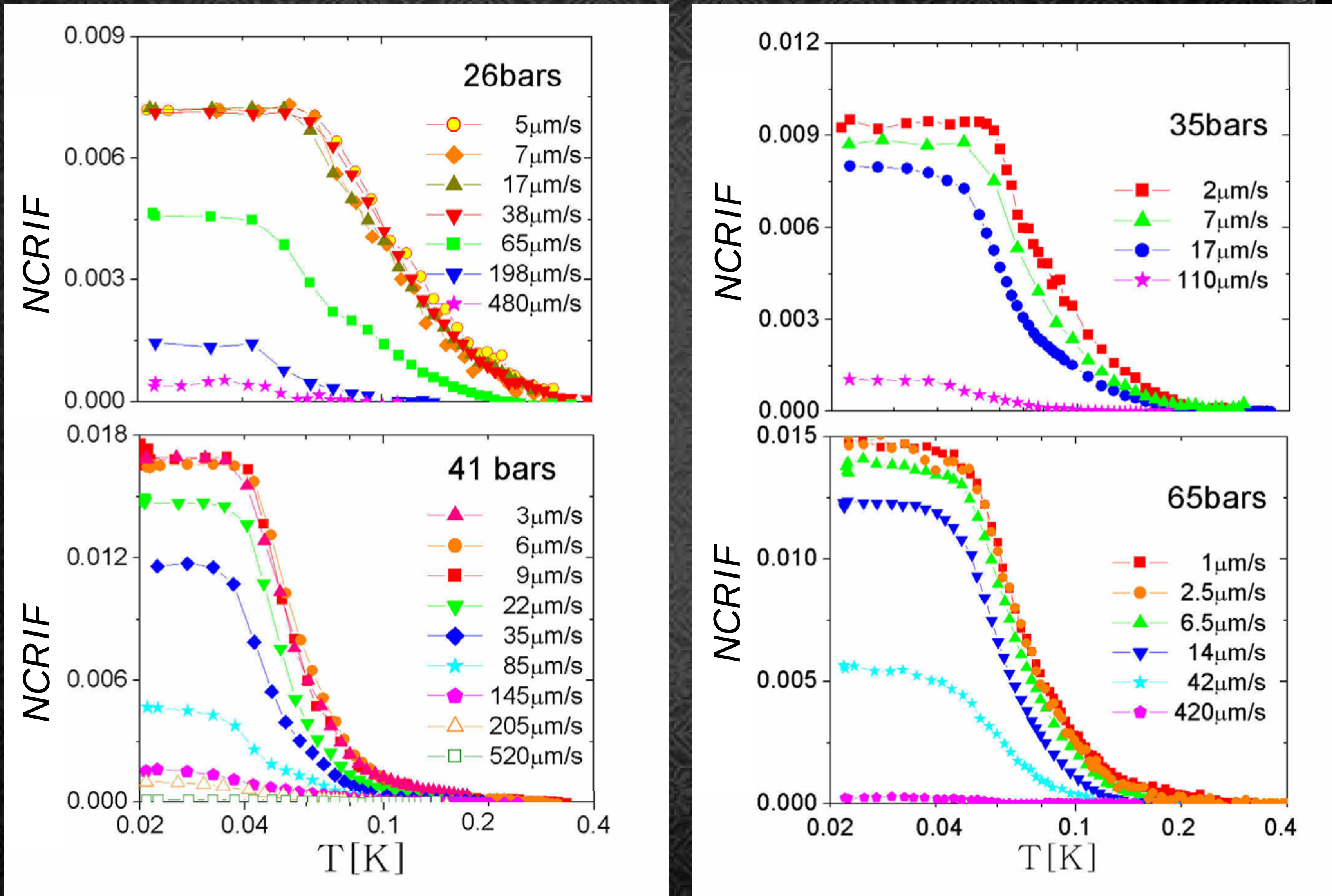

Pressure dependence of NCRI

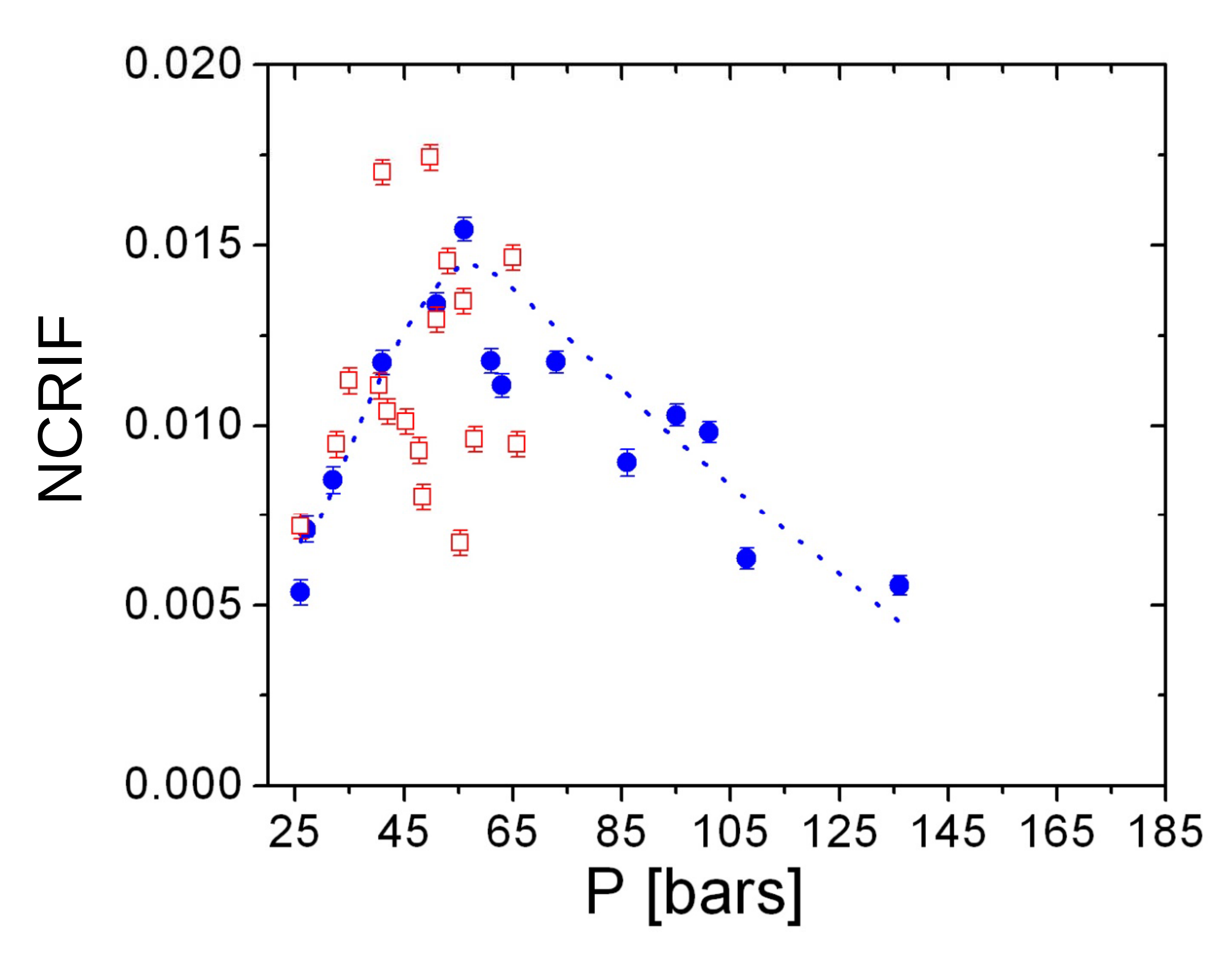

Blue data points were obtained by seeding the solid helium samples from the bottom of the annulus.

What are the causes of the scatter in NCRIF?

Scatter in NCRIF is larger In bulk than in Vycor!

Strong and ‘universal’ velocity dependence in all annular samples

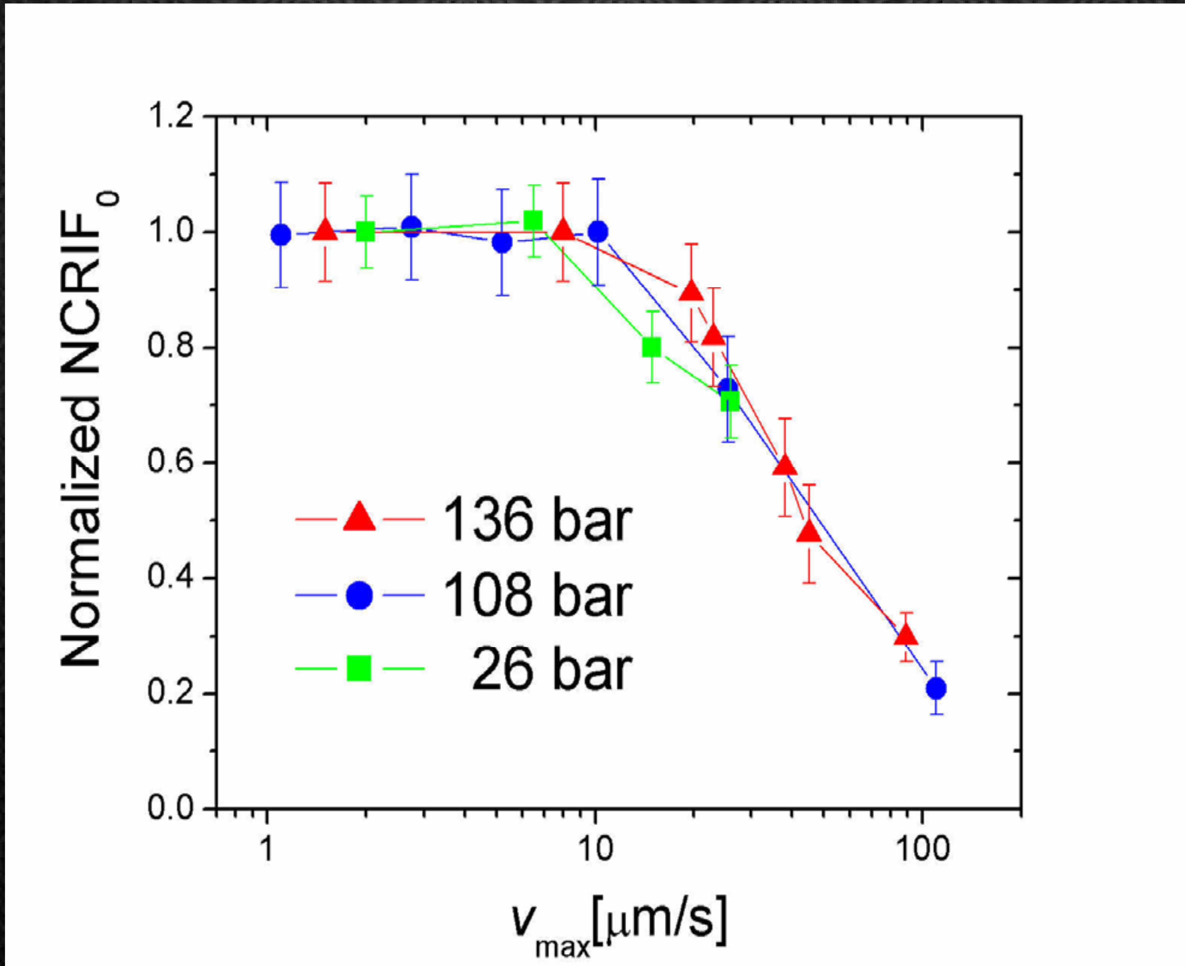

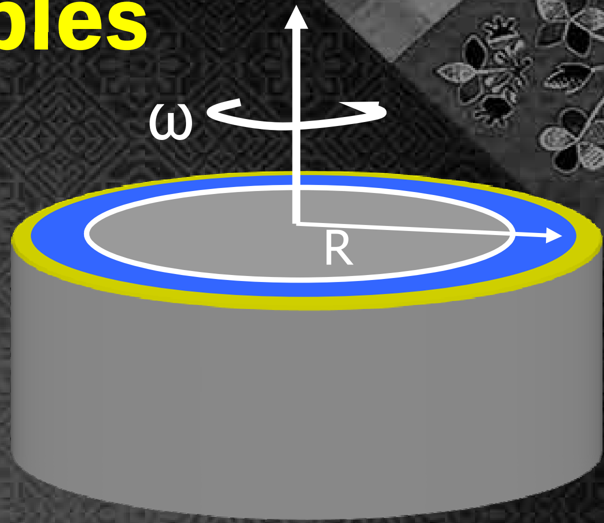

$v_C \sim 10\mu m/s$

$$\oint v_s \, dl = \frac{h}{m} \cdot n$$

$$v_s = \frac{h}{2\pi R m} \cdot n$$

$=3.16\mu m/s$
for $n=1$

Evidence of vortices ?
V_c is larger for cylindrical samples

Control experiment: blocked annulus

With a barrier in the annulus, there is no simple superflow and the measured superfluid decoupling should be vastly reduced

Torsion cell
with helium in annulus

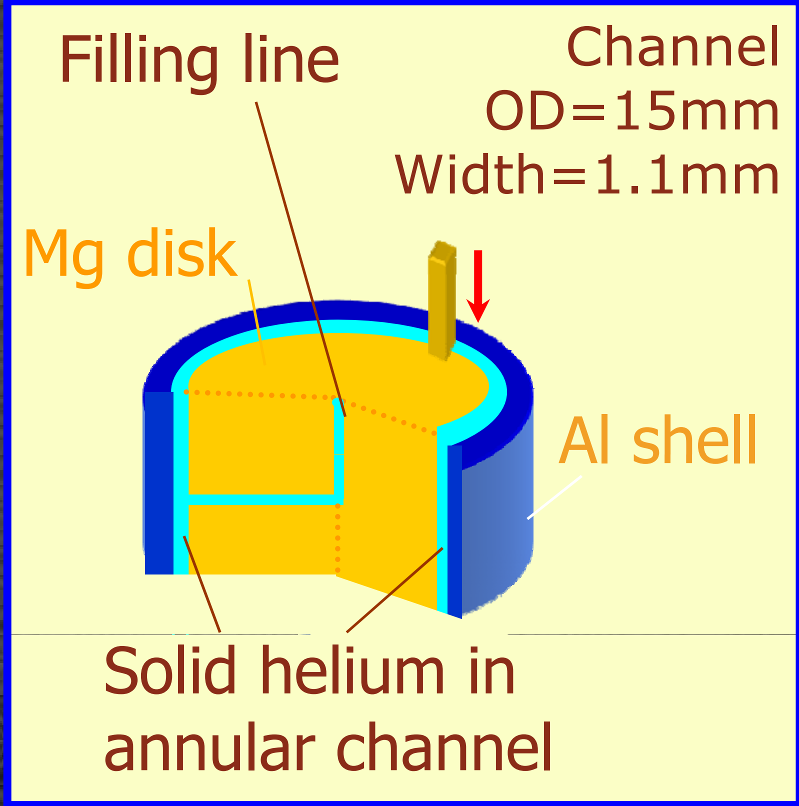

Irrotational Flow

- Superfluids exhibit potential (irrotational) flow
  - For our exact dimensions, NCRIF in the blocked cell should be about 1% that of the annulus*

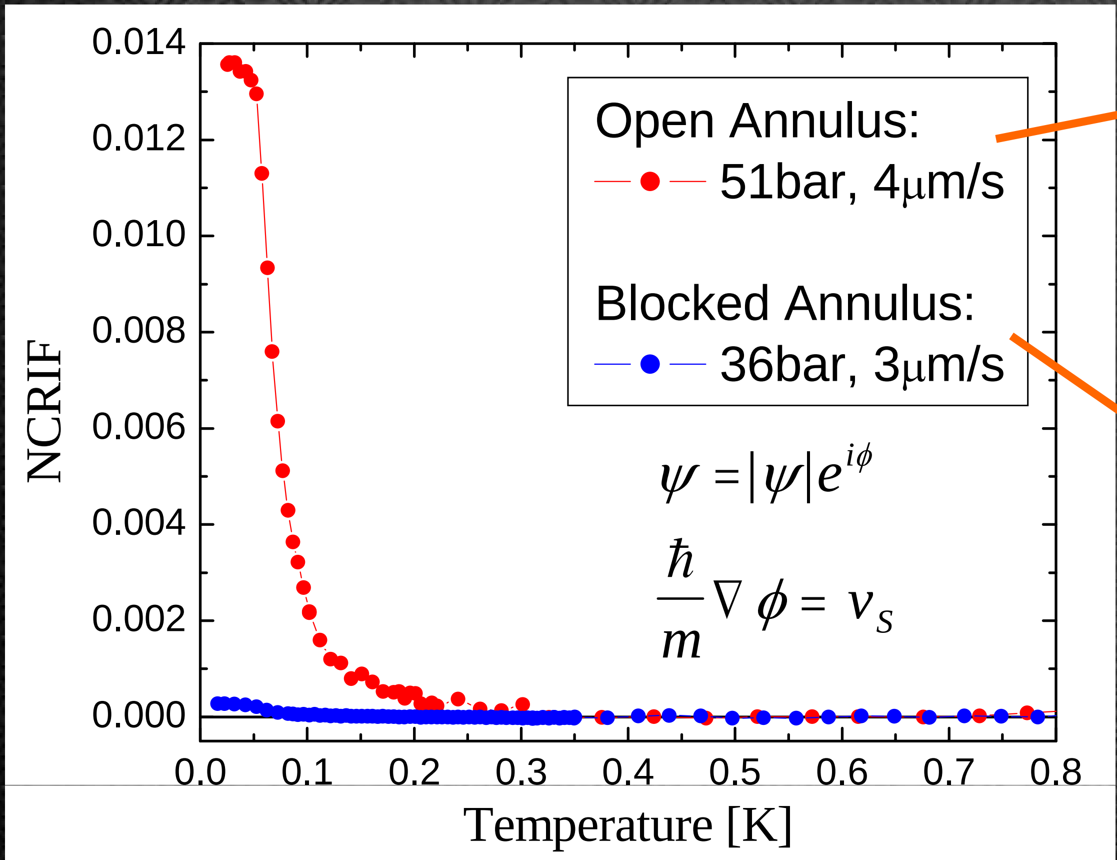

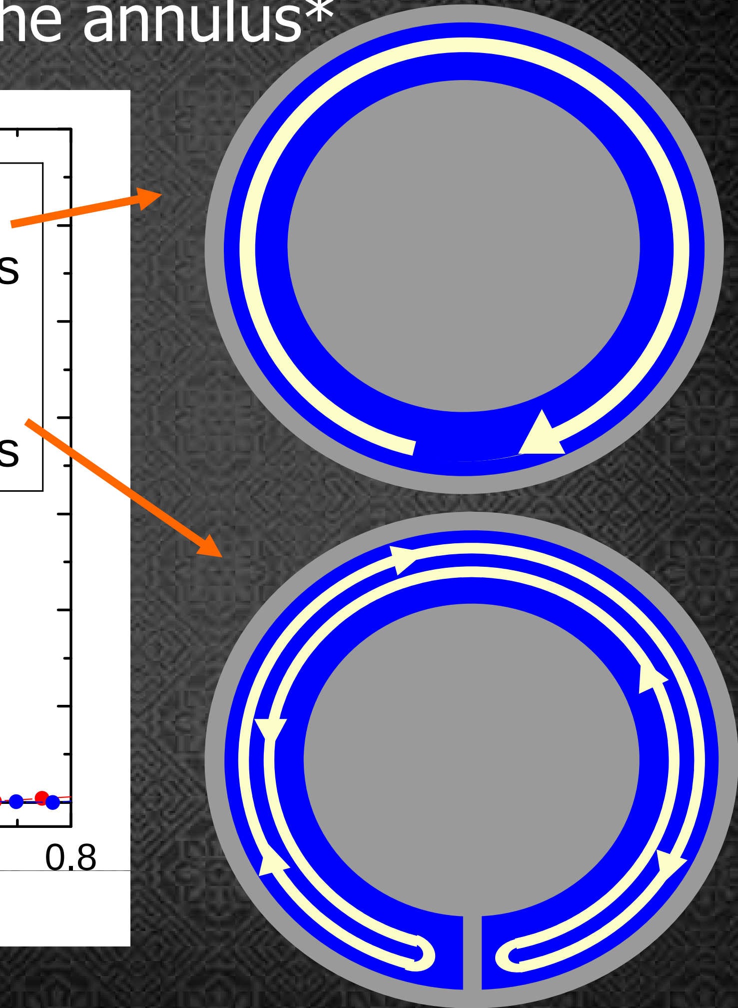

*E. Mueller, private communication.

Reversibly blocked annulus

Rittner & Reppy at Cornell

Blocked cell

Solid inertia

Open cell

Nonclassical rotational inertia

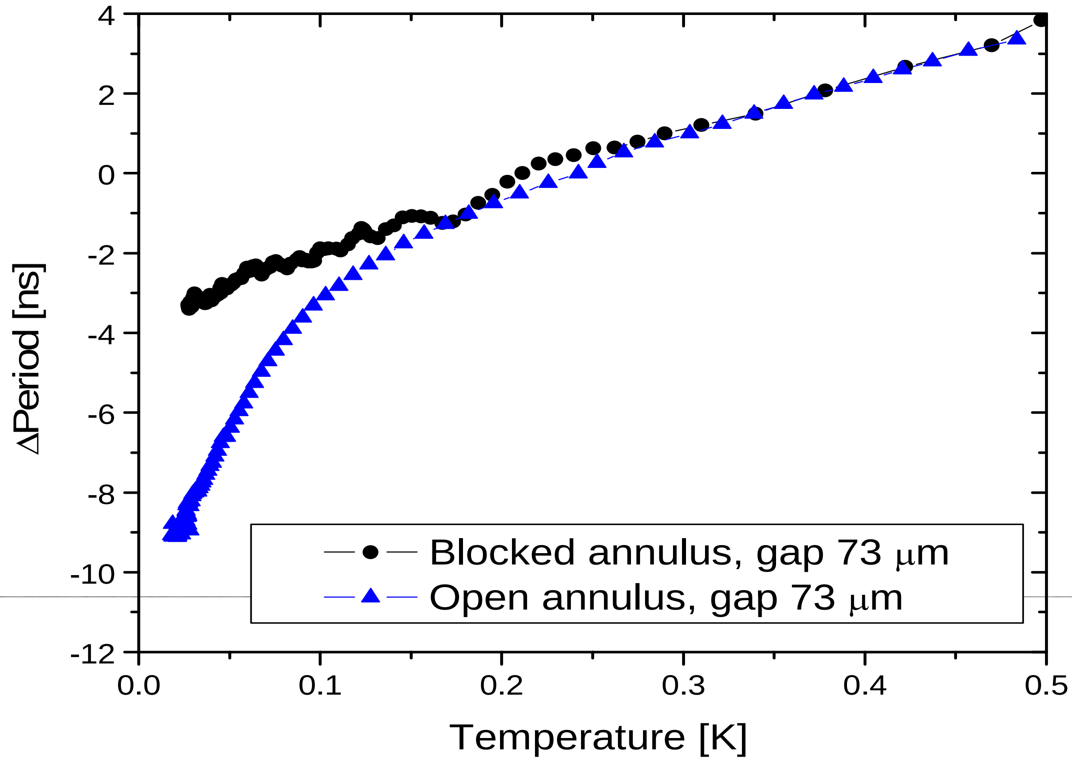

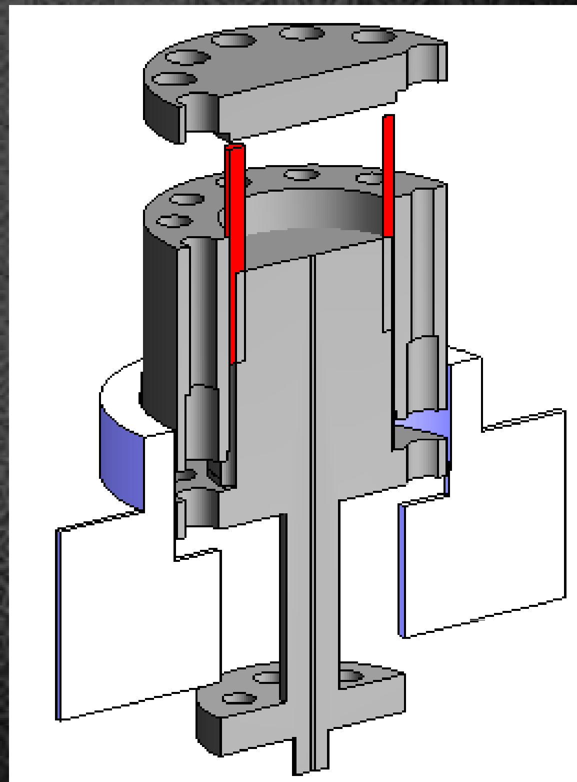

NCRI has been reproduced by

- Reppy group
  - Disorder & Supersolidity: annealing and confinement effect
- Shirahama group
  - NCRI in nano pores & 2D supersolid on Grafoil
- Kubota group
  - Solid helium under rotation: New vortex state ?
- Kojima group
  - Frequency dependence & hysteresis
- Kim Group at KAIST

Recent experiments other than TO

- DC flow
  - NO pressure driven flow by Beamish group
  - $\Delta\mu$ driven flow at LS coexistence through liquid channel by Balibar group
  - Umass Sandwich by Hallock gorup
    High P Liquid in Vycor – Solid – High P Liquid in Vycor
- Pressure measurements
  - No anomaly on L-S boundary at low temperature: $P \sim T^4$
  - Extra T^2 dependent term detected away from melting boundary
- Neutron scattering and X-ray diffraction
  - The resolution is marginal to see the effect
- Shear modulus measurement
  - Frequency, ^{3}He impurity, temperature dependence, & hysteresis qualitatively similar to NCRI

Heat Capacity signature

X. Lin, A. C. Clark, and M. H. W. Chan, Nature **449**, 1025(2007)

- Deviation from Debye solid T^3 dependence
- Coincide with NCRI

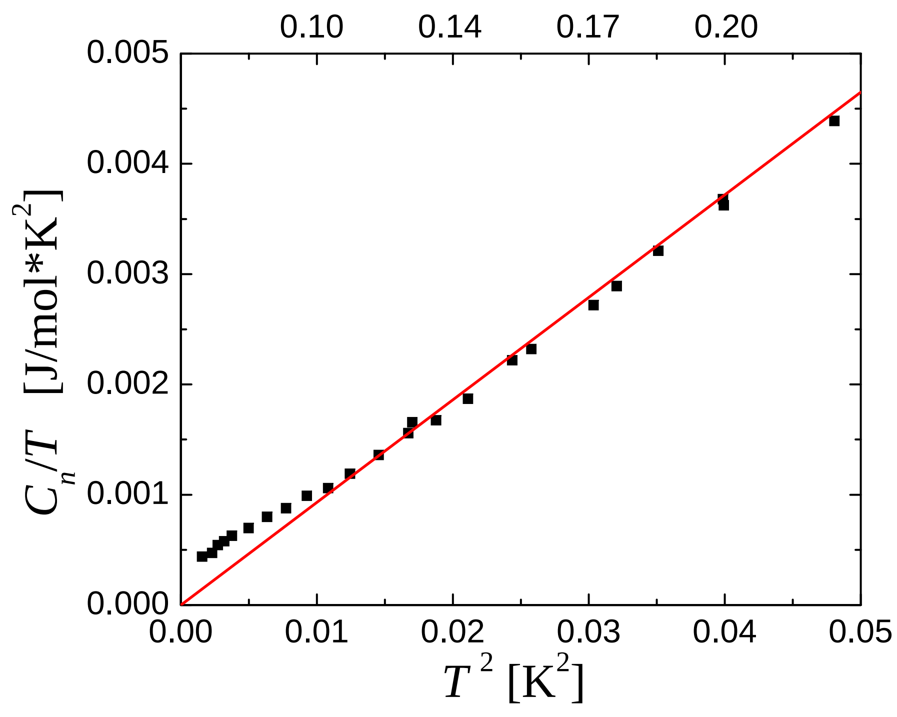

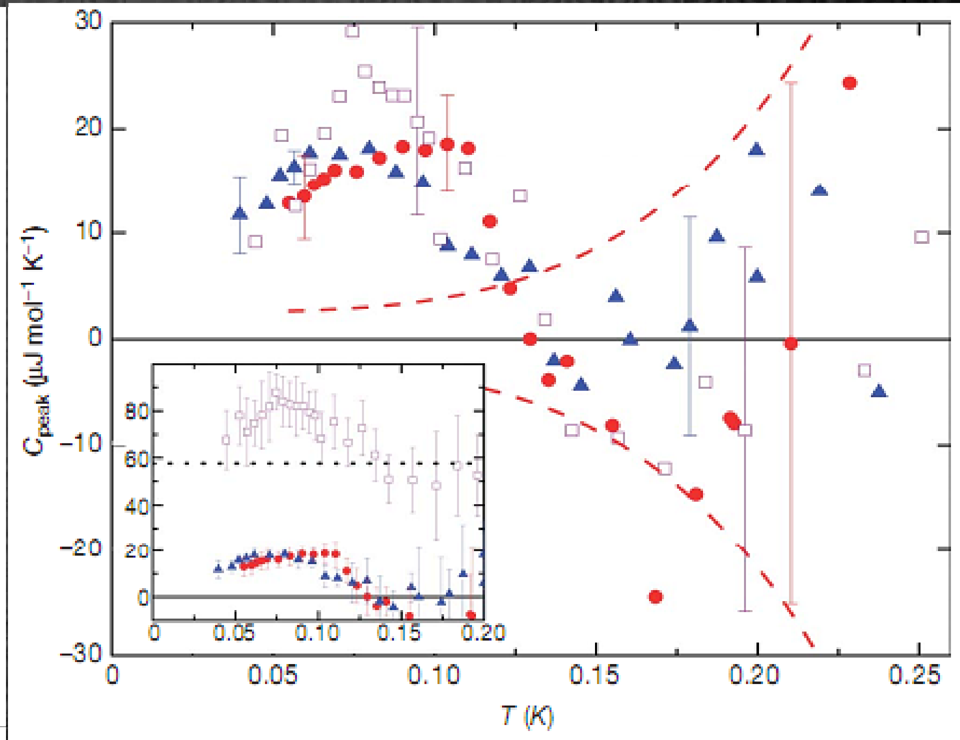

Summary 1.

NCRI observed in solid helium below ~ 0.2K

Temperature dependence reproducible,
but NCRIF varies by 3 orders of magnitude.

Strong velocity dependence observed

The addition of 3He impurities enhances the onset.

Part 2

^{3}HE EFFECTS

Dislocations and NCRI

Kim, Xia, West, Xi, Clark, and Chan

^{3}He Impurity effect (in Vycor)

E. Kim & M.H.W. Chan Nature **427**, 225 (2004)

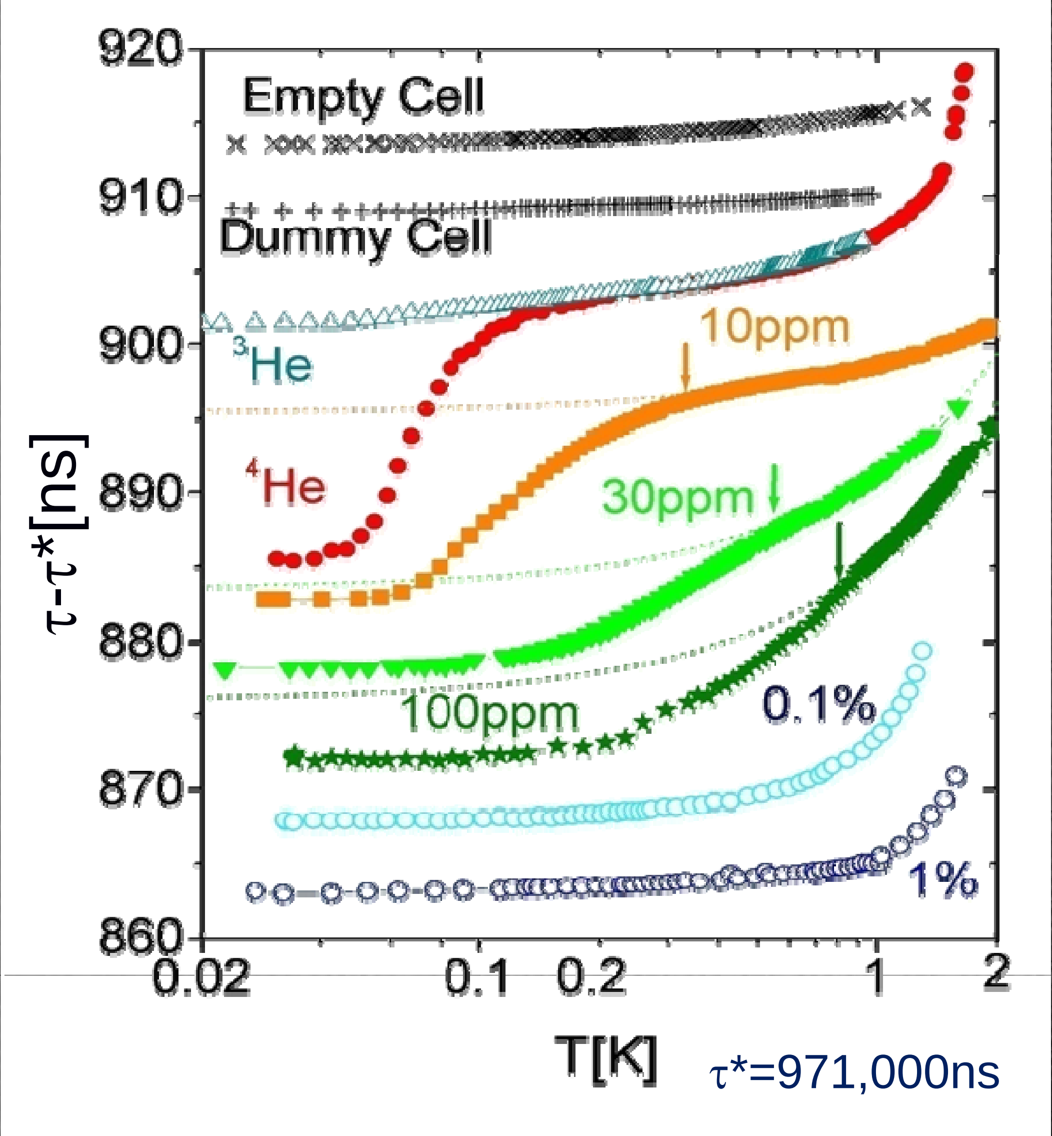

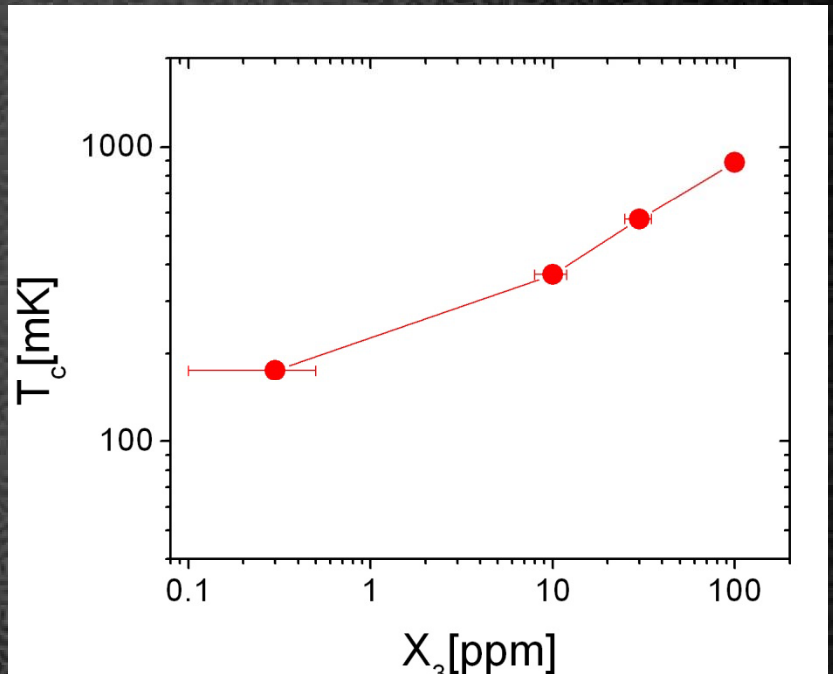

Data shifted vertically for easy comparison

Two torsional oscillators for ^{3}He dependence studies

	Open Cylinder TO1	Open cylinder TO2
Confining dimension	0.7cm	1 cm
A/V (cm^2/cc)	5.9	7.2
Resonant Frequency	783Hz	1298Hz
Covered X_3 concentration	47ppb - 30ppm	1ppb-100ppb

Isotopically-pure* ^{4}He (*X_3<1ppb)

This work is done in the B/T facility of the high magnetic field lab.
Dr. Xia (University of Florida)

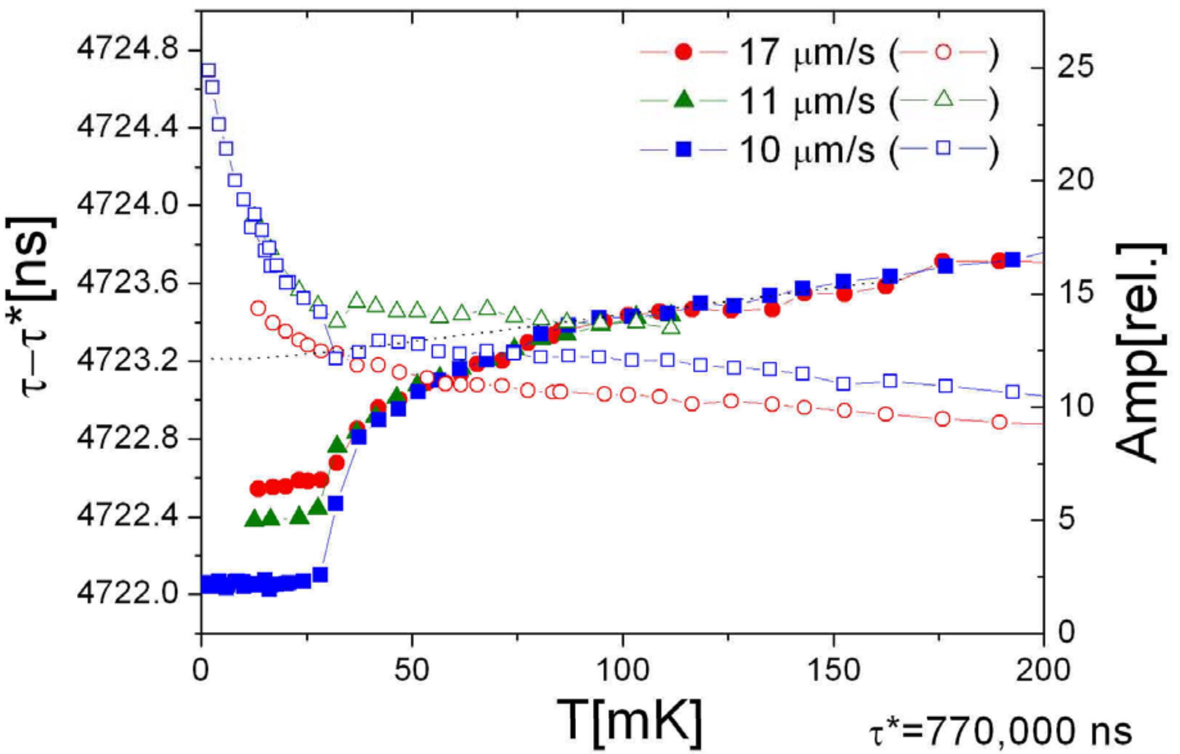

Total mass loading due to solid helium
$\tau_{He}-\tau_{empty}$=3939ns

Shift in the period
$\Delta\tau$=1ns

Supersolid fraction
~1ns/3939ns
~0.025%

Torsional oscillator
f_0= 1298Hz, Q~1x10^6

Effects of ^{3}He impurities In bulk solid samples in cylindrical torsion cells

Kim et. al, PRL 100,065301 (2008)

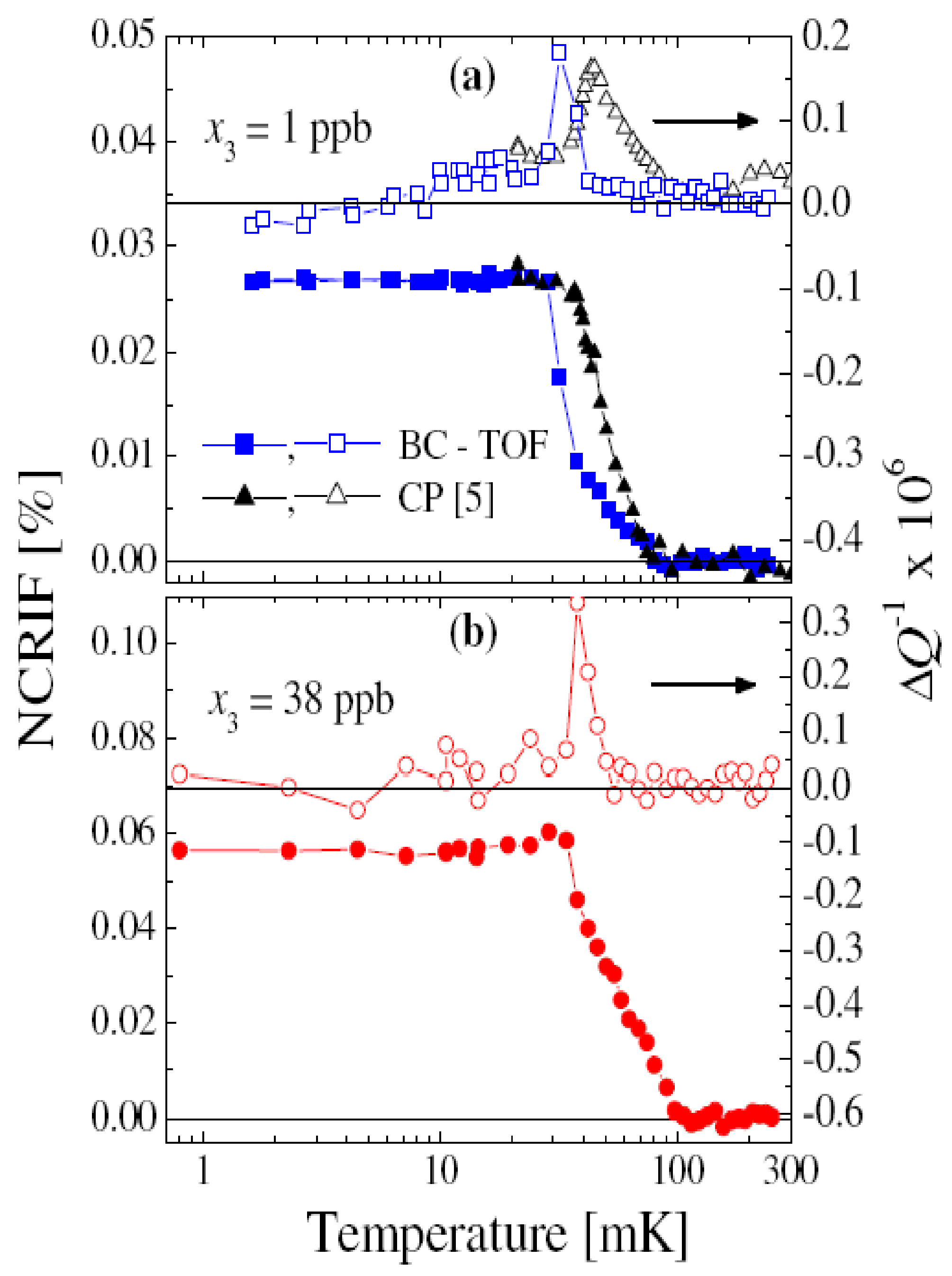

Effects of ^{3}He impurities

Addition of ^{3}He

1) enhances the onset of NCRI
2) broadens transition (longer high temperature tale)

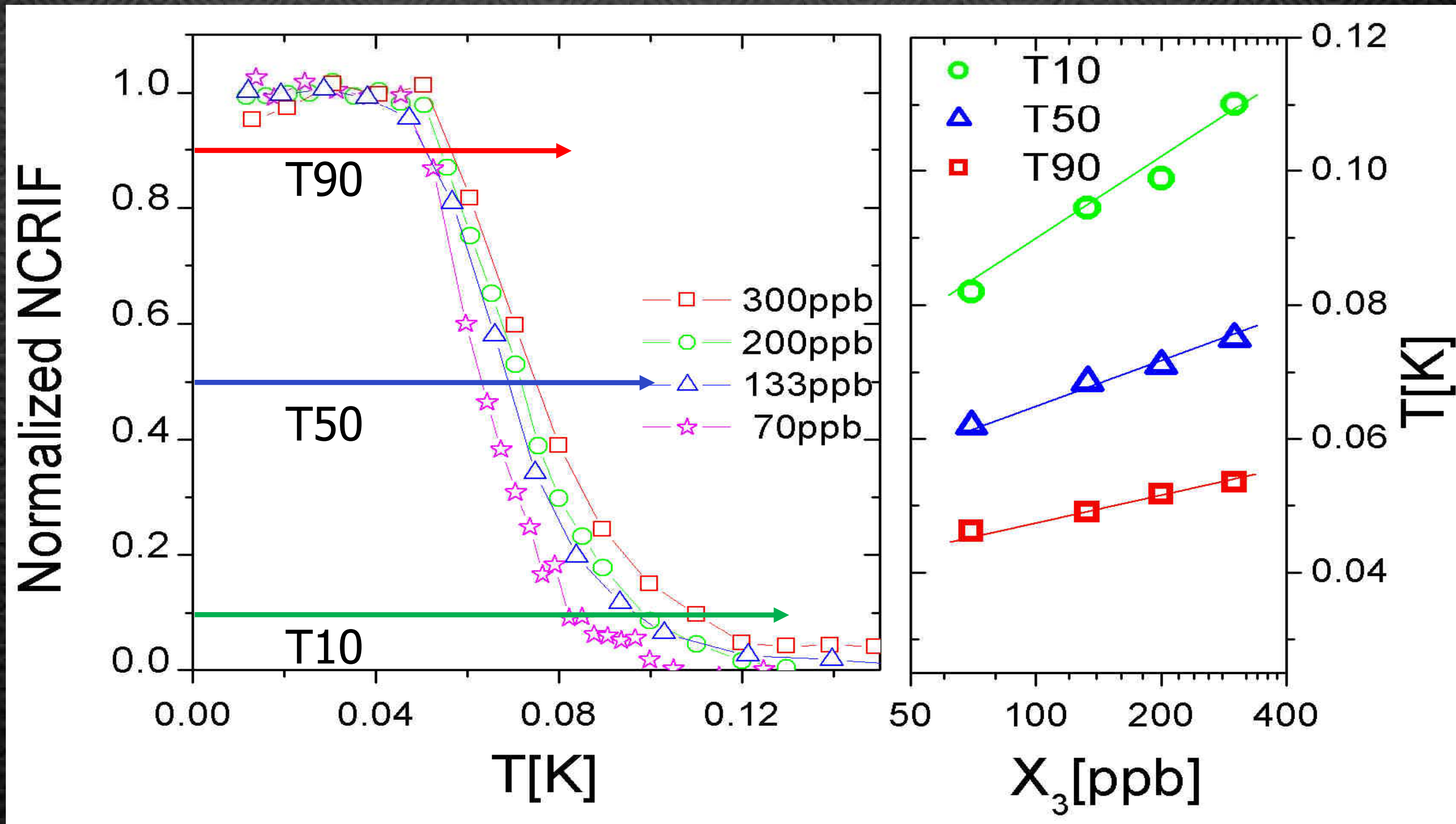

NCRI marches up to higher temperature with increasing ^{3}He concentration.

Effect of ^{3}He impurities in bulk samples

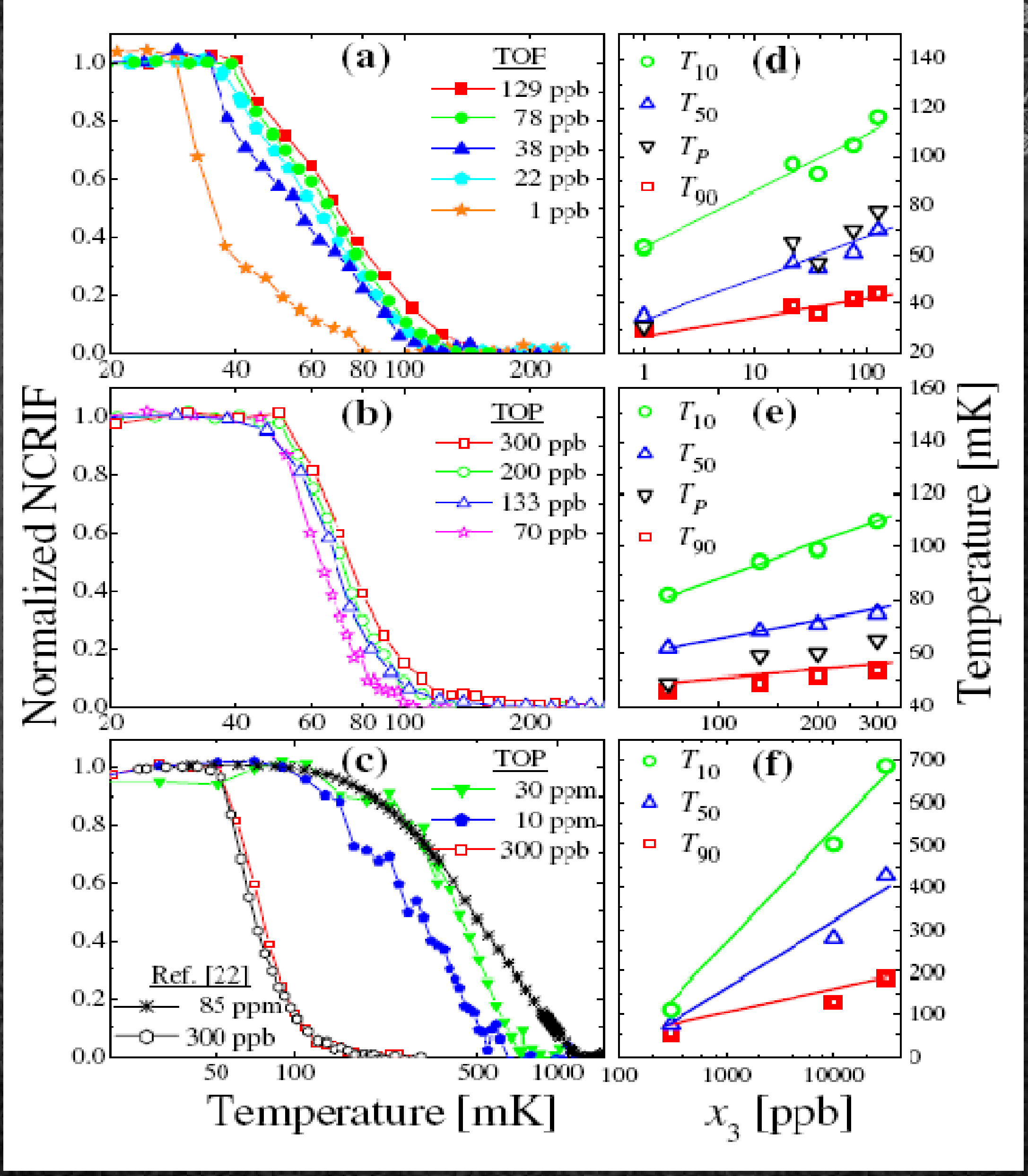

Onset T vs. ^{3}He impurities

Kim et. al, PRL 100,065301 (2008)

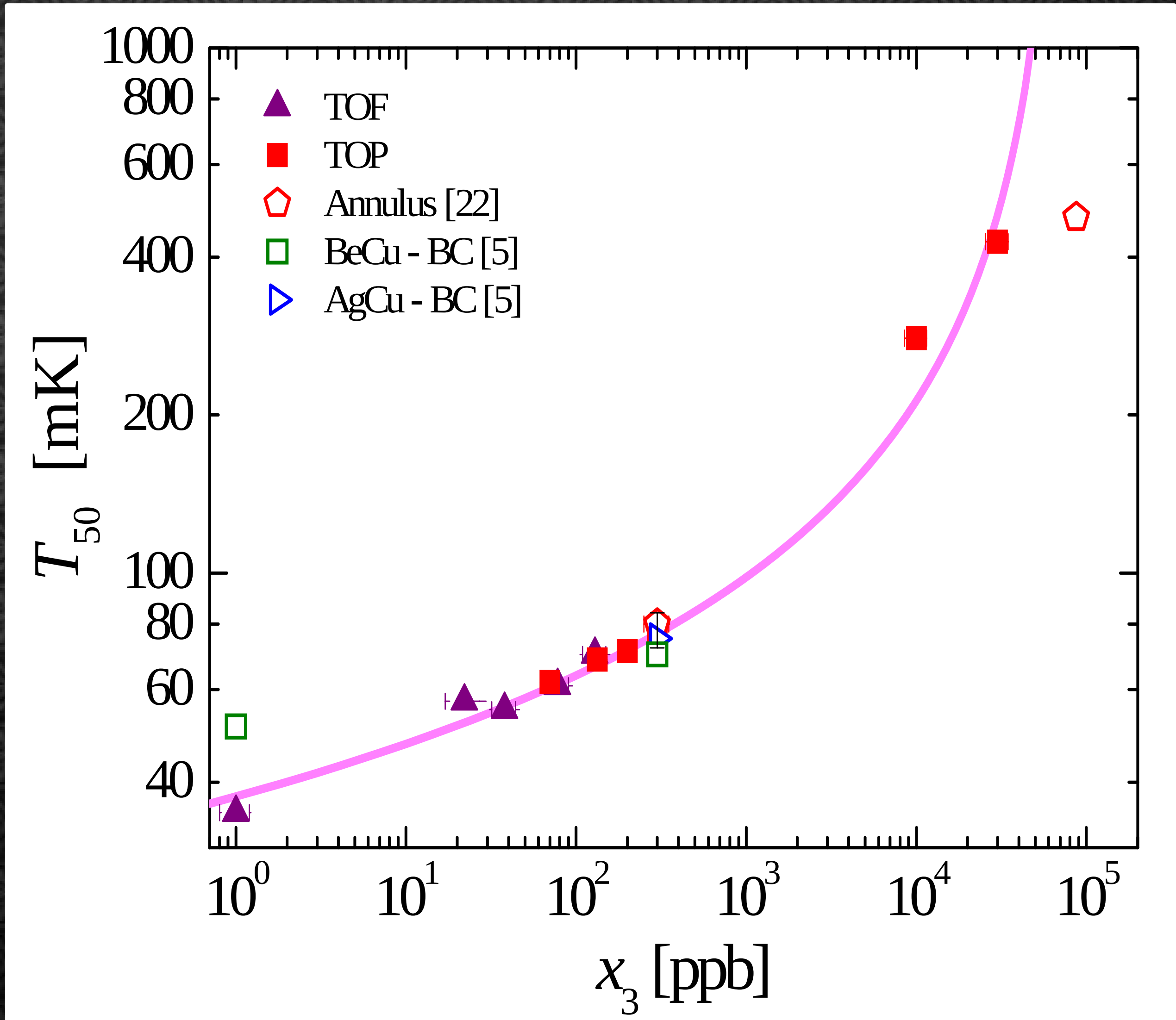

Observations

- Strong ^{3}He impurity dependence

Only 1ppb of ^{3}He impurity introduces very dramatic change in the onset.

- Addition of ^{3}He enhances the onset temperature and broadens the transition

The characteristic behavior is very similar to the observed **^{3}He impurity pinning (by condensation) of the dislocation line**.

Dislocations

- Dislocation line is common defect in crystals
- Created by thermal and mechanical stresses

Two of the common types: edge & screw

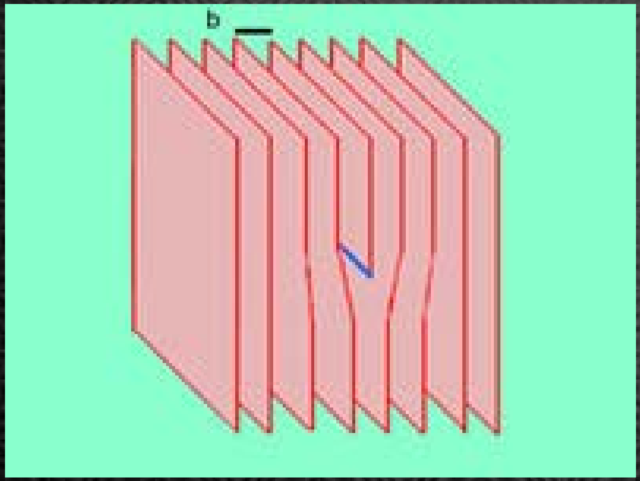

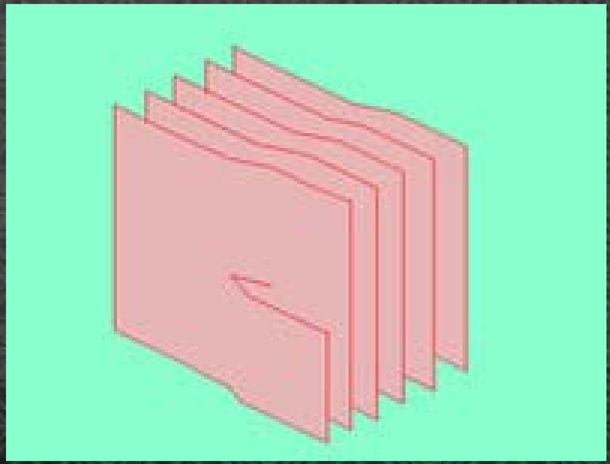

Dislocations

- Dislocation line is common defect in crystals
- Created by thermal and mechanical stresses

Dislocation density, Λ, : Total length of dislocation lines per unit volume. (cm^{-2})

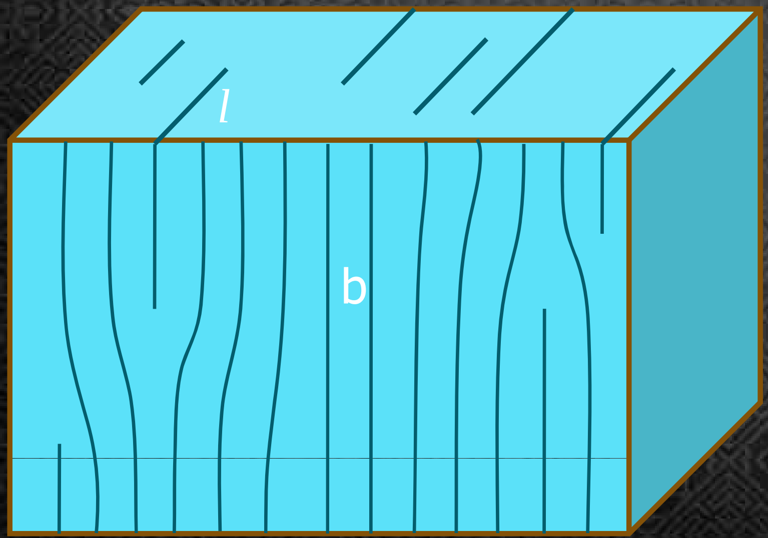

Dislocation lines form complicated networks and intersect at nodes which are localized.

Dislocations

❖The density of dislocations in crystals determined by an analysis based on the vibrating string model of dislocation.

$$\frac{\Delta v_d}{v_0} = R \int \frac{\Delta v(l)}{v_0} l N(l) dl$$

$$\alpha = R \int \alpha(l) l N(l) dl$$

Dislocations

- Information on Λ comes mostly from ultrasound attenuation measurements between 5 to 50 MHz.

$$\frac{\Delta v(l)}{v_0} = -\frac{4v_0^2}{\pi^3}\frac{\omega(l)^2-\Omega^2}{[\omega(l)^2-\Omega^2]^2+(B\Omega/A)^2}$$

$$\alpha(l) = \frac{4v_0}{\pi^3}\frac{\Omega^2 B/A}{[\omega(l)^2-\Omega^2]^2+(B\Omega/A)^2}$$

- Dislocation density in poor crystals ~ 10^9 per cm^2
- (constant volume[1])
- Dislocation density in good crystals ~ 10^5 - 10^7 per cm^2
- (constant pressure[2] or temperature[3] above ~ 0.5K)
- Dislocation density in best crystals ~ 0 to 100
- (constant temperature[4] growth below ~ 0.2K)

1. S.H. Castles & E.D. Adams, JLTP 19, 397 (1975).
2. I. Iwasa, K. Araki & H. Suzuki, J. Phys. Soc. Jap. 46, 1119 (1979).
3. V.L. Tsymbalenko, Low Temp. Phys. 21, 129 (1995).
4. J.P. Ruutu, P.J. Hakonen, A.V. Babkin, A.Ya. Parshin & G. Tvalashvili, JLTP 112, 117 (1998).

Granato-Lücke theory

◆ Dislocations intersect on a characteristic length scale of $L_N \sim 1 \rightarrow 5\mu m$

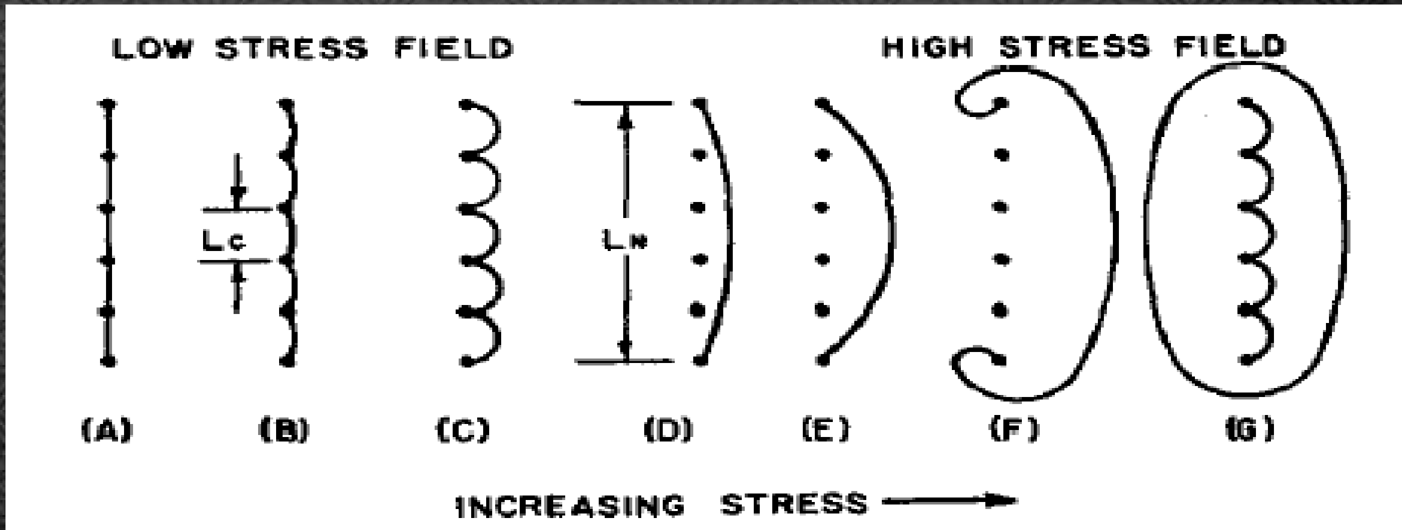

◆ ^{3}He atoms also can be detached

Break-away of ^{3}He impurities → Reduces shear modulus

Dislocation pinning

- Dislocation density, $\Lambda = 5 \sim 10^{10}\ cm^{-2}$

  Solid helium grown by a constant volume method; $\Lambda = 10^5$ to $10^9\ cm^{-2}$

- Dislocations intersect on a characteristic length scale of L_N

  (if $\Lambda \sim 10^5$ to$10^9\ cm^{-2}$)

  $0.1 < \Lambda L_N^2 < 0.3 \rightarrow L_N \sim 0.1$ to $10 \mu m$

- Dislocations can also be pinned by ^3He impurities

  $L_{IP} \sim$ Distance between ^3He atoms

^{3}He and dislocation

- Actual ^{3}He concentration on dislocation line is thermally activated

$$x_3 = x_0 \exp\left[\frac{W_0}{T}\right]$$

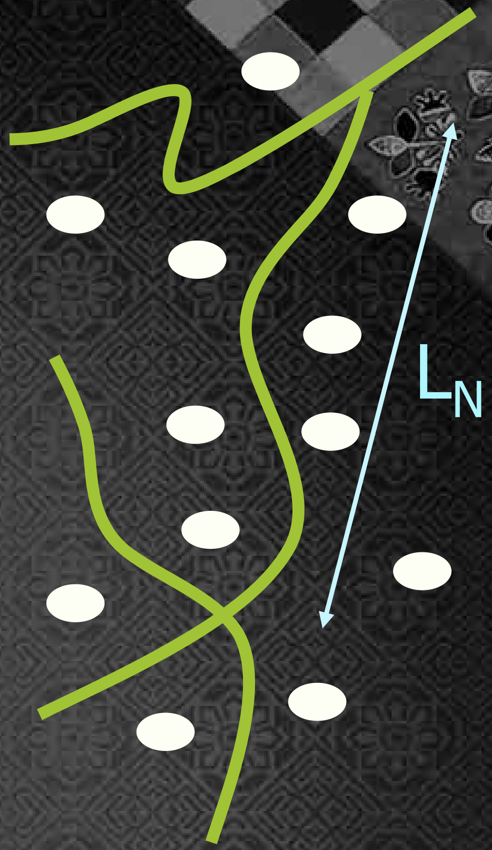

^{3}He and dislocation

- Actual ^{3}He concentration on dislocation line is thermally activated

$$x_3 = x_0 \exp\left[\frac{W_0}{T}\right]$$

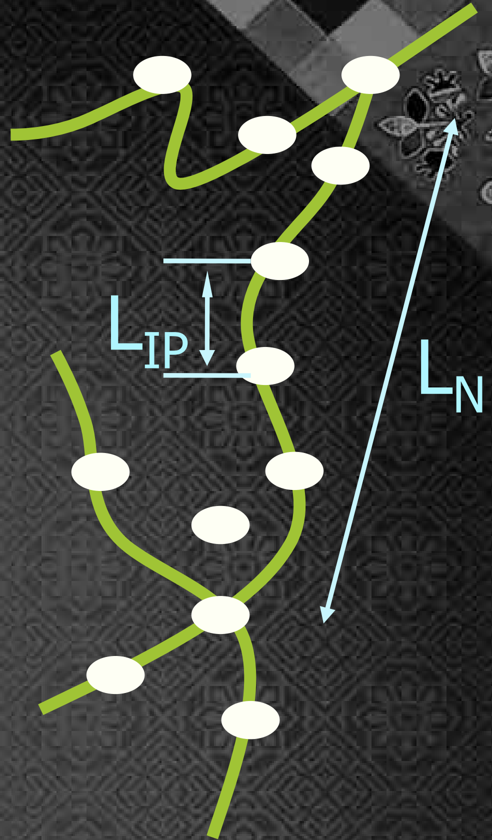

*Typical binding energy is very small , W_0 is 0.3K to 0.7K

^{3}He and dislocation

- Actual ^{3}He concentration on dislocation line is thermally activated

$$x_3 = x_0 \exp\left[\frac{W_0}{T}\right]$$

*Typical binding energy is very small , W_0 is 0.3K to 0.7K

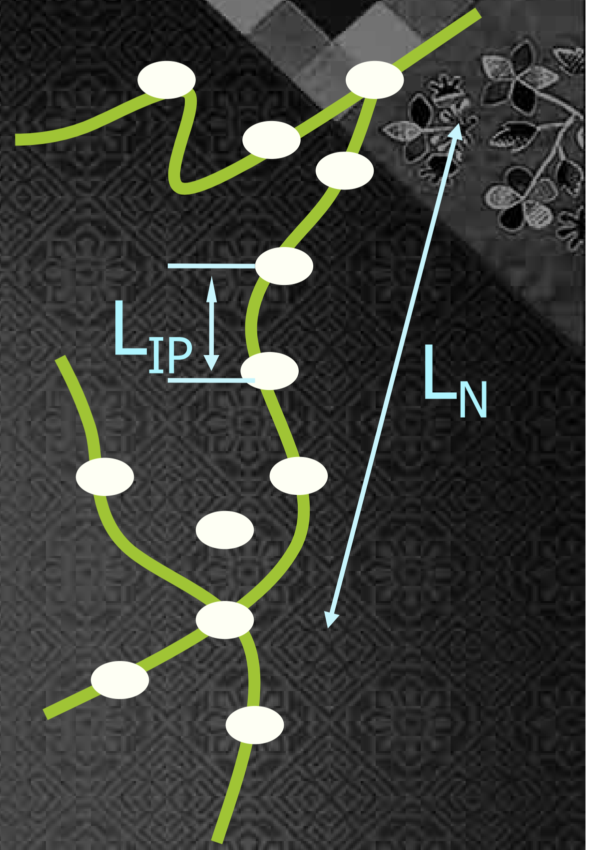

- Pinning length due to ^{3}He impurity

$$L_{IP} = (4\mu)^{1/3} b^2 W_0^{-1/3} x_0^{-2/3} \exp\left[-\frac{2W_0}{3T}\right]$$

^{3}He-dislocations interaction

Line was drawn by considering W_0=0.42K and average L_{IP} pinning length~ 1.9μm.

Smaller lengths are expected for larger dislocation densities

$$T_{IP} = -2W_0 \left(\ln \left[\frac{x_3^2 L_{IP}^3 W_0}{4\mu b^6} \right] \right)^{-1}$$

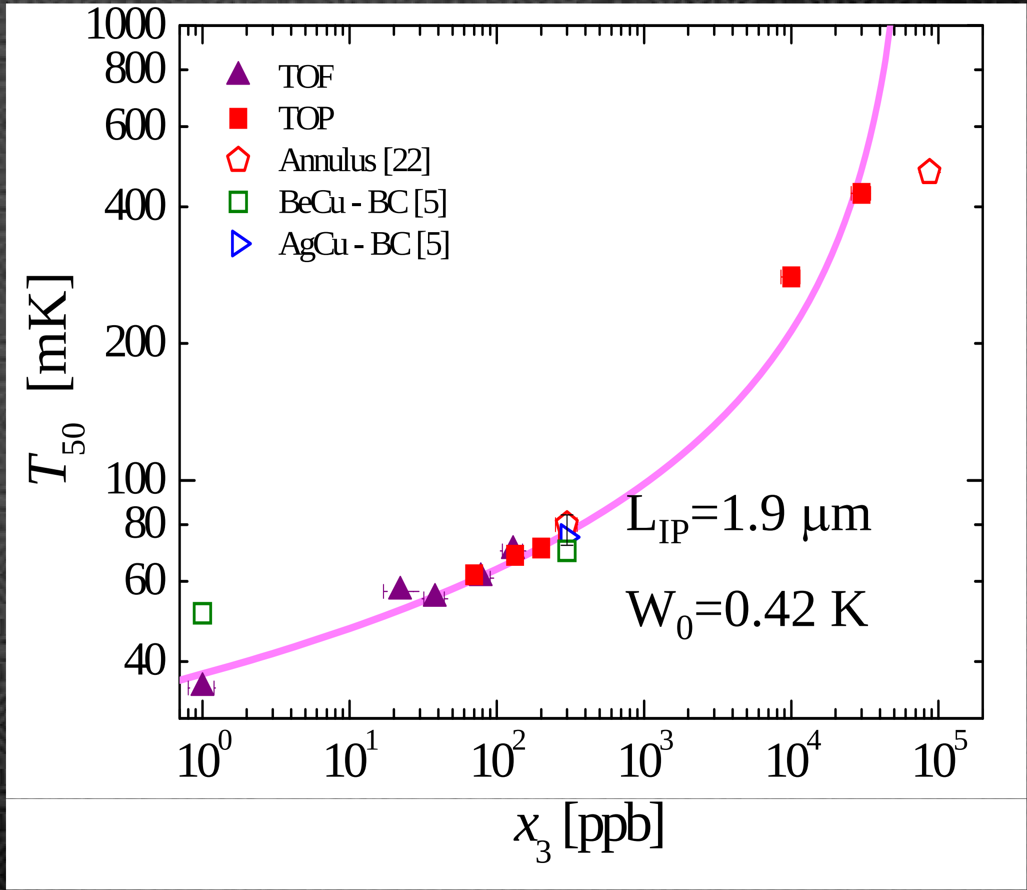

L_{IP} ^{3}He pinning length
μ, shear modulus,
b, Burger's vector

Kim et al, Phys. Rev. Lett 100, 065301 (2008)

^{3}He-dislocations interaction

Line was drawn by considering W_0=0.42K and average L_{IP} pinning length~ 1.9μm.

$$T_{IP} = -2W_0\left(\ln\left[\frac{x_3^2 L_{IP}^3 W_0}{4\mu b^6}\right]\right)^{-1}$$

Smaller lengths are expected for larger dislocation densities

→ cross-over from network pinning to ^{3}He pinning

T_{50}~T_P : Below this temperature dislocation network is pinned by impurity

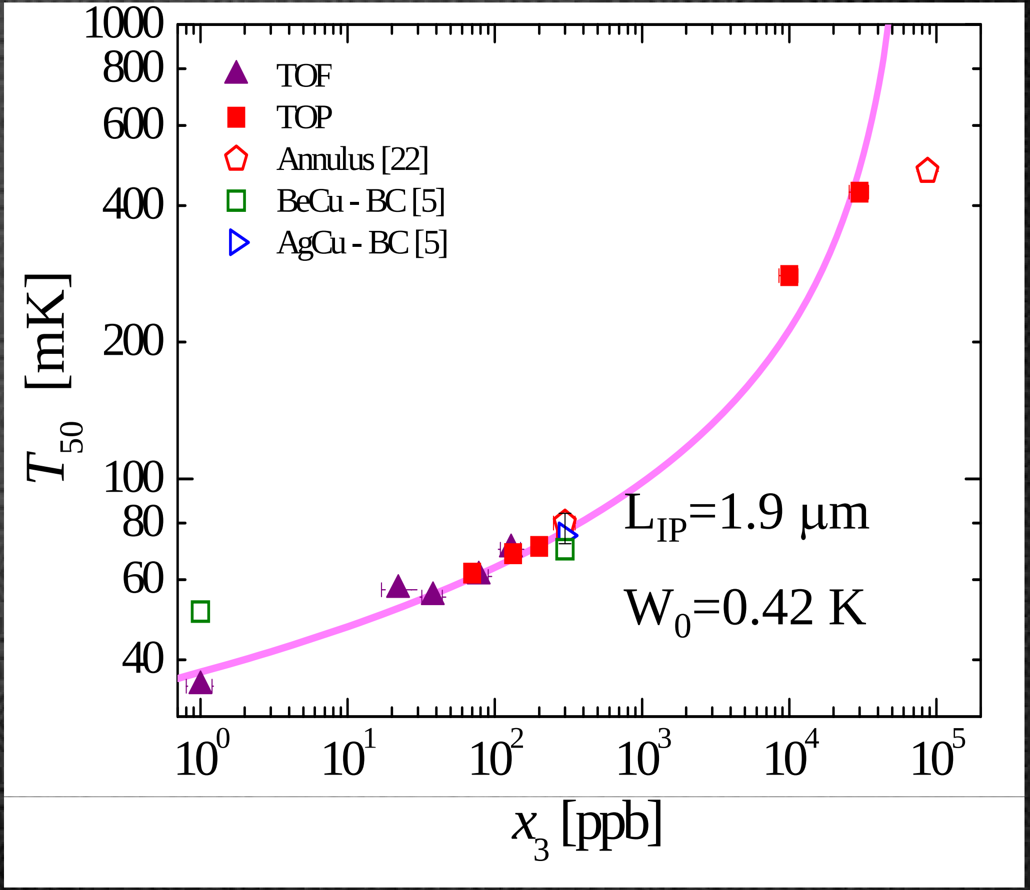

Kim et al, Phys. Rev. Lett 100, 065301 (2008)

Stiffening of solid helium responsible for NCRI ?

Why no difference in Vycor?

Much smaller pinning length is expected in Vycor glass (most of all dislocations are pinned)

Vycor TEM picture

Porous media: no substantial shear stress applied due to tortuous structure and small pore.

Vycor glass 7nm pores at 20 μm/s: $\sigma \sim 10^{-6}$ dyne/cm^2=10^{-7} Pa

100,000 times smaller stress causes similar strain of dislocation?

With strong confinements?

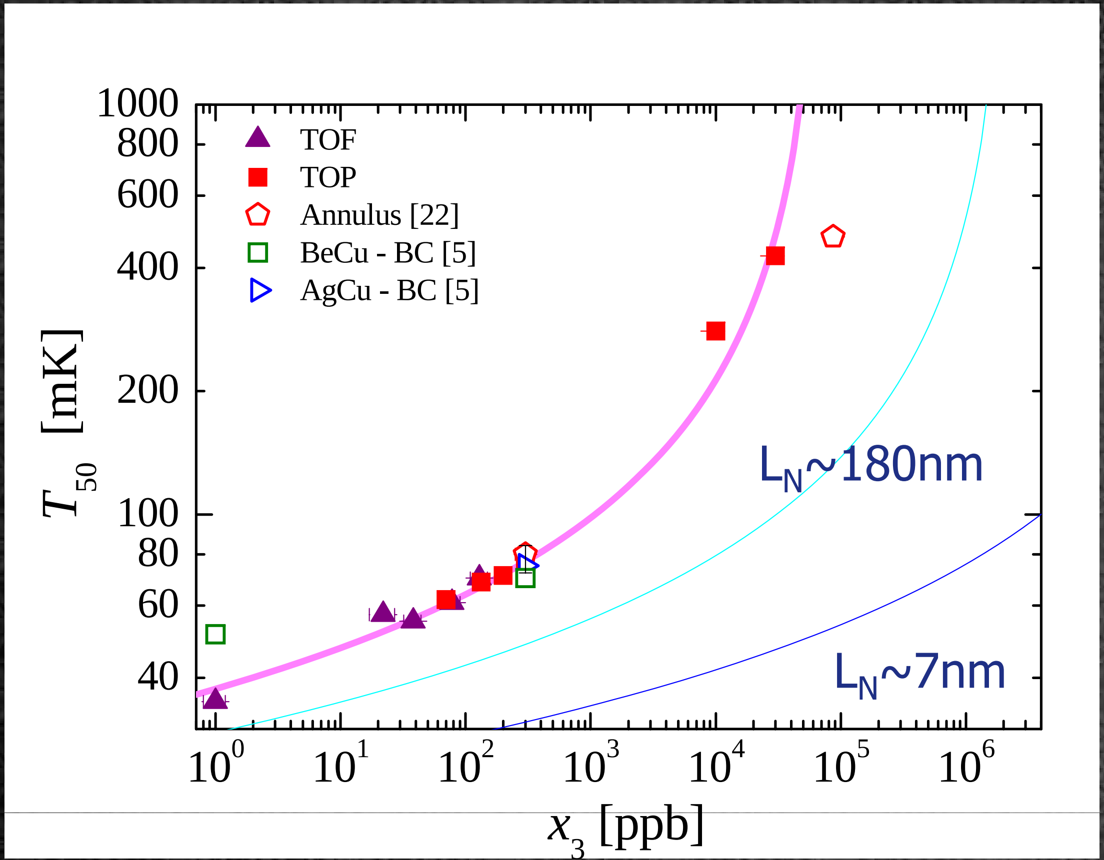

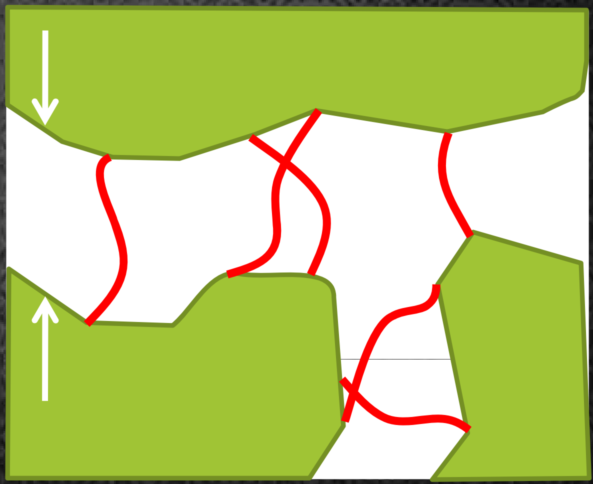

Elastic properties of solid helium

- Shear modulus change

J. Day, and J. Beamish, Nature **450**, 853 (2007)

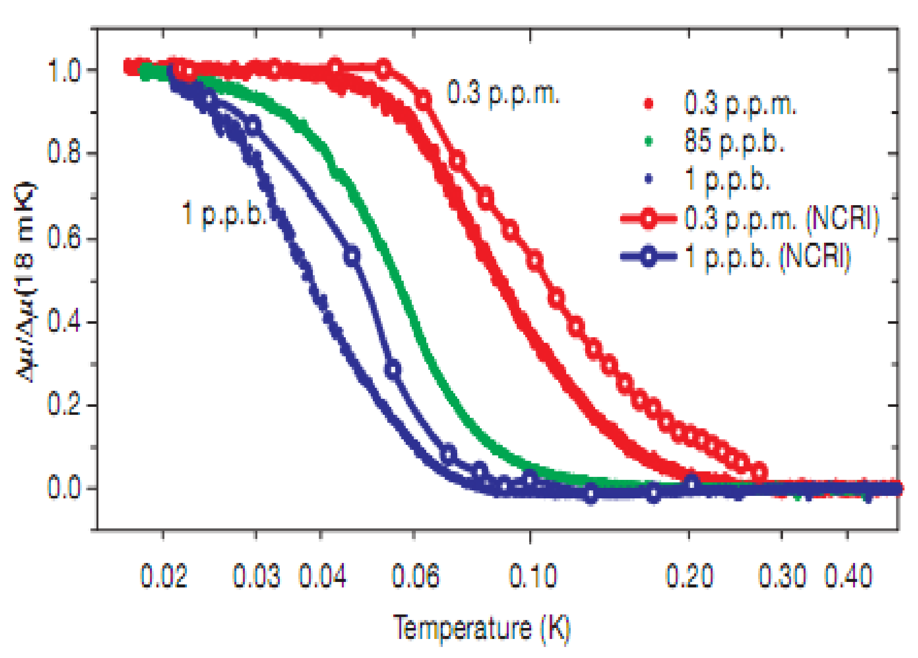

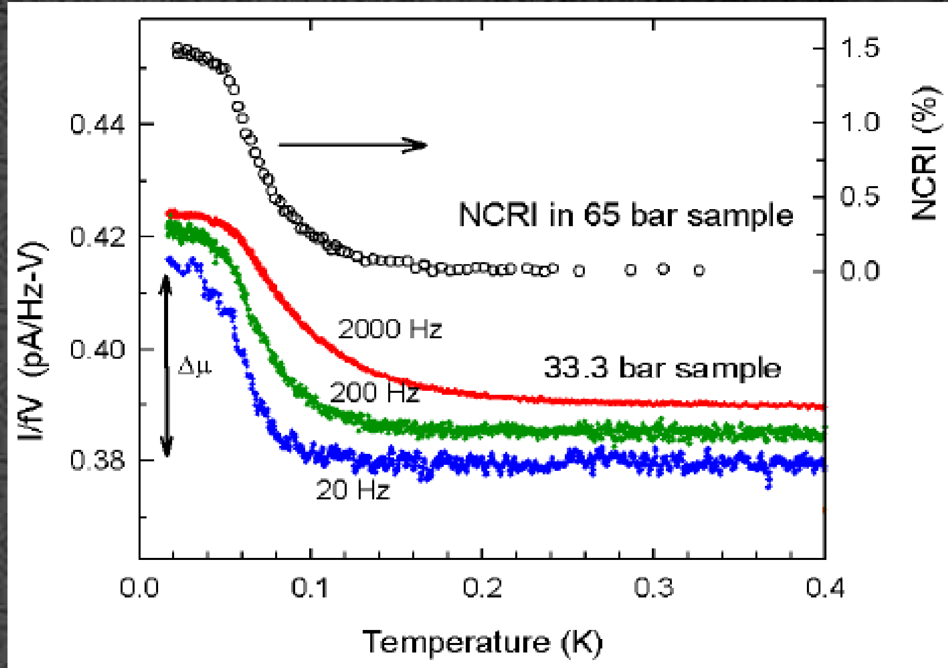

Shear modulus stiffened from dislocation pinning

Similar T, drive, freq, ^{3}He dependence with NCRI

Question: Stiffening of solid helium responsible for NCRI ?

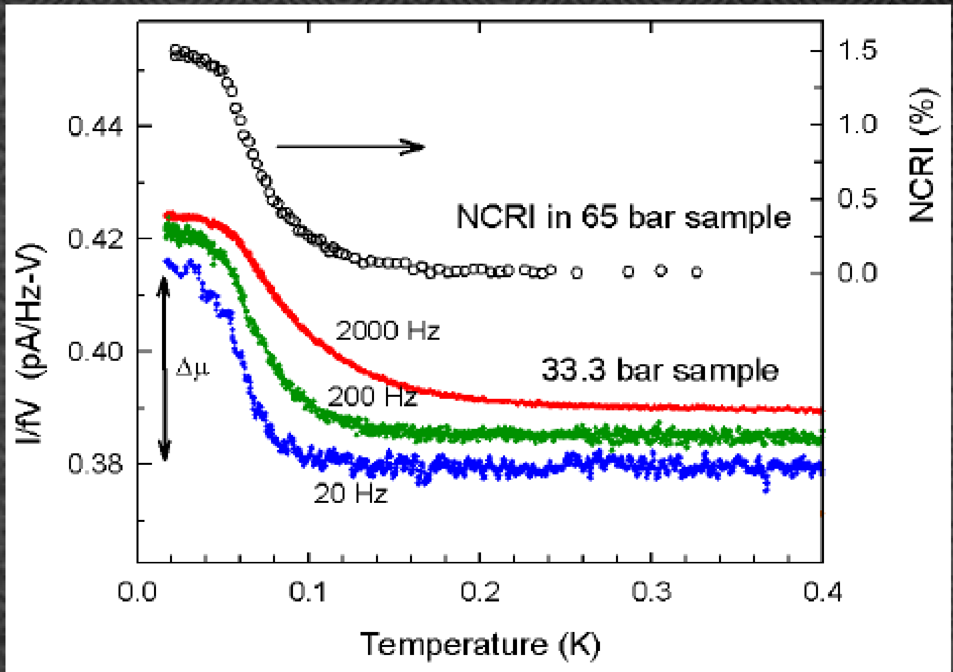

Elastic stiffening of solid helium at low temperature make the mechanical response faster. Accordingly increase the resonant frequency of TO

Nussinov et al PRB 76, 014530(2007)

Stiffening of solid helium responsible for NCRI ?

No

Clark et al PRB 77 184513(2008)

Stiffening of solid helium increase the resonant frequency of TO. However, observed 5-20% shear modulus increase is too small to explain the NCRI

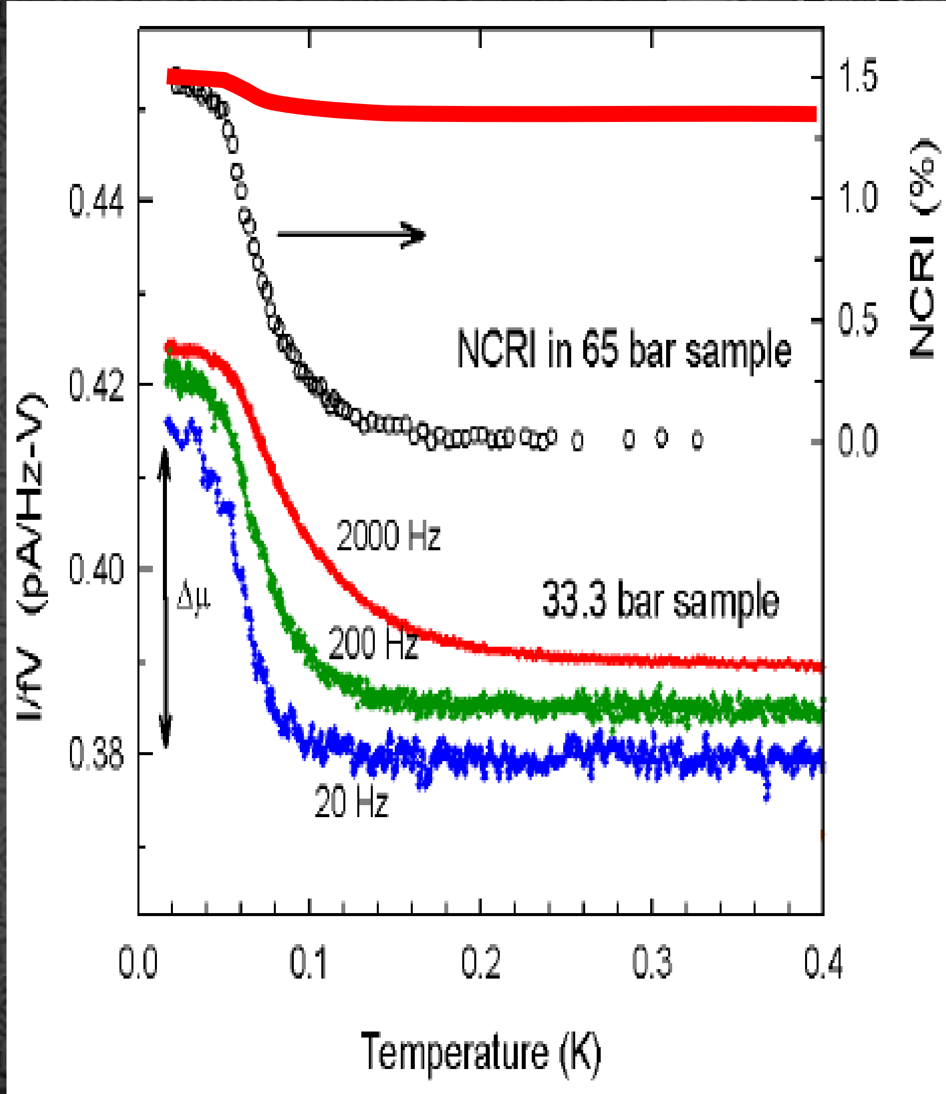

Blocked annulus results cannot be explained by shear modulus change

Summary

- **Dramatic effect of ^{3}He impurities on supersolid ^{4}He.**

  The addition of ^{3}He impurity broadens transition and enhances the onset temperature.

- **NCRI is not solely due to ^{3}He impurities**
- **The effect is probably related with dislocation pinning by ^{3}He.**

  After dislocation motion pinned by ^{3}He impurities supersolid phase appears.

  He3 impurities pin down dislocation lines and help to appearance of NCRI

Part 3

New experiments at KAIST

2D SUPERSOLID & DYNAMIC RESPONSE STUDY


©2006 Europa Technologies
Image © 2006 NASA
Image © 2006 TerraMetrics
Image
not
found
Image
not
found
Pointer 20°50'12.57" N 113°38'49.57" E
Streaming |||||||||| 100%
Eye alt 3958.94 mi


Vladivostok
Shenyang
Fushun
Tong Hua
Anshan
Dalian
North Korea
Pyongyang
Incheon
Seoul
Qingdao
South Korea
Daejeon
Daegu
Kwangju
Busan
(Pusan)
Shimane
Yamaguchi
© 2006 Europa Technologies
Image © 2006 NASA
Image © 2006 TerraMetrics
Image not found
Image not found
Pointer 38°20'08.58" N 128°00'00.84" E elev 1442 ft
Streaming 100%
Eye alt 727.28 mi

Image not found
Image not found
© 2006 Europa Technologies
Image © 2006 DigitalGlobe
Pointer 36°22'14.97" N 127°21'46.08" E elev 159 ft
Streaming |||||||||| 100%
Eye alt 9189 ft


SNOWD FEELING
Visit: http://snowdrop.new21.net


2005/05/05 11:51:38

New LT Lab at KAIST

New LT Lab at KAIST

Interior

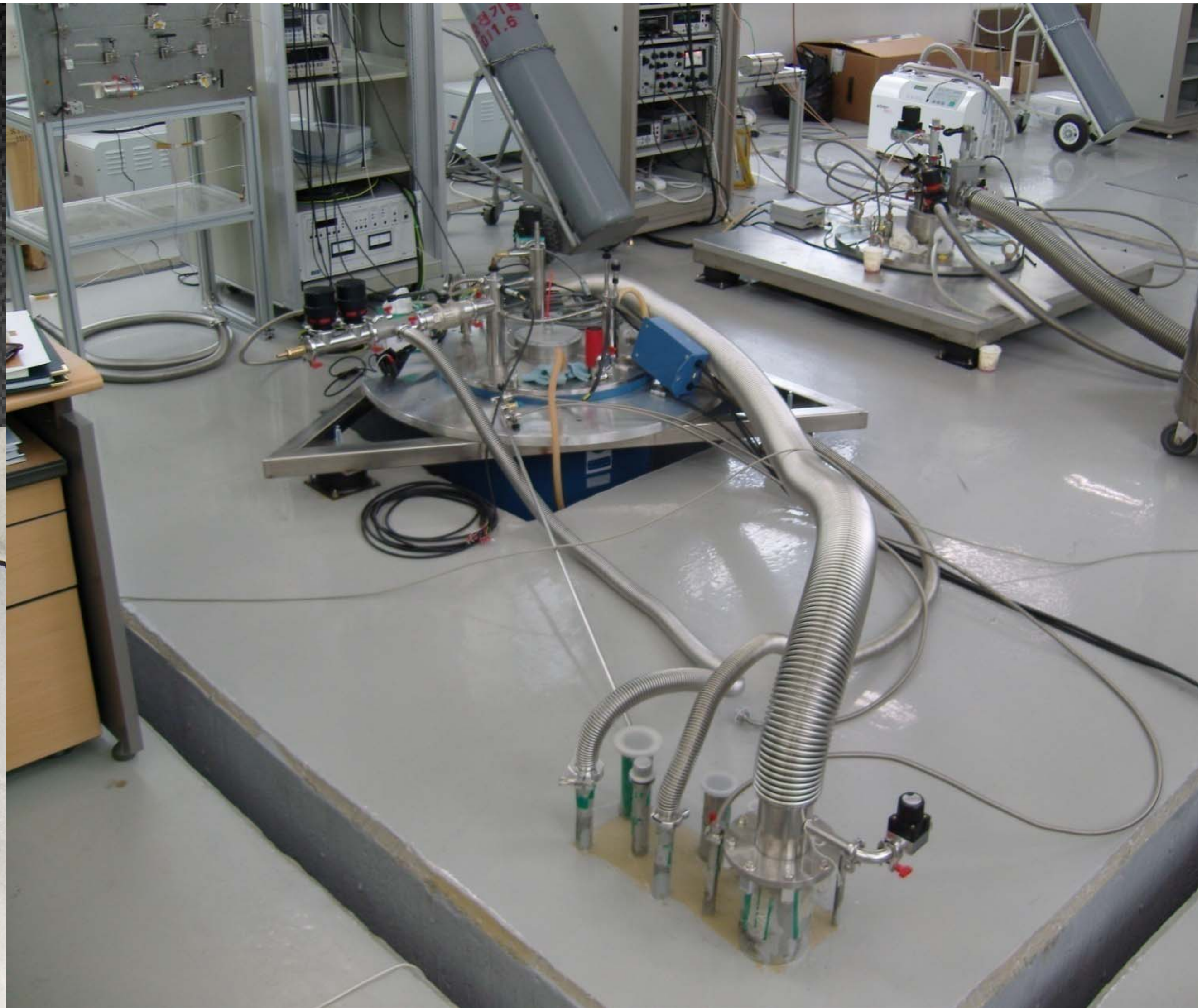

Pumping room(basement) vibration is olated with double gymbal structures.

Search for the supersolidity in 2D

❖ Motivation

The nonsuperfluid inter layer

$$\rho_S\left(T=0\right) = n_4 - n_0$$

n_4 : Total ^{4}He coverage
n_0 : Inert layer coverage

From the Lennard-Jones potential

$$V(z)=\frac{4C_3^3}{27D^2}\frac{1}{z^9}-\frac{C_3}{z^3}$$

We can calculate the attractive force between the atoms of the substrate and the atoms in the film.

25 atm >

Atomic layer	Pressure by van der Waals force
1st layer	306.0 atm
2nd layer	19.1 atm
3rd layer	11.3 atm
4th layer	4.8 atm

Helium films

- Helium films below the coverage for onset of superfluid can be a supersolid system.

  J. Sarfatt, *Phys. Lett. A* **30**, 300(1969)

Helium films

- Reentrant superfluid phase in the second layer of ^{4}He adsorbed on grafoil.
- They discussed "possible 2D supersolid"

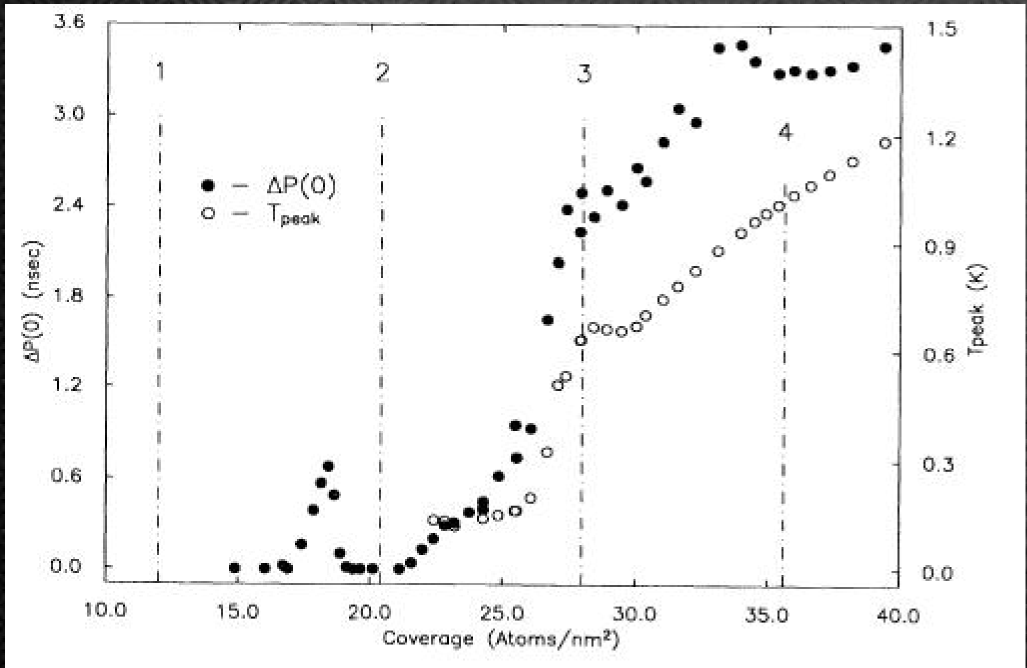

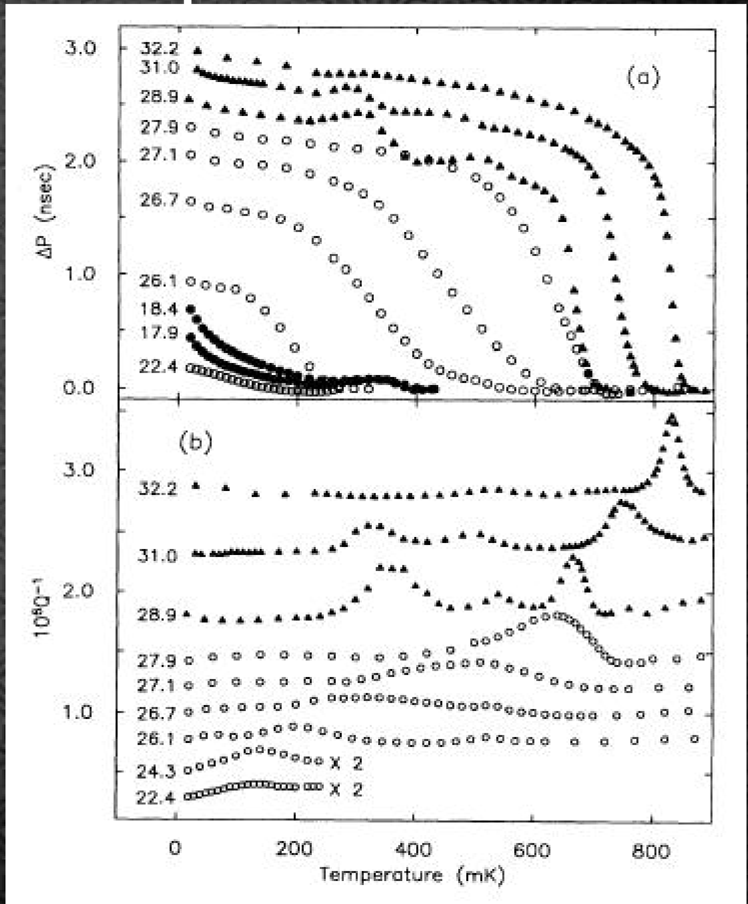

Helium films

- Reentrant superfluid phase in the second layer of ^4He adsorbed on graphite.

- M. Hieda and Moses made very interesting observation on 2D amorphous solid helium, so called inert layer. Resonant frequency of QCM increased at very low temperature.

- NO clear velocity dependence

Search for the supersolidity in 2D

- Porous Vycor glass
- Mass loading : 458 ns/layer

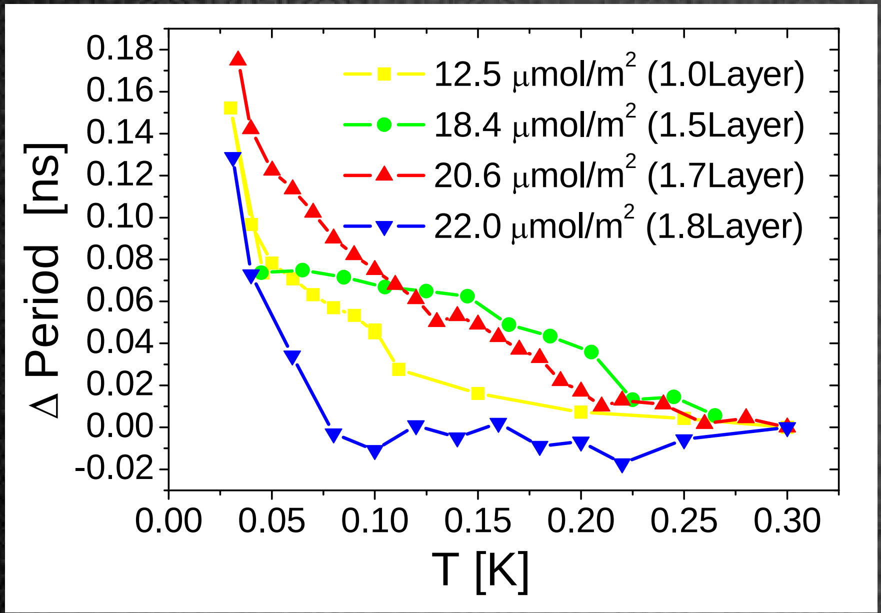

Period change in the inert layer

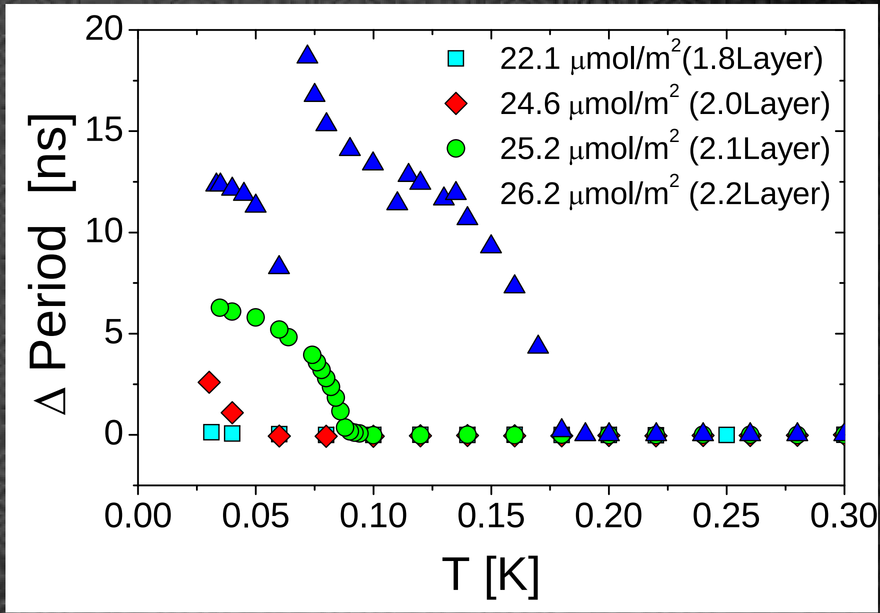

Superfluid transition of He films

Quest for lower amplitude

Vycor tube glued by stycas1266

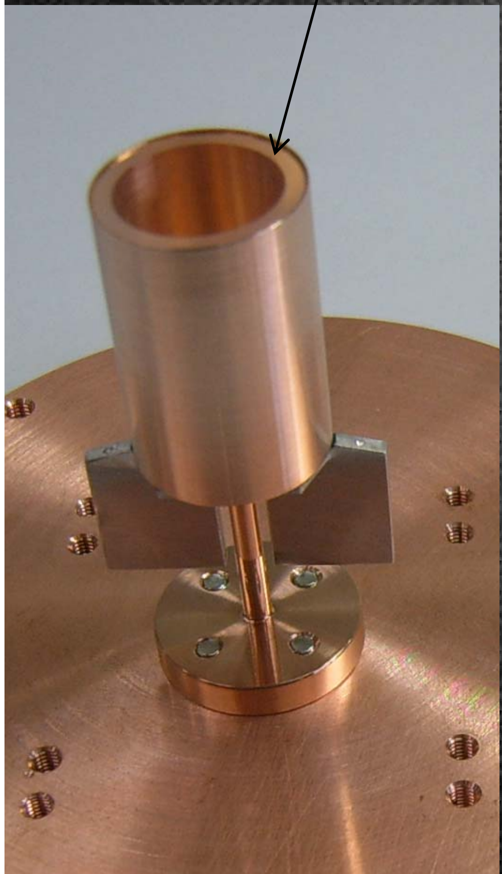

CuNi capillary for feeding helium

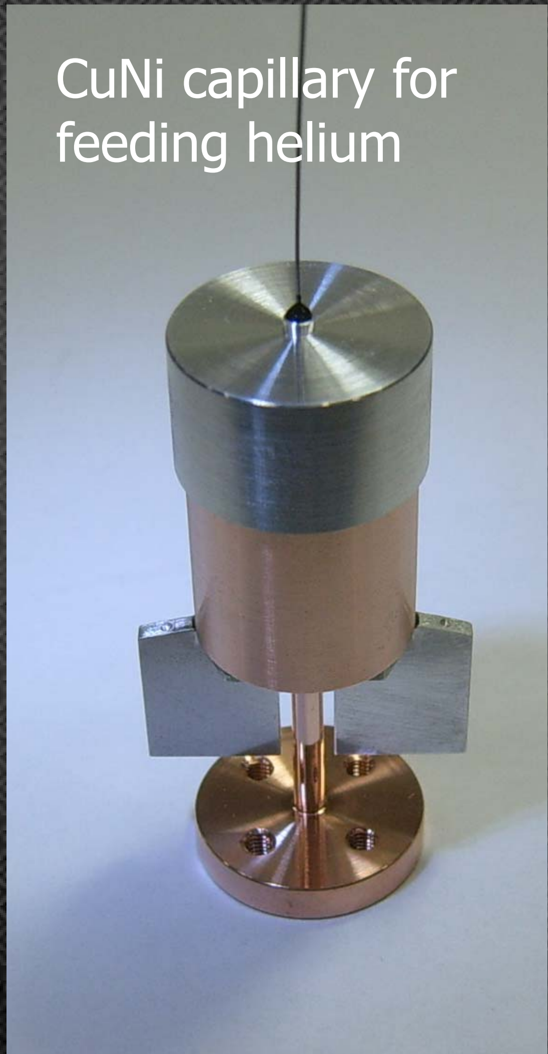

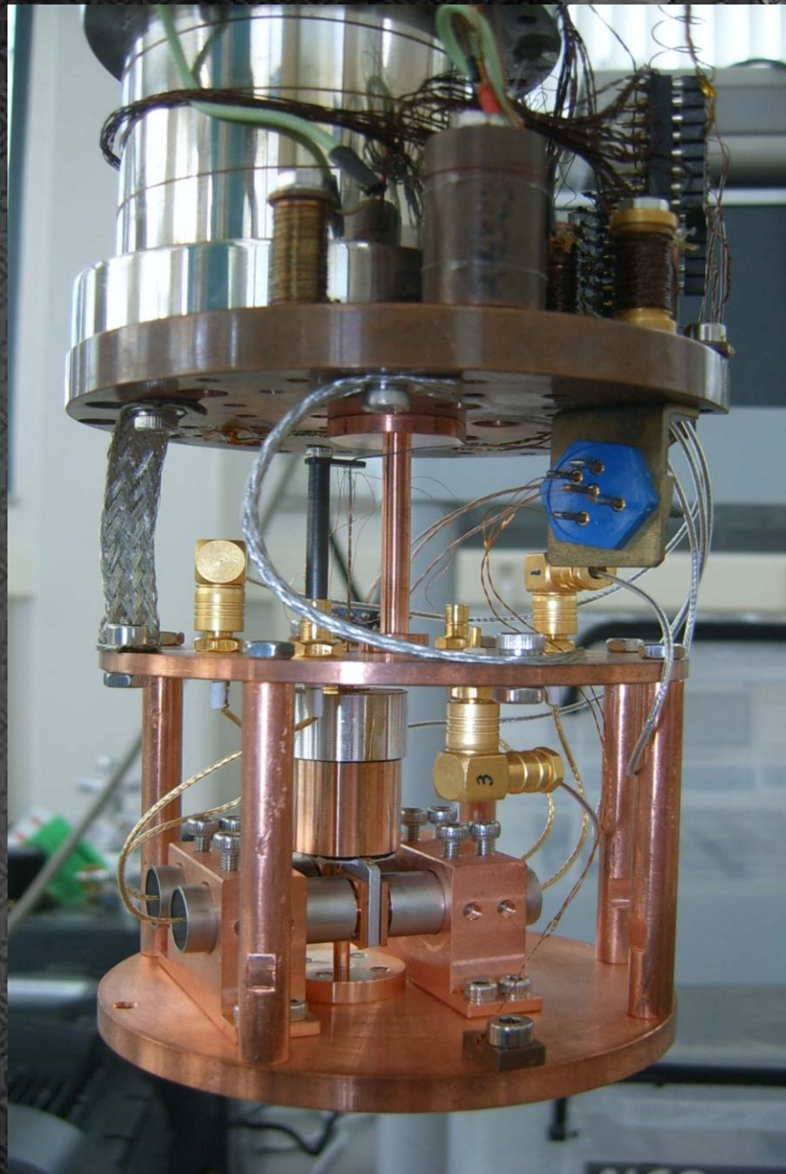

Resonant frequency 738 Hz, Q-factor $8 * 10^5$

Amorphous solid helium film on Vycor

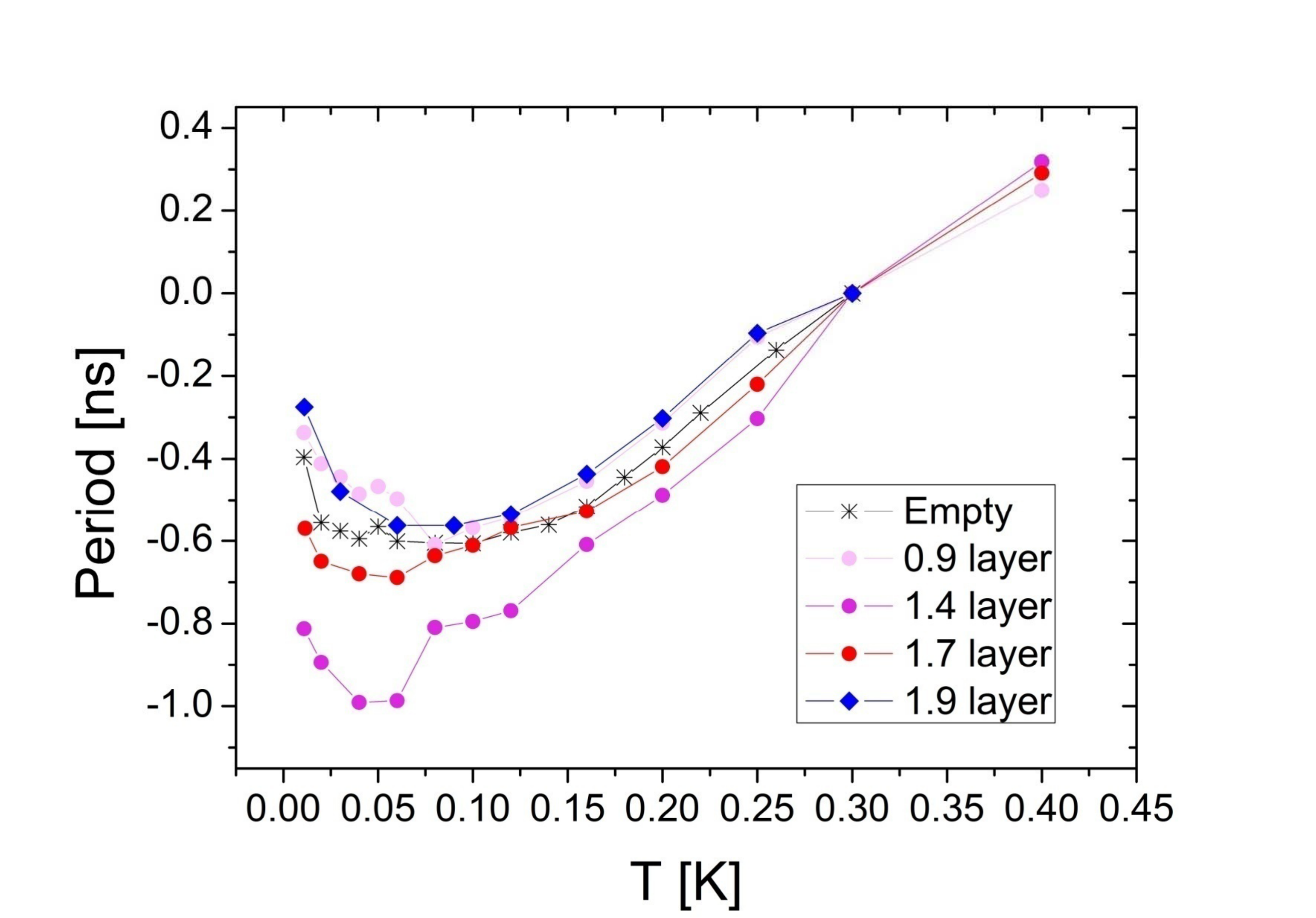

Thermal history:

Unusual long time constant

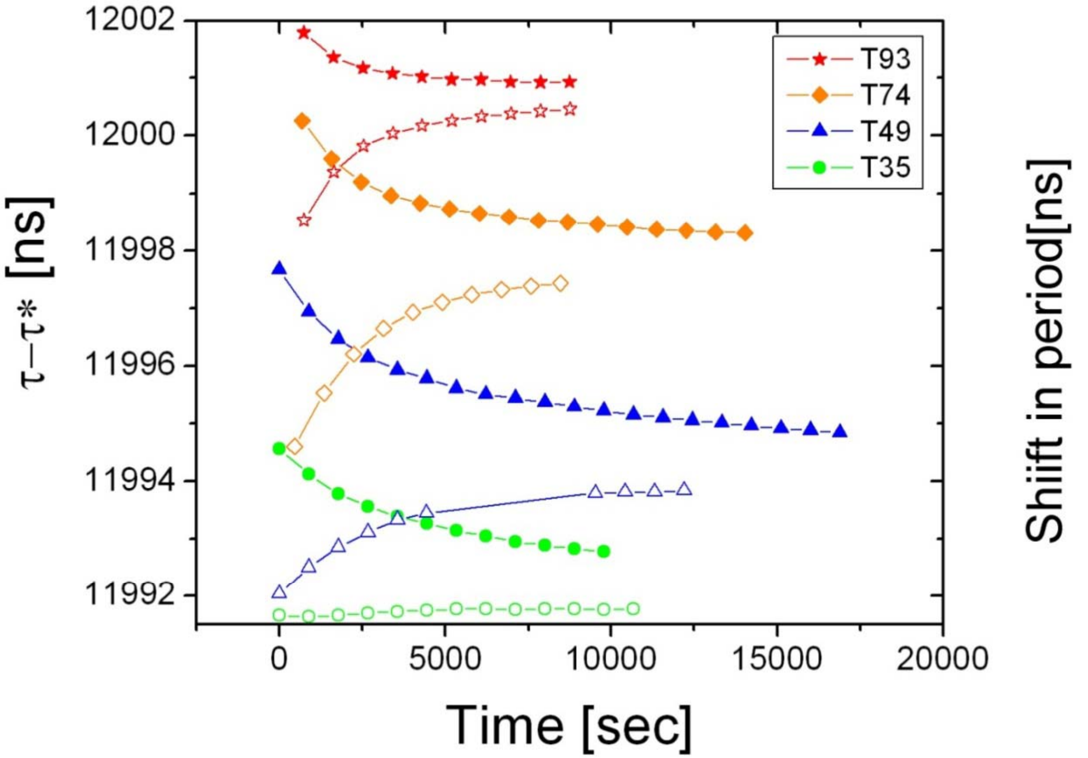

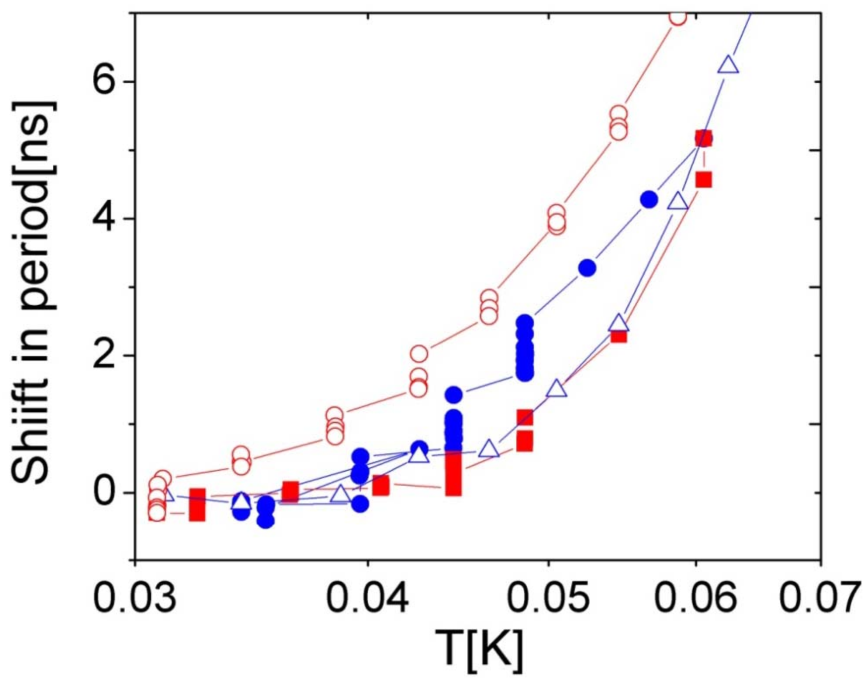

Typical equilibration time of TO due to very high mechanical Q-factor at low temperature: ~ 1000sec

Below 0.1K we observed unusually extended equilibration time.

Not fitted well with exponential decay function only.

After few thousands sec. logarithmic time dependence is dominant.

Thermal history dependence was carefully revisited. Clark et al PRB 77, 184513(2008)

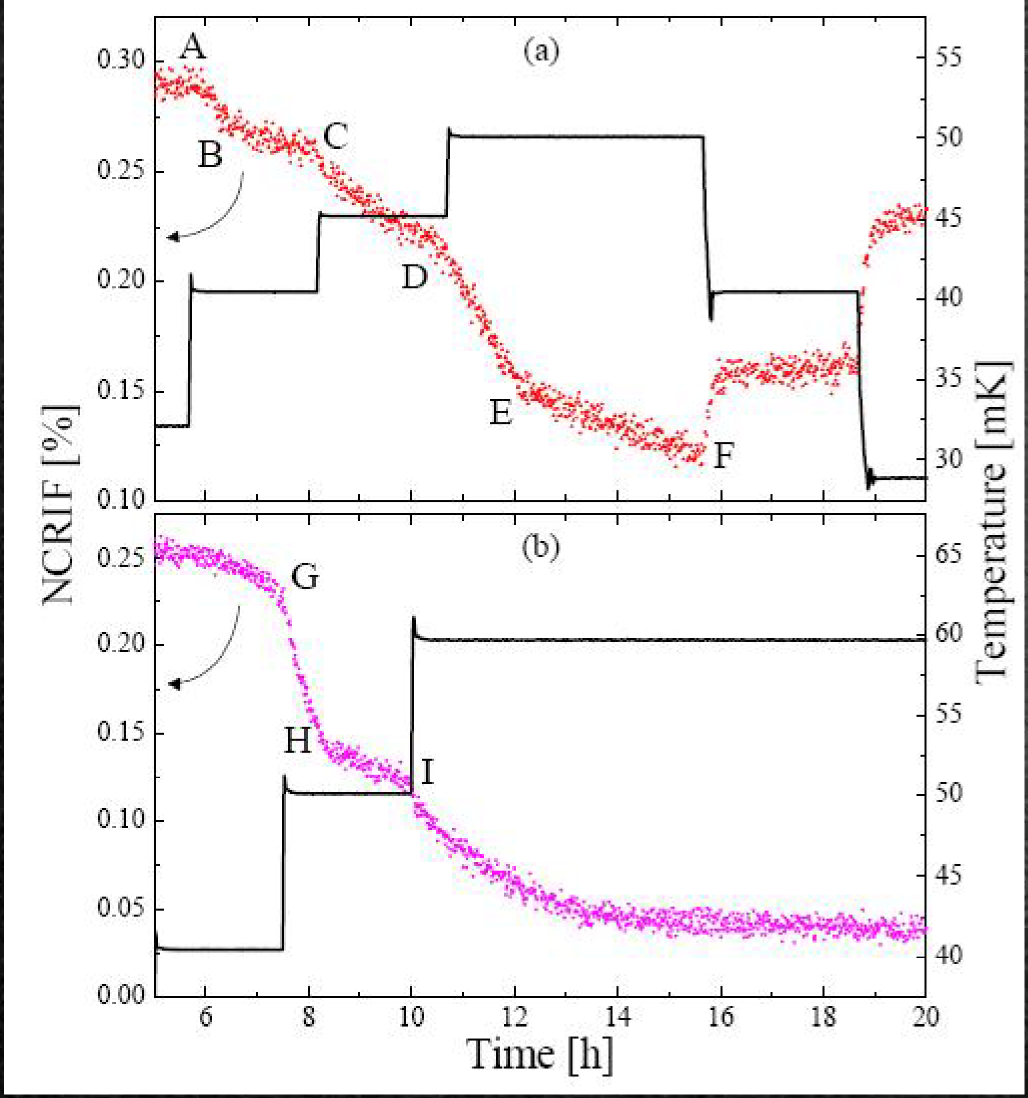

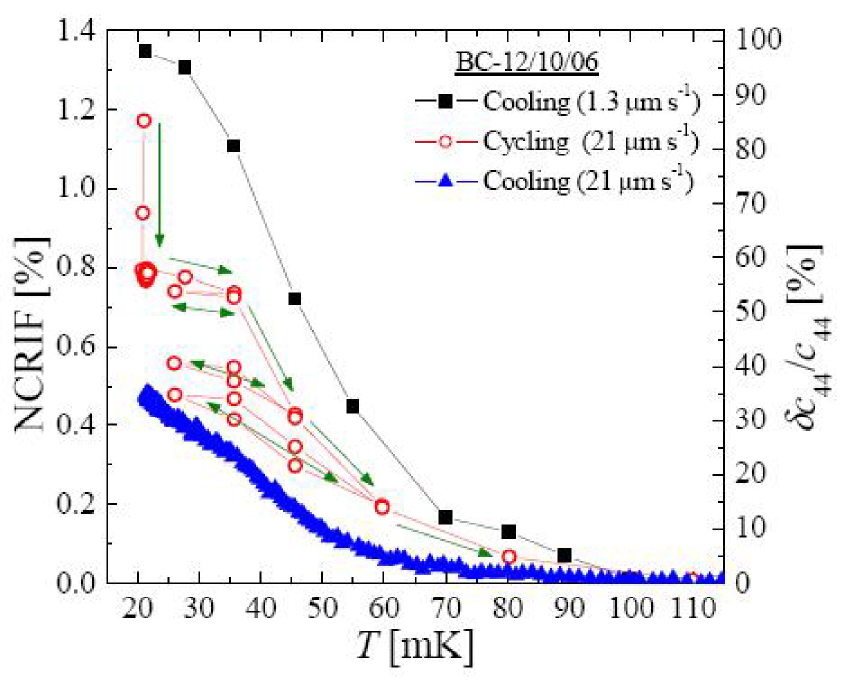

Meta-stable state

Vortex pinning mechanism or elastic anomaly could explain hysteresis

Long dissipation(amplitude) relaxation in bulk solid helium

Long time constant observed upon the change of TO drive amplitude in bulk TO cell. Aoki et al PRL 100, 215303 (2008)

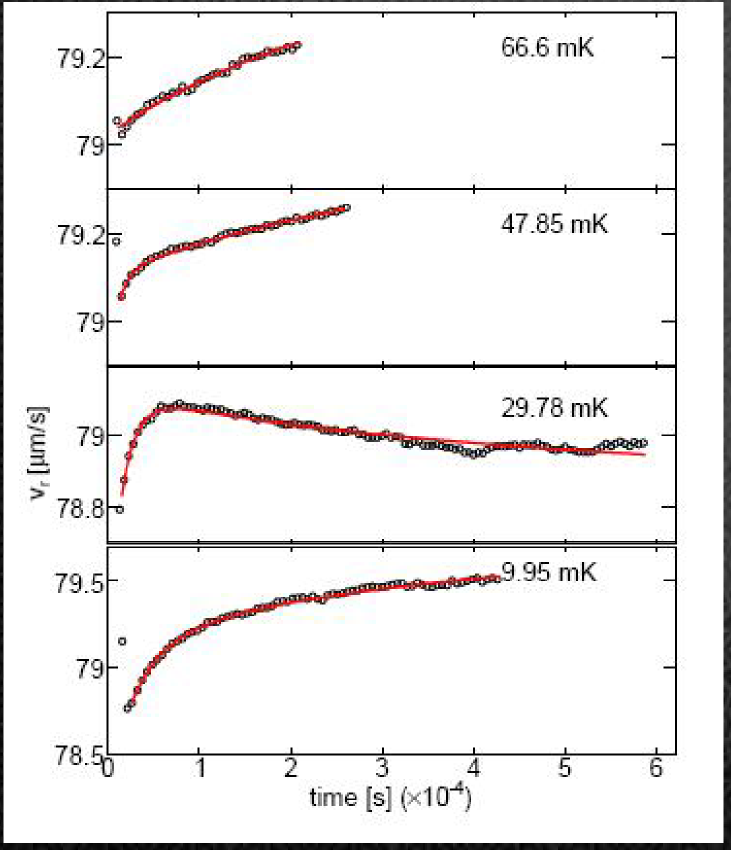

$$v_r = v_0 + A\exp(-t/\tau) + B\ln[t + t_0]$$

The exponential dependence: The mobility of dislocation (and pinning by 3He impurities) and vortex liquid interpretation are discussed in their paper. They argue that long dissipation relaxation is likely due to vortex liquid in solid helium.

Solid ^{4}He confined in porous gold

The motion of the shear modulus change in porous media is reduced by small confinements.

- Porous Gold
  - Pore size ~180nm
  - Porosity ~71%
  - Surface area 0.66m^2

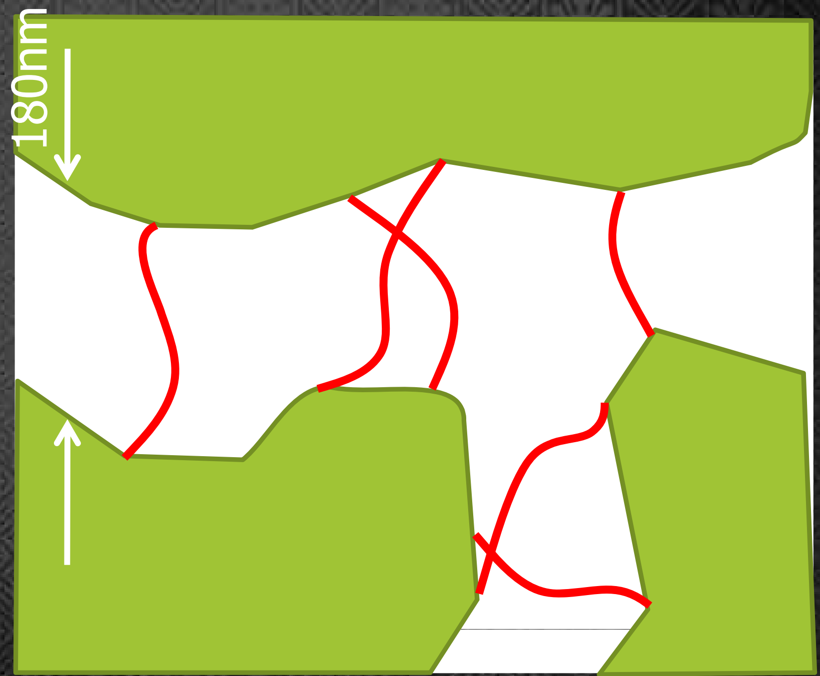

Solid ^{4}He confined in porous gold

- Tostional oscillator
  - Resonant frequency ~ 948 Hz
  - Q ~ 3 x 10^5
  - No bulk space

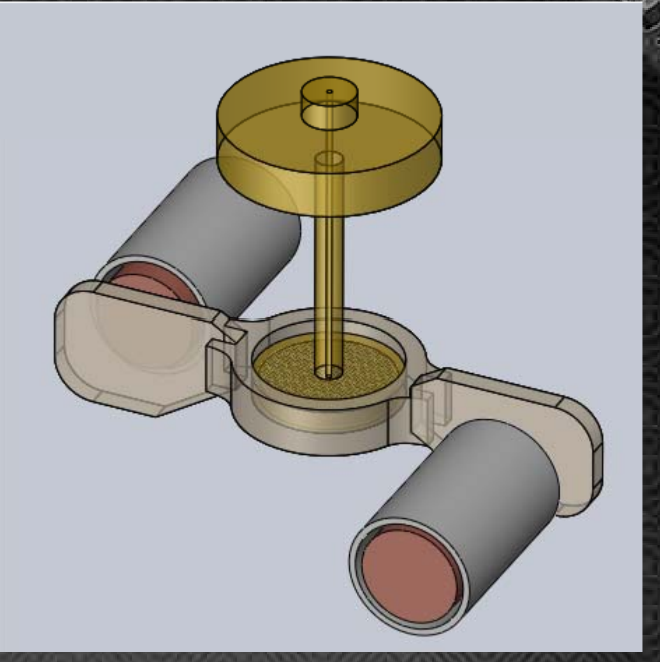

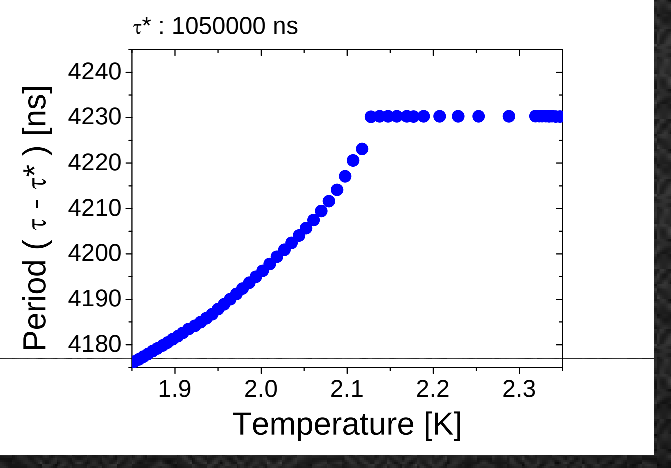

Superfluid ^{4}He in the porous gold

Solid ^{4}He confined in porous gold

- Solid Helium was prepared by the BC (blocked capillary) method

- Starting Pressure : 60 bar
- Measured Sample pressure : 53 bar

- Samples grown by quench cooling
  3K -> 1K for 15 min.

- ^{3}He : 0.3 ppm

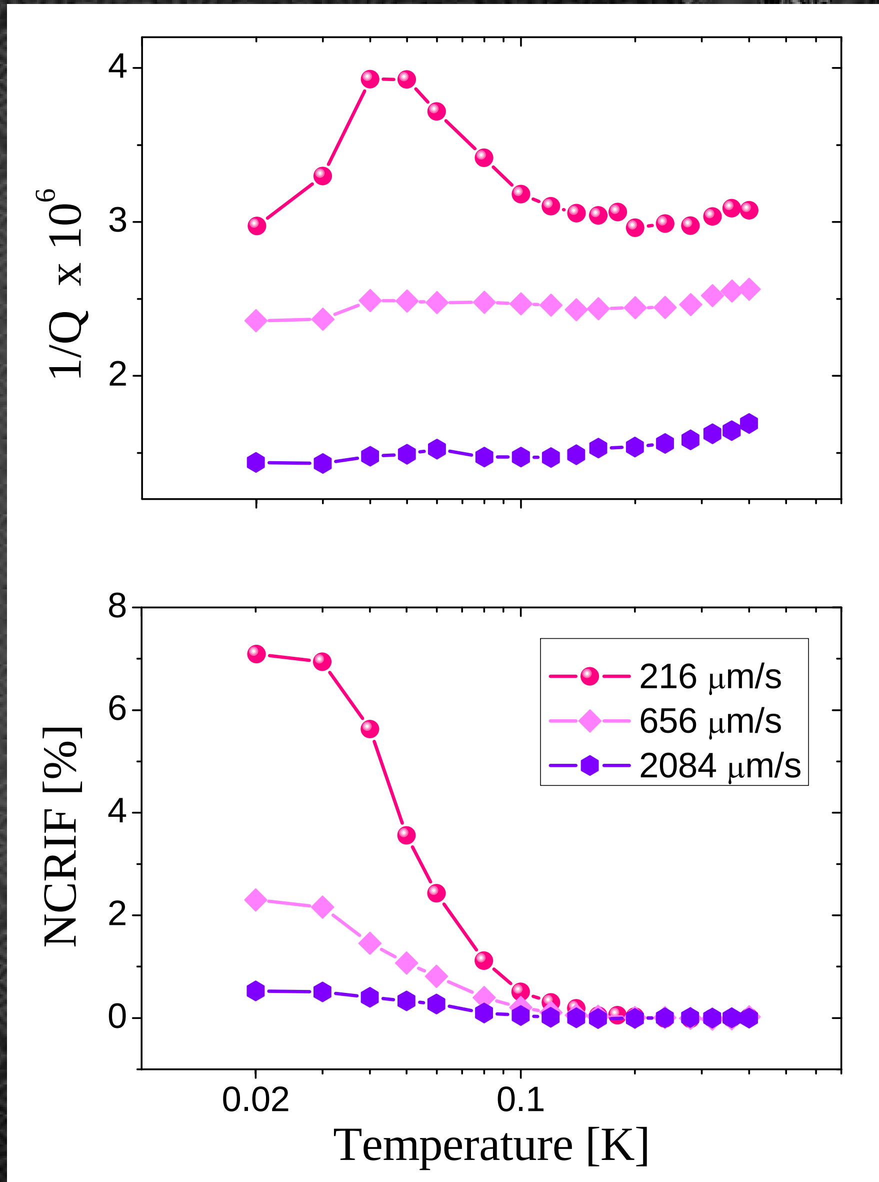

Response to drive change

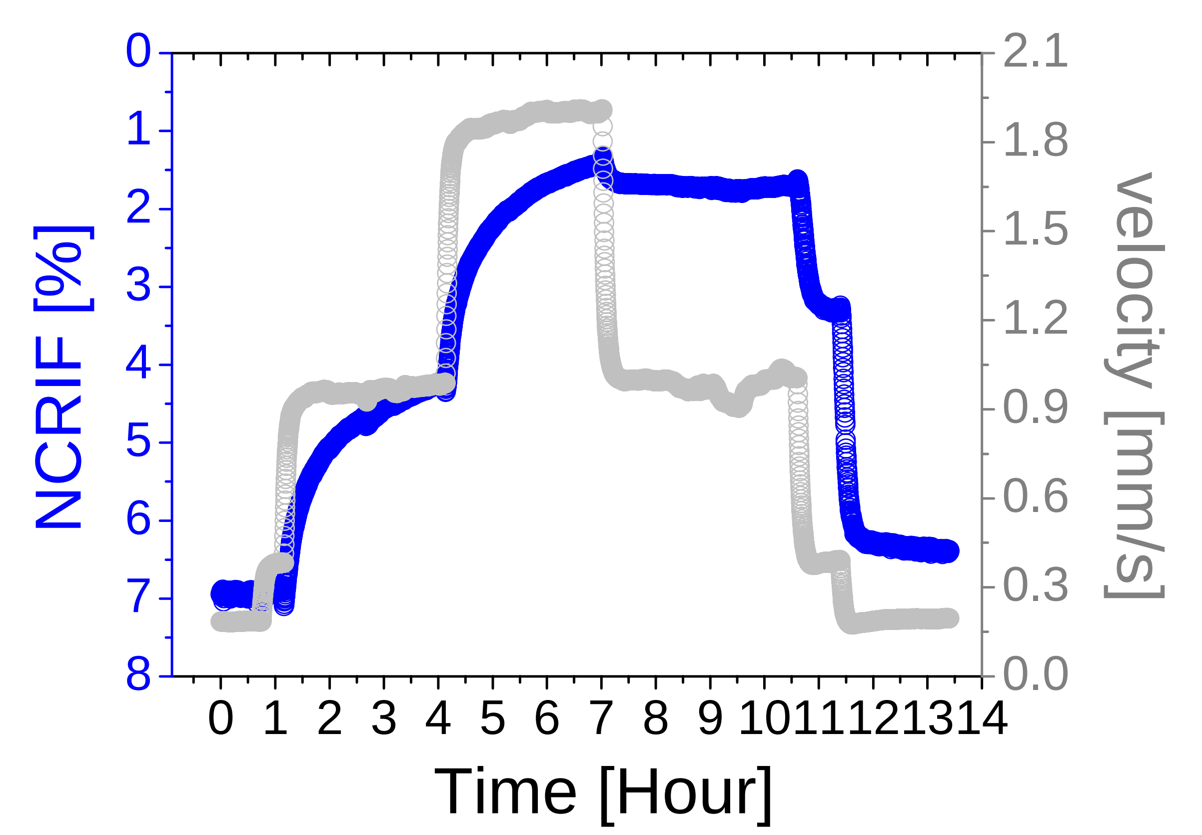

Long relaxation of NCRI when drive increases.

NCRI change looks hysteretic according to the drive change.

Response to drive change

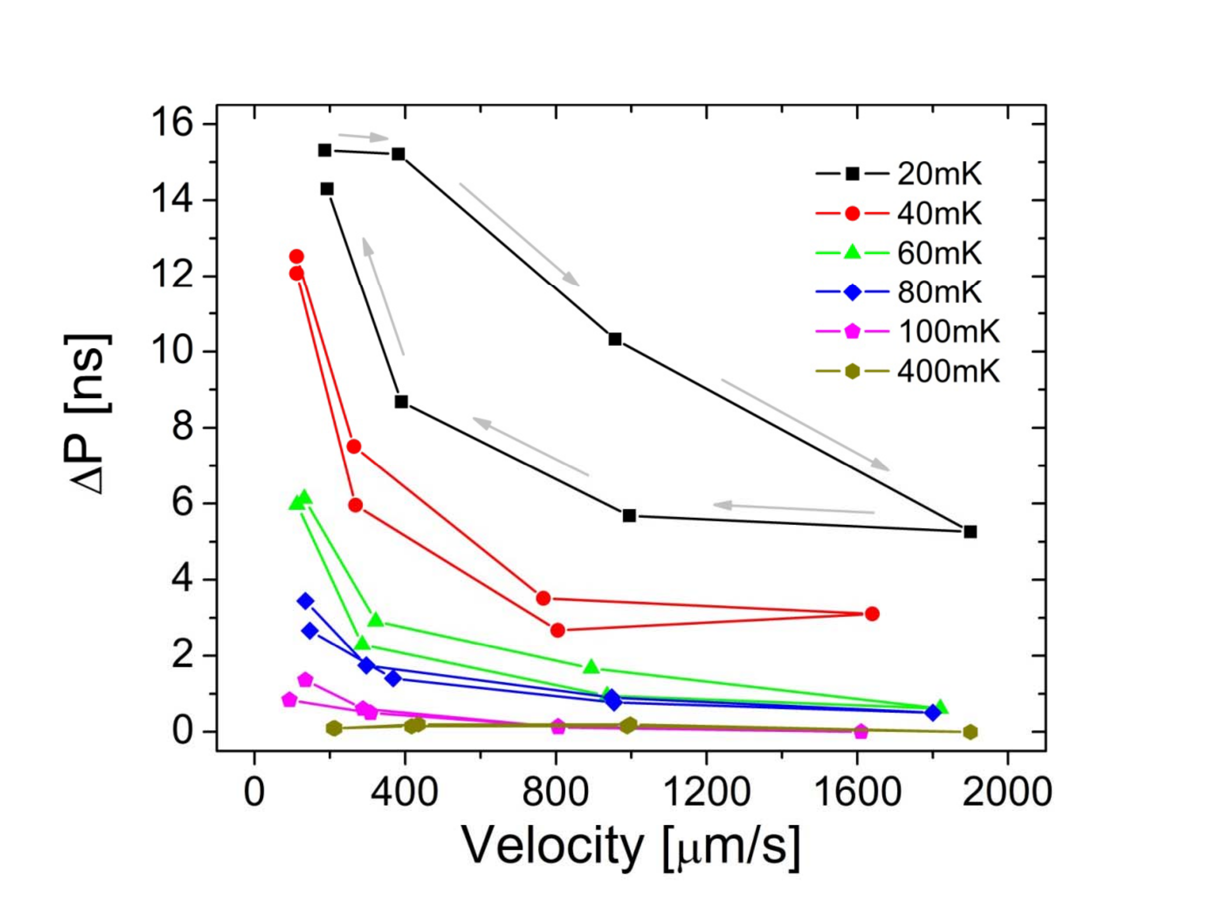

Long relaxation of NCRI when drive increases.

NCRI change looks hysteretic according to the drive change.

Thank you for your attention!